Acquisition Techniques for Direct Sequence Spread Spectrum Packet Radio Systems

by

Zhen-Liang Shi

B.Sc., Northern Jiao-Tong University, Beijing, 1983
M.Sc., Northern Jiao-Tong University, Beijing, 1986

A Dissertation Submitted in Partial Fulfillment of the
Requirements for the Degree of

DOCTOR OF PHILOSOPHY

in the Department of Electrical and Computer Engineering

We accept this dissertation as conforming to the required standard

Dr. Peter A. Driessen, Supervisor (Department of ECE)

Dr. J. Bornemann, member (Department of ECE)

Dr. F. El-Guibaly, member (Department of ECE)

Dr. C. J. Pritchet, outside member (Department of PHYS)

Dr. A. Polydoros, External Examiner (Dept. of EE, Univ. of S. Cali.)

Abstract

The thesis focuses on fast acquisition techniques for spread spectrum packet radio communications systems. Matched filters are often used to achieve fast acquisitions. A new synchronizer using *multiple acquisition detection* is designed to achieve a highly reliable synchronization with a very simple receiver structure. Since PN codes, in practice, cannot be made too long due to the difficulty of manufacturing long matched filters and the limitation on the bandwidth of the frequency spectrum for the system, the reliable synchronization can be only obtained by repeating the transmission of the acquisition code at the beginning of each packet. The verification or coincidence detection is done by means of a marker detection following an acquisition. A hard-limiting synchronizer is also examined combined with the *multiple acquisition detection*. The hard-limiting synchronizer is simpler to implement and suitable for receiving signals with a large SNR dynamic range, but it cannot work well when multiuser interference and multi-path interference are present. For this reason, a new linear Automatic Threshold Control (ATC) synchronizer is developed for detecting signals with a large amplitude dynamic range while preserving good performance in multi-path and multi-user interference. The idea of the ATC scheme is to adjust the receiver acquisition threshold level according to the SNR of the received signal such that the largest (or the most likely) correlation peak in a short time period is selected for the synchronization alignment. Therefore false acquisitions caused by strong correlation side-lobes during the acquisition can be eliminated. For the more realistic situation where the multi-user interference or near-far effect causes severe performance degradation, we proposed a novel non-linear multi-user detector or multistage detector which is suitable for both the synchronous and asynchronous CDMA systems. This sub-optimal detector is able to achieve the performance of the optimal detector with very small computation complexity. The near-far effect will no longer exist because the interference from

the unexpected users is considered to be not always harmful for the detection of a specific users' message. To apply this detection technique to asynchronous CDMA systems, acquisition for each users' PN code becomes more critical, because during the acquisition, the information from the other users' PN codes is usually not available, which means that acquisition still suffers the near-far effect. The proposed acquisition scheme based on interference cancellation technique and the ATC scheme can alleviate the near-far effect significantly, and provide the necessary condition for the appropriate operations of multi-user detectors.

Examiners:

Dr. Peter F. Driessen, Supervisor (Department of ECE)

Dr. J. Bornemann, member (Department of ECE)

Dr. F. El-Guibaly, member (Department of ECE)

Dr. C. J. Pritchet, outside member (Department of PHYS)

Dr. A. Polydoros, External Examiner (Dept. of EE, Univ. of S. Cali.)

Acknowledgements

I would like to thank Dr. Peter Driessen very much for his profound help in directing my research and reading many drafts of my dissertation. I must also thank the many friends and colleagues who have helped and encouraged me during my studies at the University of Victoria. My special thanks should go to Dr. Weixiu Du for his many good suggestions and helpful comments for some part of the thesis. In addition, I especially wish to thank Shujian Zhang for his consistent encouragement and helps.

I would also like to thank Professor Bornemann, Professor El-Guibaly and Professor Pritchet for serving on my supervisory committee, and Professor Polydoros for serving as the external examiner in my Ph.D oral examination.

Finally, I want to thank my wife and my parents, who have been supporting and understanding me beyond measure. The thesis is dedicated to them.

To

My Parents

and

Wenli

Contents

List of Tables

List of Figures

List of Symbols

SYMBOL	*MEANING*	*PAGE*
A_k	signal amplitude of user k	132
A_{J_1}	interference amplitude vector to user 1	134
α	$\bar{B}/\bar{I}$	24
α_n	$\alpha_n = \sqrt{\sigma_i^2(0)/\sigma_i^2(n)}$	149
B	receiver blocking time (random variable)	21
B_{J_1}	interference data matrix	134
$\bar{B}$	average receiver blocking time	21
b	data bit vector of K users	86
b_0	threshold for acquisition detection for linear MF	17, 20
	initial threshold for the ATC scheme	67
b_1	threshold for coincidence detection for linear MF	17
b_c	coincidence detection threshold for the ATC scheme	67
$b_{J_1}(i)$	the ith data bits of the interfering users to user 1	134
c_k	unit-amplitude signature waveform of user k	132
$\tilde{\eta}_i$	minimum asymptotic efficiency of user i	111
η_i	asymptotic efficiency of user i	111
f_m	minimum function value	93
Φ	modifying matrix	88
g_i	the ith column vector of the inverse of Q	90

g_{ii}	the ith diagonal element of the inverse of Q	89
γ_o	SNR at the output of the linear MF	20
H_1	signature sequence matrix of user 1	133
H_{J_1}	signature sequence matrix of interfering users to user 1	134
H_i'	signature sequence matrix of user 1 to user i	142
$\bar{H}^\dagger$	pseudoinverse of $\bar{H}$	110
$\bar{H}$	signature waveform matrix	86
h	error tolerance of the acquisition detection	43
h_1	digital threshold of the HLMF for acquisition	43
h_e	error tolerance for the marker detection	27
h_x	erasure tolerance for the marker detection	27
$h_0(n)$	Hamming distance test measure for HL acquisition	43
$\hat{h}_0(\hat{n})$	Hamming distance between the replica marker and the received marker without and interference	27
I	receiver idle time (random variable)	21
$\bar{I}$	average receiver idle time	21
J_1	multiuser interference to user 1	133
J_i'	multiuser interference to the first i users	142
m	PN sequence length in chips	18
L_D	number of data bits for a packet	18
λ_f	arrival rate of false acquisition in noise alone	23
M'	minimum number of data bits required for acquisition	141
N_h	number of PN code periods used for acquisition	16
N_s	number of PN code periods used for coincidence detection in the preamble	16
$P(h_e, h_x, \hat{n})$	probability of marker detection in a particular position	27
$P_{acq}(i)$	probability of acquisition for the ith signal	148

$P_{acq}(i,k)$	probability of acquisition in the ith PN period given k chips lost	25
P_B	probability of receiver blocking due to false alarms	20
$P_c(i)$	probability of coincidence detection when the acquisition occurs in the ith period	25
P_{cd}	probability of successful coincidence detection	75
P_d	probability of initial acquisition	20
$P_d(i)$	probability of acquisition at the ith stage	148
P'_d	probability of initial acquisition for the constant threshold receiver	74
P_f	probability of false acquisition at incorrect phase for the ATC scheme	73
P'_f	probability of false acquisition at incorrect phase for the constant threshold receiver	73
P_{fan}	probability of false acquisition	20,72
P_{fcn}	probability of false coincidence detection	23
P_{fc}	same as P_{fan} with threshold b_c	72
$P_{fd}(n)$	probability of false acquisition at incorrect phase	20
P_{fn}	probability of false marker detection at an incorrect phase	28
$P_{pass}(i)$	probability that a detector passes stage i	148
P_{syn}	overall synchronization probability	24
$P_{syn}(k)$	probability of acquisition provided that k chips are blocked and lost	23
P_L	probability of packet loss	18
$P_L(min)$	minimum packet loss probability	29
P_{w_k}	probability that the window w_k is initiated	72

Q	Hessian matrix of the minimization problem	87
p	symbol error probability	27
p_c	chip error rate	43
q	symbol detection probability	27
Q_j	$Q_j = I - H_j H_j^{\dagger}$	151
Q_{p_j}	$Q_{p_j} = Q_j Q_{j-1} \cdots Q_1$	151
p_n	symbol error probability when no signal is present	27
q_n	symbol detection probability when no signal is present	27
R	normalized cross-correlation matrix	111
R_{1J_1}	cross-correlation matrix between user 1 and the interfering users	135
$r_c(j)$	residual signal after the j cancellation	151
$r_{1k}(0)$	partial cross-correlation between user 1 and user k	135
$r_{1k}(1)$	partial cross-correlation between user 1 and user k	135
s	symbol erasure probability	27
s_n	symbol erasure probability when not signal is present	27
ρ	autocorrelation coefficient of the PN code	19
$s_k(t)$	signature waveform for the kth packet	86
σ^2	power of noise	19
$\sigma^2_{Y_n}$	statistical variance of Y_n	45
T	duration of a PN code period	18
T_1	busy period after a false acquisition	21
T_2	busy period after a false coincidence detection	21
T_D	packet length	23
T_c	chip duration of PN codes	19
τ_k	delay for signal of user k	132
θ_1	vector to be estimated for signal of user 1	133

0_{J_1}	vector which is interference to user 1	133
w_k	bit energy of user k	107
x^I	the 0-1 minimum solution	88
$\hat{x}^I$	binary quantization of $\hat{x}$	92
$\hat{x}$	the continuous minimum solution	88
x_m	$\hat{x}^I$ with the smallest function value	92
Y_n	output sample from the digital matched filter	43
$\bar{Y}_n$	statistical mean of Y_n	44
$Z(t)$	envelop of the output from linear MF	71
Z_k	$Z(kT_c)$, input sample to the hardlimiter	72

List of Acronyms

ACRONYM	*MEANING*	*PAGE*
ADTLC	automatic decision threshold level control	65
ATC	automatic threshold control	66
CD	coincidence detection	10
CT	constant threshold	64
CDMA	code-division multiple-access	2
CSK	code-shift-keying	16
DS	direct sequence	2
ED	envelope detector/detection	17
FEC	forward error control	14
FH	frequency hopping	2
FDMA	frequency-division multiple-access	83
LIA	linear independent assumption	109
LS	least-squares	134
MAE	minimum asymptotic efficiency	111
MF	matched filter	7
OBO	one-by-one	138
PCN	personal communications network	2
PCS	personal communications service	1
PN	pseudo-noise	2

SAW	surface-acoustic-wave	7
SEC	simultaneous estimation and cancellation	141
SSMA	spread spectrum multiple-access	2
TDMA	time-division multiple-access	83
TL	two-level	14

Chapter 1

Introduction

1.1 Introduction

In the past few decades spread spectrum technology has been used for military communications, where it was attractive because of its capability of various interference resistance, secure communications and its capacity for high-resolution ranging. Just as spread spectrum signals are unlikely to be intercepted by a military opponent, so are they unlikely to interfere with other signals intended for commercial users - even ones transmitted on the same frequencies. Such an advantage opens up crowded frequency spectra to vastly expanded use. Two typical examples of commercial applications of spread spectrum are given by the Digital Cellular System of Qualcomm Inc. and the Broadband Personal Communications Systems (PCS) [55][38].

Spread spectrum is a kind of modulation and demodulation technique. With this technique, the conventional digital transceivers, such as PSK, DPSK, MSK transceivers etc, can be used to communicate digital information in channels where a variety of interference exist. As the name implies, spread spectrum technique converts digital signal into the transmission signal which has a bandwidth much greater than the minimum bandwidth required to transmit the digital information.

The two commonly used techniques for this conversion are direct sequence (DS) modulation and frequency hopping (FH) modulation . Both techniques spread the transmitted power over a wide frequency band so that the power per unit bandwidth (Watts pe. Hertz) is very small; then at the receiver the signal is compressed into its original narrow band - even while leaving the power of other (interfering) signals scattered over that same extremely wide transmission band.

Spread spectrum modulations can be used as a multiple-access scheme in which users share the same bandwidth without interfering with each other by using different codes or FH patterns. This is called code-division multiple-access (CDMA) or spread-spectrum multiple-access (SSMA) . Some specific CDMA systems are *Personal Communication Networks* (PCN) , *Digital Cellular Systems* (DCS) [38][55].

The key to success in spread spectrum operation is that the transmitted signal for a given user is "tagged" with a direct-sequence (pseud-noise (PN) code) or a frequency hopping pattern that only the designated receiver can recognize. The receiver knows in advance how the transmitter will spread the spectrum and acquires the signal and continues to track the transmitted pattern. The technique for acquiring and tracking the transmitted pattern is called synchronization.

The chapter is organized as follows. In sections 1.1.1 and 1.1.2, the principles of the frequency-hopping (FH) and direct sequence (DS) spread spectrum technologies are introduced. In section 1.1.3, some aspects of CDMA are discussed. In section 1.2, packet radio technique is presented. The importance of synchronization for spread spectrum systems is emphasized in section 1.3. Finally, an outline of the dissertation is given in section 1.4.

1.1.1 Frequency hopping spread spectrum

The type of spread spectrum in which the carrier hops randomly and rapidly under the control of a random sequence is called *frequency-hopping (FH) spread spec-*

trum. Typically, each carrier frequency is chosen from a set of 2^k frequencies which are spaced approximately the width of the data modulation spectrum apart. The spreading code in this case does not directly modulate the data-modulated carrier but is instead used to control the sequence of carrier frequencies. In the receiver, the frequency hopping is removed by mixing (down-converting) with a local oscillator signal which is hopping synchronously with the received signal.

When a FH system coexists with a few other conventional narrow-band users, the interference from the narrow-band users can be greatly reduced because the existing narrow-band users only occupy a small fraction of the total frequency slots available for the hopping. Therefore the FH system transmits data without interference most of the time. On the other hand, the conventional narrow-band users may encounter severe interference from the FH users. An example is shown in [38]. Therefore, FH spread spectrum may not be the best choice if the system is required to coexist with some other conventional communications systems.

1.1.2 Direct sequence spread spectrum

Direct sequence spread spectrum transmission spreads the spectrum by modulating (multiplying) the digital data bits with a pseudorandom sequence of very high chip rate. Because of the high rate of the sequence, the bandwidth after the modulation is much wider than the bandwidth of the original information.

A typical DS coherent PSK spread spectrum system is shown in figure 1.1. At the transmitter, the digital data bits $b(t)$ are modulated (multiplied) by a high rate PN code $c(t)$ and then up-converted to the transmission band. The signal is assumed to be added with narrow-band interference in the channel. At the receiver, the signal is compressed into its original narrow band while leaving the power of interfering signals scattered over the same extremely wide transmission band. The data bits are recovered by the conventional PSK demodulation. The process at

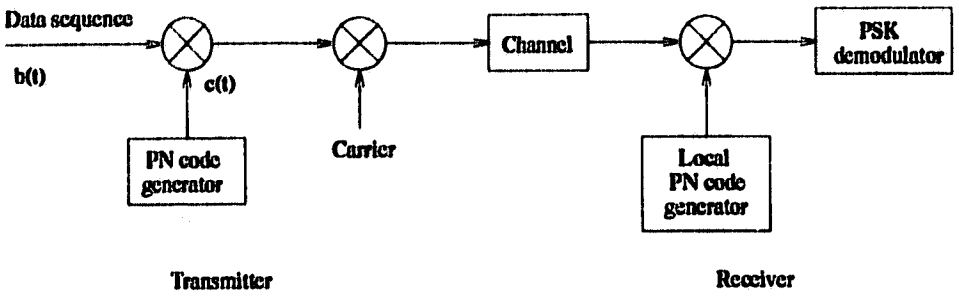

Figure 1.1: Direct sequence PSK spread spectrum transceiver

the receiver is usually called despreading. Because the despreading recovers the original signal energy while suppresses the interference, the signal to interference ratio after despreading is increased. The amount of the increase is called *processing gain* which is traditionally defined as the ratio of transmission bandwidth to digital data bandwidth.

The key to success in the despreading operation is that the receiver has the exactly same DS sequence (replica) as the transmitter has. In other words, only the given receiver can recognize this pattern. The receiver knows in advance how the transmitter will spread the spectrum and acquires (at the beginning of reception) the signal and continues to track the transmitted pattern.

1.1.3 Code-division-multiple-access

More recently, commercial applications of spread spectrum have attracted considerable attention. One useful form of applications is called code division multiple access (CDMA). A typical CDMA system is shown in figure 1.2 where coherent reception is assumed. In the CDMA system, a group of individual signals can be multiplexed onto a communication medium via a set of distinct sequences. Each of the sequences identifies a user. For example, if user 1 has a sequence c_1, and user 2 a sequence c_2, etc., then a receiver, desiring to listen to user 1 will receive at its antenna all of the

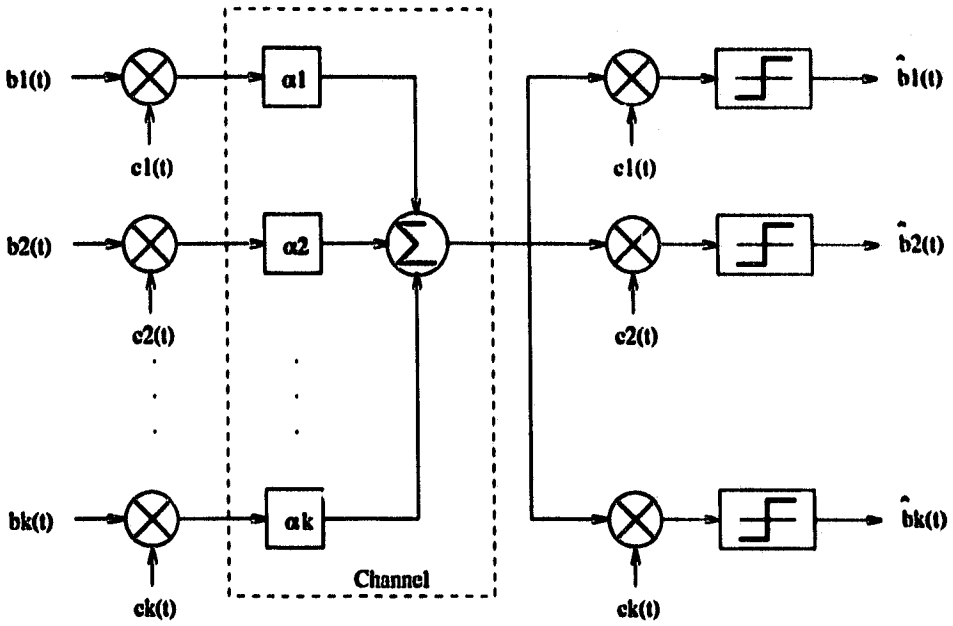

Figure 1.2: Conventional coherent CDMA signal detection

energy sent by all of the users. However, after despreading user 1's signal, it will see all the energy of user 1 and expect a small fraction of the energies sent by other users.

Typical applications of CDMA include personal communications service (PCS), cellular telephone, and wireless networks. In these systems spread spectrum is likely to be used to improve the performance in multipath, to make possible coexistence with the other systems, and to provide resistance to various interference. Several spread spectrum systems using CDMA have been described in [39][38][37] and [55]. The PCS system presented in [37] has demonstrated that DS spread spectrum users can share a frequency band with conventional microwave radio users without one group interfering with the other while achieving a good performance in fading channel.

The demodulators illustrated in figure 1.2 were referred to as the conventional single-user detectors [54]. Although this type of demodulators achieves the minimum

bit-error-rate in additive white Gaussian noise channel, it is no longer optimum in the multiple access channel. Its performance is only acceptable when the energies of the received signals are not too dissimilar and the PN codes are relatively long compared to the number of users in the system, i.e., in low bandwidth efficiency situations. If the received signal energies are indeed dissimilar, i.e., some users are very weak in comparison to others, then the demodulators are not able to recover the weak signals reliably, even in low power bandwidth efficiency situations. This is known as the *near-far* effects and is the main shortcoming of currently operational CDMA systems.

Power control technology is currently applied to remedy the near-far problem. However such a strategy may be self-defeating [54] [51] because it may dictate a significant reduction in most transmitter powers to accommodate the weakest transmitter, thereby diminishing the multiple access capability of the overall system.

A complete solution to the near-far problem relies on the development of cost-effective multi-user detectors. A lot of work has been done by Verdu, Lupas, Varanasi and Aazhang [52][53][25][26] [49][50]. Verdu and Lupas focused on the development of linear type multi-user detectors which do not require the energy information of users. Varanasi and Aazhang studied non-linear type multi-user detectors which can achieve better performance than the linear ones provided that the energy information is known. In addition, the computation complexity is still linear with the number of users.

1.2 Packet radio

Packet radio is a technology that extends the application of packet switching which evolved for networks of point-to-point communication lines to the domain of broadcast radio. It offers a highly efficient way of using a multiple access radio channel

with a potentially large number of mobile subscribers to support computer communication and to provide local distribution of information over a wide geographic area.

In a packet-switched network, the unit of transmission is called a packet. It contains a number of data bits, and is usually of variable length up to a maximum of a few thousand bits. Packet switching was originally designed to provide efficient network communications for "bursty" traffic and to facilitate computer network resource sharing. It is well known that the computer traffic generated by a given user is characterized by a very low duty cycle in which a short burst of data is sent or received followed by a longer quiescent interval after which additional traffic will again be present.

The rapid development in packet radio technology has been greatly stimulated by the need to provide computer network access to mobile terminals and computer communications in the mobile environment.

Spread spectrum technology is often applied in packet radio systems to provide the capability of reducing intersymbol interference, to improve performance in multipath fading channel and to make possible for CDMA communications, i.e., allowing various groups of users to coexist in the same area.

The signal processing of spread spectrum packet radio systems is based on matched filters (MF) such as charged-coupled-devices (CCD), digital matched filters and surface-acoustic-wave (SAW) convolvers. Among them, SAW convolver is probably the most attractive one because of its large time-bandwidth product and programmability. A sufficient processing gain may be obtained by the time-bandwidth product. However, in some cases where even larger processing gain is needed, a hybrid correlator technique can be applied [10]. The programmability allows the transmitting signal to be changed. Thus, each data bit can have a new PN code. For the high data rates on the order of 1 Mbits/s or higher, this could help

ease the suffering from intersymbol interference in typical broadcast environments.

More detailed design issues of SS packet radio are given in [10] and the papers therein. A complete tutorial about packet radio is given in [16].

1.3 Synchronization for spread spectrum

One may have noticed from the previous description of spread spectrum technology that those attractive benefits of spread spectrum can only be obtained under the vital condition of the alignment of phases/frequencies between the received spreading pattern and receiver pattern. At the beginning of signal reception, the difference between these two phases/frequencies is a random variable which mainly corresponds to the propagation delay. Since typical spreading waveform period is quite long and bandwidth is large, the uncertainty in the estimated propagation delay translates into a large number of symbols of code phase uncertainty. Synchronization is a method to reduce the uncertainty until the two sequences are in alignment. Synchronization for spread spectrum basically consists of two steps. The first step is called acquisition which brings the difference of the two sequences to within an uncertainty unit (usually called a cell). At the same time, the SNR at the output of the receiver detector is large enough to do further synchronization adjustment. The second step is called fine synchronization which brings the difference to within a small fraction of an uncertainty unit. In this thesis, we will consider the acquisition.

1.3.1 Synchronizations for systems with non-limited permitted synchronization time

In such a system, communication can be assumed to be in operation forever. There is no time limit on the synchronization procedure. Theoretically, synchronization time could be any value from 0 to ∞ seconds. The objective of synchronization is

to reduce the average synchronization time as efficiently as possible. To judge the performance of an acquisition system, one needs to calculate the average acquisition time and its variance. Intuitively, the acquisition time will increase as the uncertainty region increases and SNR decreases. There are a lot of acquisition methods available. Among them, the serial search method is probably the earliest and most commonly one used for military spread spectrum systems. The method includes single dwell search and multiple dwell search which have been generalized by the unified method in [31]. Other acquisition schemes include sequential estimation [56][34] and sequential detection [5][4][44]. Each method has its own particular application case and to some extend reduces the acquisition time or simplifies the system complexity. There is no versatile method existing for all kinds of applications. An optimum synchronizer can be defined to be a synchronizer which can achieve synchronization with a given probability in the minimum possible time [60].

The analysis of acquisition consists of two parts. First, the model of the acquisition process must be established. For different methods, different models (usually represented by signal flow graphs) can be employed. Using the technique of signal flow graph or Markov chain, the characteristics of time and frequency domain of acquisition time can be obtained. The second part is to calculate the probabilities of detection and false alarm at each decision moment. The exact calculations sometimes are not easy for most of the receiver constructions, and approximated results are often obtained.

1.3.2 Synchronizations for systems with limited permitted synchronization time

Until now, few papers gave a complete analysis for the synchronization of spread spectrum packet radio systems. For this kind of system which has a limited synchronization time, the optimum synchronizer defined before is no longer appropriate.

Nh Bits For Acquisition	Ns Bits For Frame Sync	LD Data Bits

Figure 1.3: Packet structure

A new optimal synchronizer needs to be defined. From the structure of a packet in figure 1.3, we see that a packet is mainly composed by two portions. The first portion, the head of a packet, is called *preamble* which is used mainly for synchronization. The other portion is the text/data of the packet. It is obvious that the correct reception of a packet is dependent upon acquisition of the preamble as well as correct decision for each data bit. Since the presence of interference or noise, the operation of synchronization in the preamble can not be perfect. In other words, synchronization may fail so that the whole packet is lost. The minimum packet loss synchronizer may be defined as an optimal synchronizer to minimize the probability of packet loss by synchronization failure given the length of the preamble.

Some of the fast acquisition schemes which use matched filtering technique can be adopted for packet radio with the attention focusing on the minimization of probability of packet loss due to synchronization failure. The basic idea is to use a passive correlator (matched filter) to correlate with the received sequence and find the most likely correlation peak as the synchronization phase. The selected phase is then verified by the followed *coincidence detection* (CD) which is usually based on majority logic algorithm [32]. Acquisition schemes using matched filters for packet radio were presented in [22][23] [43]. More complicated schemes based on SAW matched filters can be found in [28][12].

1.4 Dissertation outline

In chapters 2 and 3, an acquisition scheme based on multiple acquisition prefixes are analyzed for linear and hardlimiting matched filters, respectively. The scheme is similar to the two-level scheme in [35][58], but with much simpler receiver construction because it does not need any active correlators for the coincidence detection. Besides, the scheme will be shown to has better performance than the single prefix scheme. The *masking effect* caused by false alarms at high SNR will be diminished by a two-level threshold decision scheme in the linear matched filter and can be totally eliminated by the hardlimiter.

In chapter 4, an automatic threshold control scheme is proposed and analyzed to reject the masking effect and thus increase the dynamic range of the received signal. This scheme will be shown to be most appropriate for sequence acquisitions in a CDMA system because the effective SNR for a specific user fluctuates according to the number of active users in the system.

Starting from chapter 5, we introduce some basic concepts for optimum and sub-optimum multi-user detection. A new non-linear multistage multi-user detector is proposed in chapter 5. The method will be shown to outperform other detection methods for CDMA signals. The comparison of existing multi-user detection schemes for asynchronous CDMA is addressed in chapter 6.

With the knowledge introduced in chapters 5 and 6, it will be easier to understand the acquisition scheme for CDMA signals based on interference cancellation technique presented in chapter 7. Since any multi-user detection requires the knowledge of signature sequences of all users in the CDMA system, the acquisition for these sequences becomes the most important task. The difficulty is that the near-far effect cannot be avoided during acquisition, although it can be alleviated by our method. Acquisition process in such a system involves more signal processing computations than those in other conventional systems, which may result in some delay

for the signal receptions. For packet radio, each packet can be temporally stored in buffers, the induced delay by acquisition does not cause too much performance degradation. However, searching for efficient acquisition algorithms to achieve the near-real-time communication is still a challenging topic.

Chapter 2

Acquisition Using Linear Matched Filter

2.1 Introduction

Direct sequence spread spectrum systems operating in burst or packet mode transmit user data in packets of a few thousand bits where each packet begins with a short synchronization preamble. Such burst or 'push-to-talk' techniques are commonly used in tactical military communications as well as indoor wireless computer communications [34][29]. Thus for receivers which use matched filters like SAW devices spanning one PN code period, only a finite number L PN code periods in the preamble are available at the beginning of a burst for PN acquisition and to determine the start of user data. Because synchronization must be achieved during the limited time of the preamble, one measure of system performance is the probability of not achieving synchronization within this limited permitted time, i.e. missing the packet. However, packets may be also lost because a false alarm in noise can cause the receiver to be busy, and thus unavailable (blocked) when the packet arrives. Thus the overall system performance is characterized by the probability of packet

loss caused by either failed synchronization (missed packet) or receiver blocking.

For maximum information throughput, a tradeoff is made between the probability of successful synchronization and the overhead time needed for synchronization. Thus the length L of the preamble which yields maximum throughput will depend on the number of information symbols in each data burst and the symbol error rate [45].

One previous scheme requires code acquisition at the first PN code period, followed by coincidence detection (verification) on the remaining $L-1$ PN code periods [29]. For any particular choice of acquisition threshold and corresponding false alarm rate, the matched filter may not be long enough for reliable acquisition at low SNR, although the message with forward-error-correction (FEC) could be decoded successfully. Therefore, most of the packet losses may be caused by synchronizations failure.

The two-level code acquisition (TL) scheme presented by Rappaport and Wilson [35][58] may be used to improve the performance of synchronization to burst mode communication. The reliable sync is guaranteed by the use of several active correlators following one or more fast (short) acquisition matched filters. In the scheme, the detection threshold can be set to be reasonably low for reliable detection in low SNR, because most of the "false-start" signals may be dismissed by a number of long active correlators. However, this method needs a long preamble relative to the message length, thus it may not be suitable for packet-switch communication. Furthermore, the hardware complexity may impose an upper limits to the number of correlators in a receiver.

Logically thinking, for the same length of the preamble, we can have fewer PN codes with longer code period. Thus the corresponding matched filter will be longer. The detection performance will be better than that by using shorter codes. However, the tradeoff with L is usually made according to the possible size of the matched

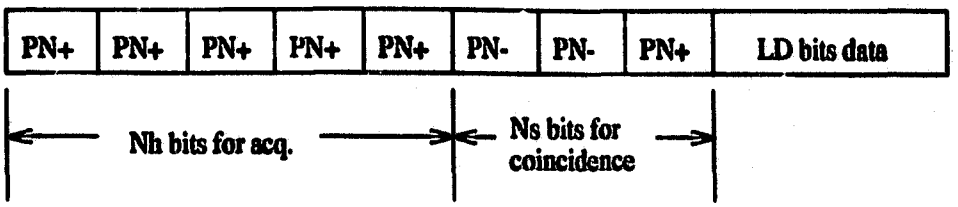

Figure 2.1: Packet format for the proposed acquisition scheme

filter being used. As a matter of fact, since longer matched filters are difficult to be built, the above two-level scheme has been considered.

The comparisons given at the end of the chapter show that the proposed scheme in this chapter yields much better performance than the scheme of [29], and is better than or equivalent to that of the scheme of [35][58] with comparable receiver complexity. We have found that the performance of the TL scheme of [35][58] can not be significantly improved by increasing the number of active correlators. This is due to the fact that increasing the active correlators means that one can make the acquisition threshold lower to reduce the possibility of missing signals. But on the other hand, the lower threshold may bring too many false acquisitions which the active correlators cannot handle. The maximum amount of improvement over the proposed scheme is limited by this method. In addition, the new scheme has a much simpler receiver structure

The chapter is organized as follows. In section 2.2, the acquisition technique is described. The performance analysis is carried out in section 2.3, followed by numerical results and the appropriate comparisons of the proposed scheme with the other schemes in section 2.4 and summary in section 2.5.

2.2 Acquisition technique

In this section, a new construction of preamble is proposed for fast acquisition. The designed preamble is mainly used for enhancing the acquisition reliability. Accord-

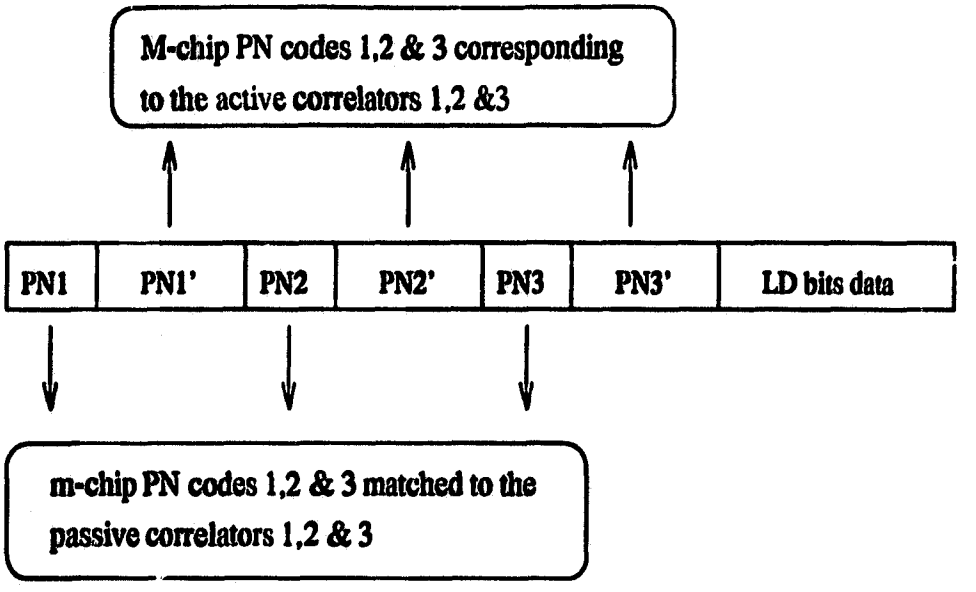

Figure 2.2: Packet format for the two-level acquisition scheme

ingly, the acquisition process is presented.

Figure 2.1 shows the data format used by the proposed technique for a preamble with length of $L = 8$ PN code periods. This preamble is divided into two portions. The first one consists of N_h unmodulated PN code periods, while the second portion is made up of N_s PN codes modulated by a marker. In the above example, $N_h = 5$ and $N_s = 3$. We assume one data bit per PN code period, so that the preamble consists of the data string 11111001. For comparison, figure 2.2 illustrates the preamble data format for the TL method of [35][58]. It is assumed that the length of the preamble of the TL method is the same as that of the proposed method. In addition, same passive correlators or matched filters are used for the two schemes. The length of the active correlators for the TL scheme will depend on the number of prefixes in the preamble. The more the prefixes, the shorter the length of the active correlators.

Figure 2.3 shows a simplified code-shift-keying (CSK) receiver structure. A band-pass filter eliminates out-of-band noise. The noncoherent matched filters (MF) are

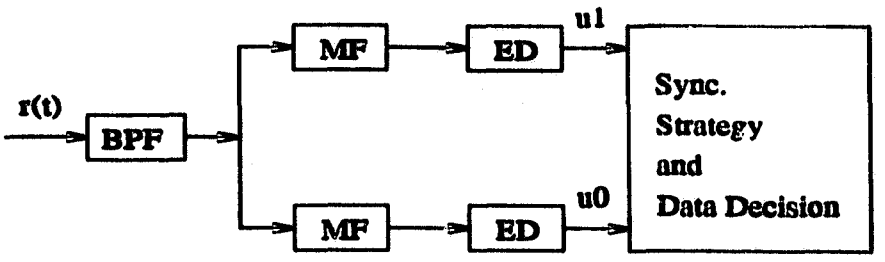

Figure 2.3: Simplified CSK receiver

designed to match two orthogonal PN codes corresponding to ones and zeros, and are followed by envelope detectors (ED) with a detection threshold. After synchronization is achieved, bit decisions are made by comparing the two ED outputs and selecting the larger output.

The receiver operates by searching the incoming data stream for synchronization in two steps: initial acquisition (correlation detection) and coincidence detection (frame synchronization).

Initial acquisition is achieved when the MF output $y(t)$ exceeds the threshold b_0 . This may occur in any one of the N_h PN code periods in the preamble, not necessarily the first one. When this first step is complete, the receiver sets the threshold to a new value b_1 and samples the MF output once per code period. The coincidence detection is achieved when the current data symbol $\hat{a}\epsilon\{-1, 1, erasure\}$ plus the previous $N_s - 1$ symbols match the N_s symbol marker within a specified symbol error and erasure tolerance. Since it is not known a priori at which point in the N_h preamble symbols acquisition occurred, the marker search (symbol-wise correlation) is performed in successive positions of the marker until a match is found or N_h positions have been tested. If no match is found, then the receiver resumes the search for initial acquisition. If a match is found, then the receiver starts to process the L_D symbols of user data.

The marker of length N_s is chosen to be a sequence with minimum correlation

sidelobes when preceded by the N_h '1' symbols in the preamble, while also preserving minimum sidelobes when preceded by random data or noise. The optimum marker sequences for selected values of N_s are determined in [7].

The advantage of this acquisition scheme for packet radio is that successful acquisition can be achieved even if several PN sequences are missed due to noise, thus increasing the synchronization reliability at low SNR. The technique in [29] is a special case where $N_h = 1$, so that if the receiver does not achieve acquisition in the first PN code period, then the packet is missed.

2.3 Performance analysis

In this section, the synchronization performance of the proposed rapid acquisition technique is analyzed in terms of the probability P_L of packet loss versus SNR. The system parameters which determine P_L are the PN sequence length $m, N_h, N_s, L_D, b_0, b_1$ and the symbol error tolerance in the marker. An expression for P_L is determined and each component of this expression is evaluated in terms of the system parameters. This is followed by consideration of threshold selection and the use of two-level threshold.

2.3.1 Preliminaries

A binary code shift keying (CSK) direct-sequence spread-spectrum system is briefly reviewed to establish notation. The received signal at the output of the bandpass filter is

$$r(t) = [\sum_k A a_{i_k}(t - \tau - kT) + n_I]\cos\omega_0 t - n_Q \sin\omega_0 t \qquad i_k = 0, 1 \quad (2.1)$$

where A is the amplitude of the signal, and $a_0(t)$, $a_1(t)$ are assumed to be orthogonal spreading sequences time-limited to $[0, T]$ which represent ones and zeros of the

binary message. n_I and n_Q are the in-phase and quadrature components of the white Gaussian noise with two sided power spectral density $N_0/2$. The noise power at the output of the bandpass filter is $\sigma^2 = N_0/T_c$. The sampling rate at the output of the matched filter is $1/T_c$. Let m be the total number of chips in a PN code period, we have $T = mT_c$. m will determine the processing gain of the spread spectrum system and is often from 30 to 500.

Consider the acquisition procedure in which the detector observes $a_1(t)$ over a period $0 \leq t \leq N_h T$. The test statistic at the output of the matched filters is

$$y(t) = \{AN\rho(t) + n_I'\}\cos\omega_0 t - n_Q' \sin\omega_0 t \tag{2.2}$$

where n_I', n_Q' in (2.2) are filtered noise, and

$$\rho(t) \equiv \begin{cases} \frac{1}{T}\int_0^t a_1(\tau)a_1(t-\tau)d\tau & t < T \\ \frac{1}{T}\int_0^T a_1(\tau)a_1(t-\tau)d\tau & t \geq T \end{cases} \tag{2.3}$$

is the normalized autocorrelation function of the PN sequence $a_1(t)$ and is usually not negligible since the PN codes are not m-sequences or orthogonal sequences. The upper equation in (2.3) corresponds to the partial correlation when the first PN code period of the preamble has not yet come into the matched filter completely, i.e. only a fraction of the first bit (PN period) is in the matched filter. The lower one corresponds to the whole period autocorrelation after the first whole PN period has come into the matched filter.

Assuming that the receiver has no knowledge of the amplitude A of the received signal, we select the threshold of the acquisition for an acceptable probability of false alarm P_{fan} caused by the noise alone. From [57], the output of the envelope detector is according to the Rayleigh distribution when no signal is present. Accordingly, the probability of false alarm is

$$P_{fan} = \exp(-\frac{b_0^2}{2}), \tag{2.4}$$

where b_0 is the acquisition threshold normalized to σ. Also from [57], the output of the envelope detector is according to the Rician distribution when signal plus noise is present. Thus the probability of initial acquisition in the correct position ($\rho(iT) = 1$, $i = 1, 2, ..., N_h$) is given by

$$P_d = Q(\sqrt{2\gamma_o}, b_0), \tag{2.5}$$

where $\gamma_o = m\gamma_i = m \cdot A^2/2\sigma^2 = m\frac{E_c}{N_0}$ (E_c is chip energy) is the SNR at the output of the MF, and $Q(a, b)$ is the Marcum-Q function.

The probability of false initial acquisition at an incorrect position where $\rho(t) < 1$ can be written

$$P_{fd}(n) = Q(\sqrt{2\gamma_o\rho^2(nT_c)}, b_0), \quad n = 1, ..., N_h m. \tag{2.6}$$

In [32], it was shown that the test samples at positions $n = 1, 2, ..., N_h m$ are mutually independent if the PN sequence is long enough.

2.3.2 Calculation of performance

To detect signals at low SNR, the acquisition threshold is set to be as low as possible. But lower threshold will cause more frequent false acquisitions which may result in many packets to be blocked. An appropriate threshold may be set based on an acceptable blocking rate.

From [29], the probability P_L of packet loss may be approximated by

$$P_L = 1 - (1 - P_B)P_{syn}(0) \tag{2.7}$$

where P_B is the probability of receiver blocking due to false alarms, and $P_{syn}(0)$ is the probability of successful synchronization provided that the receiver is not

blocked and the synchronization search starts from the first chip of the preamble. $P_{syn}(0)$ will depend on the parameter N_h and the threshold b_0. P_B is estimated as $\bar{B}/(\bar{I}+\bar{B})$, where $\bar{B}$ is the average blocking time and $\bar{I}$ is the average idle time between two consecutive false alarms.

This approximation assumes that if the receiver is blocked at the time of packet arrival, then the packet is irretrievably lost. However, if the blocking period ends at some point during the preamble of an arrived packet, then the receiver can resume the search for acquisition, and that packet may still be received correctly.

To show how an incoming packet is captured and blocked/missed by a receiver, we characterize the receiver into two states when no signal is present. This is shown in figure 2.4. One is called silent or idle state (I) in which the receiver is ready for capturing a new packet (real or false). Another one is called blocking or busy state (B) in which the receiver is busy in detecting (either coincidence or data demodulation) a non-existing packet. We assume that any busy period is only caused by false acquisitions. This is equivalent to saying that the arrival rate is low enough such that no more than two packets overlap. There are two cases for a real packet to be captured. The first one is when the packet falls into a silent interval, which is illustrated in figure 2.4-b. And the sync is obtained successfully under the above condition. The second one happens when it falls in a blocking interval which ends before the last PN chip in the preamble comes into the matched filter. This is shown in figures 2.4-c, 2.4-d and 2.4-e. Up to $N_h m - 1$ correlation peaks may be lost due to the blocking, but synchronization is still possible. If it is achieved, the packet is captured. A precise approach to obtain P_L is given in appendix A by using queuing theory. However, a more straightforward analysis is described as follows.

From section 2.2, we see that the receiver will be busy for $T_1 = (N_h + N_s - 1)T$ after a false acquisition if no false coincidence occurs. If a false coincidence occurs, the receiver will be unavailable for $T_2 = T_R + T_D$ which is the time period equal

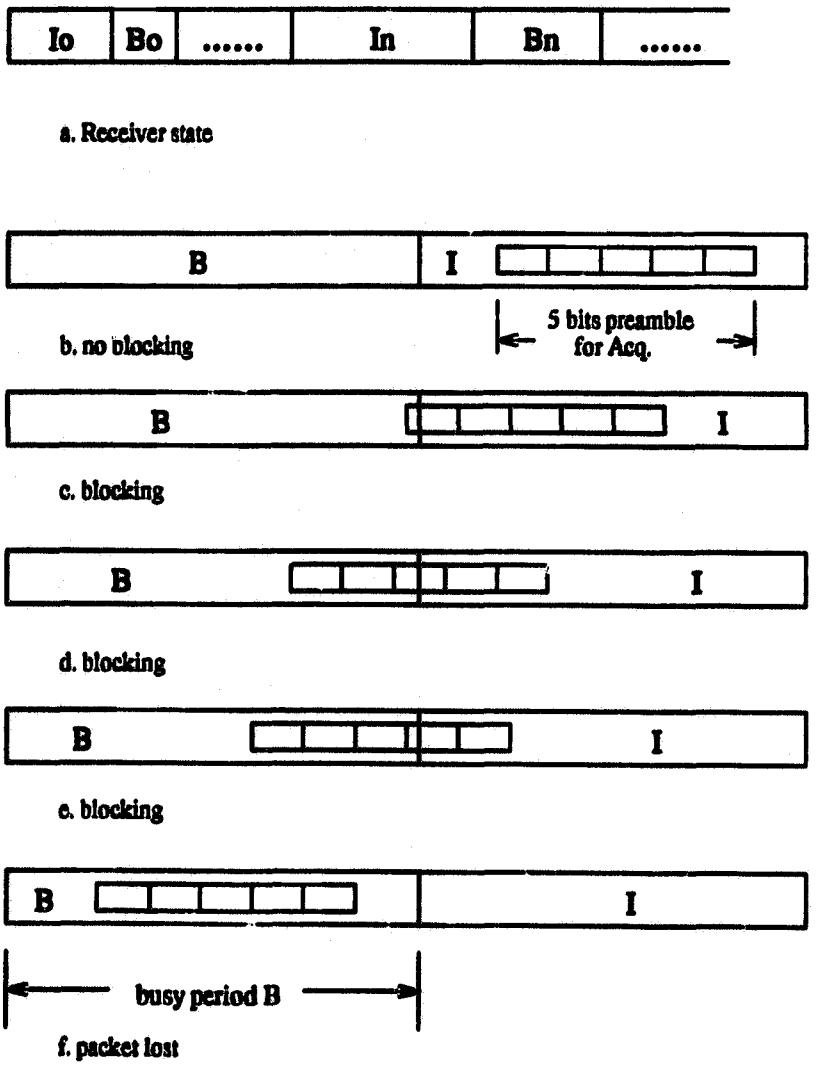

Figure 2.4: State diagram of receiver.

to the length of a packet, where $T_D = L_D T$ is the data length. T_R ($T \leq T_R \leq (N_h + N_s - 1)$T) is a random variable which depends on which of the $(N_h - 1)$ coincidence positions is detected. Thus the blocking time is at least T_1. The average blocking time $\bar{B}$ can be determined from

$$\begin{aligned} \bar{B} &= (1 - P_{fcn})T_1 + P_{fcn}T_2 \\ &= (N_h + N_s - 1)T + P_{fcn}[T_R - (N_h + Ns - 1)T + T_D] \end{aligned} \tag{2.8}$$

P_{fcn} is the probability of false coincidence in noise. Since $T_D >> T_R, N_h T$ and $N_s T$, we may have

$$\bar{B} \approx (N_h + N_s - 1)T + P_{fcn}T_D \tag{2.9}$$

The false acquisition in noise is modeled as a Poisson process with arrival rate $\lambda_f = P_{fan}/T_c$, where $1/T_c$ is the sampling rate or chip rate. Since the inter-arrival times of a Poisson process are identical-independent-distributed (i.i.d.) exponential, the average silent time can be obtained from

$$\bar{I} = 1/\lambda_f \tag{2.10}$$

Denote D as the event that the current packet is at least one-chip overlapped with a blocking interval. For the given average blocking time $\bar{B}$ and silent time $\bar{I}$, the probability that D occurs is

$$P(D) = \frac{\bar{B}}{(\bar{I} + \bar{B})} \tag{2.11}$$

Once D occurs, synchronization is still possible if less than $N_h m$ chips in the preamble are blocked/lost. Let k ($k = 1, 2, ..., N_h m - 1$) be the number of chips blocked by false acquisition, and the corresponding conditional probability $P(k|D)$ is approximately $T_c/\bar{B}$. Here we assume that the location distribution of the blocked preamble in the average blocking period $\bar{B}$ is uniform. Denote $P_{syn}(k)$ as the probability of

successful synchronization when k chips are blocked, the probability of sync when D happens can be written

$$\begin{aligned} P_{syn}(D) &= P(D)\sum_{k=1}^{N_h m-1} P(k|D)P_{syn}(k) \\ &= \frac{T_c}{\bar{I}+\bar{B}}\sum_{k=1}^{N_h m-1} P_{syn}(k) \\ &= \frac{P_{fan}}{1+\alpha}\sum_{k=1}^{N_h m-1} P_{syn}(k) \end{aligned} \tag{2.12}$$

where

$$\begin{aligned} \alpha &= \bar{B}/\bar{I} \\ &\approx P_{fan}(N_h + N_s - 1 + P_{fcn}L_D)m \end{aligned} \tag{2.13}$$

The probability $P(\bar{D})$ that no blocking occurs when a preamble comes into the receiver is

$$\begin{aligned} P(\bar{D}) &= \frac{\bar{I}}{\bar{I}+\bar{B}} \\ &= \frac{1}{1+\alpha} \end{aligned} \tag{2.14}$$

When this is the case, all the $N_h m$ chips are available for the sync, i.e. no chips are lost. Let $P_{syn}(0)$ denote the successful sync when no chips are lost, and the probability of sync when $\bar{D}$ happens is

$$P_{syn}(\bar{D}) = P(\bar{D})P_{syn}(0) \tag{2.15}$$

The total sync probability is

$$\begin{aligned} P_{syn} &= P_{syn}(\bar{D}) + P_{syn}(D) \\ &= \frac{1}{1+\alpha}P_{syn}(0) + \frac{P_{fan}}{1+\alpha}\sum_{k=1}^{N_h m-1} P_{syn}(k) \end{aligned} \tag{2.16}$$

Note that the successful sync probability $(1-P_B)P_{syn}(0)$ given in the approximation (2.7) corresponds to the first term in (2.16).

$P_{syn}(k)$ can be calculated from

$$P_{syn}(k) = \sum_{i=\lfloor \frac{k}{m} \rfloor + 1}^{N_h} P_{acq}(i,k) \cdot P_c(i) \tag{2.17}$$

where $P_{acq}(i,k)$ is the probability of acquisition in the ith PN period ($1 \leq i \leq N_h$) given k chips lost ($0 \leq k \leq mN_h - 1$). $P_c(i)$ is the probability of coincidence when the acquisition occurs in the ith PN period.

The probability P_L of packet loss is

$$P_L = 1 - P_{syn} \tag{2.18}$$

To determine P_L, it remains to evaluate $P_{acq}(i,k)$, $P_c(i)$ and P_{fcn}.

Probability of initial acquisition $P_{acq}(i,k)$

It is clear that the acquisition search starts from the $(k+1)$th ($k = 0, 1, ..., N_h m - 1$) correlation peak because k chips are lost. Figure 2.5 shows the signal flow graph of the acquisition process. From this flow graph, $P_{acq}(i,k)$ can be easily calculated with the initial condition $k+1$

$$\begin{aligned} P_{acq}(i,k) &= \prod_{j=k+1}^{im-1} (1 - P_{fd}(j))(1 - P_d)^{i-i_o} P_d, \\ & \quad j \neq m, 2m, ..., (i-1)m \end{aligned} \tag{2.19}$$

where $N_h \geq i \geq i_o$, and $i_o = \lfloor \frac{k}{m} \rfloor$.

Probability of coincidence detection

To calculate the second term $P_c(i)$ in (2.17), we note that the coincidence test is carried out in up to N_h positions of the marker. The probability of successful coincidence detection $P_c(i)$ will depend on the probability of a false marker detection when testing at an incorrect position before the correct position is reached, as well as on the probability of a successful marker test when testing in the correct position.

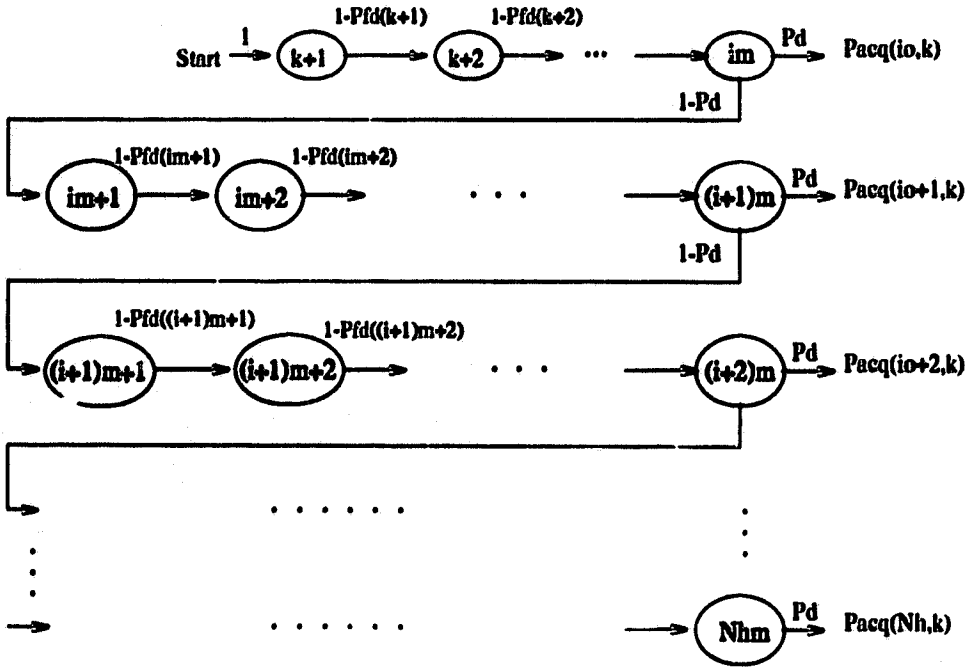

Figure 2.5: Signal flow graph of the acquisition process

The number of incorrect positions tested, and thus the probability of false marker detection, will depend on the particular PN code period i in the preamble at which the search for the marker begins.

The probability $P(h_e, h_x, \tilde{n})$ of marker detection in a particular position depends on the specific choice of marker, the amount of overlap $\tilde{n}$, the error tolerance h_e and the erasure tolerance h_x between the observed marker bits and the known or expected marker bits. The overlap $\tilde{n}$ is defined to be N_s when there is complete overlap (i.e. correct position) and may be 0 or negative if there is no overlap. The disagreements $\tilde{h}_0(\tilde{n})$ or the Hamming distance between the replica marker and the under-detected N_s bits in the absence of error is known for all $\tilde{n} > N_s - N_h$. $P(h_e, h_x, \tilde{n})$ is evaluated in [8] and reproduced here for convenience

$$
\begin{aligned}
& P(h_e, h_x, \tilde{n}) \\
= \; & \text{Prob } (h_e \text{ or fewer disagreements and } h_x \text{ or fewer erasure} \\
& \text{with overlap } \tilde{n}) \\
= & \sum_{j=0}^{h_e} \sum_{k=0}^{\min(h_x, N_s-j)} \sum_{\tilde{m}=\max(0,\, k-\tilde{h}_0(\tilde{n}))}^{\min(k, N_s-\tilde{h}_0(\tilde{n}))} \sum_{\ell=\max(0, j-\tilde{h}_0(\tilde{n})+k-\tilde{m})}^{\min(j,\, N_s-\tilde{h}_0(\tilde{n})-\tilde{m})} \\
& \binom{N_s - \tilde{h}_0(\tilde{n})}{\ell, \tilde{m}} q^{N_s-\tilde{h}_0(\tilde{n})-\ell-\tilde{m}} \; p^{\ell} \; s^{\tilde{m}} \\
& \times \binom{\tilde{h}_0(\tilde{n})}{j-\ell,\; k-\tilde{m}} q^{j-\ell} \; p^{\tilde{h}_0(\tilde{n})-j+\ell-k+\tilde{m}} \; s^{k-\tilde{m}}, \qquad (2.20)
\end{aligned}
$$

$$
\text{where } \binom{\tilde{h}_0(\tilde{n})}{\ell,\; \tilde{m}} = \frac{\tilde{h}_0(\tilde{n})!}{\ell!\tilde{m}!(\tilde{h}_0(\tilde{n}) - \ell - \tilde{m})!}. \qquad (2.21)
$$

where symbol detection probability q , error probability p and erasure probability s for noncoherent CSK receiver are derived in appendix B.

Following [8][41], $P_c(i)$ can be calculated from

$$\begin{aligned} P_c(i) &= Pr\{\text{No detection occurred at } \tilde{n} \neq N_s\} \\ &\quad \cdot Pr\{\text{Detection at } \tilde{n} = N_s \mid \text{no detection occurred at } \tilde{n} \neq N_s\} \\ &= [1 - Pr\{\text{At least one detection occurred at } \tilde{n} \neq N_s\}] \\ &\quad \cdot Pr\{\text{Detection at } \tilde{n} = N_s \mid \text{no detection occurred at } \tilde{n} \neq N_s\} \end{aligned} \tag{2.22}$$

A lower bound on $P_c(i)$ may be written

$$P_c(i) \geq [1 - \sum_{\tilde{n}=N_s+i-N_h}^{N_s-1} P(h_e, h_x, \tilde{n})] \cdot P(h_e, h_x, N_s) \tag{2.23}$$

Probability of false coincidence P_{fcn}

The probability of false coincidence in noise is written

$$\begin{aligned} P_{fcn} &= Pr\{\text{at least one false marker detection occurs} \\ &\quad \text{in noise during } N_h \text{ marker tests}\} \\ &\leq N_h Pr\{\text{one test succeeds}\} \\ &= N_h P_{fn} \end{aligned} \tag{2.24}$$

Define $\{q_n, s_n, p_n\}$ as the probabilities of decisions {+, erasure, -} in noise alone, P_{fn} can be calculated from

$$P_{fn} = \sum_{j=0}^{h_e} \sum_{k=0}^{\min(h_x, N_s-j)} \binom{N_s}{k,\ j} p_n^j\ s_n^k\ q_n^{N_s-j-k}. \tag{2.25}$$

The calculations of q_n, p_n and s_n are also given in appendix B.

2.3.3 Threshold selection for desired performance characteristics

From (2.16) and (2.18), since $P_{syn}(k) \leq 1$ for $k = 0, 1, ..., N_h m - 1$, P_L can never be less than

$$P_L(min) = 1 - \frac{1}{1+\alpha} - \frac{P_{fan}}{1+\alpha}(N_h m - 1) \tag{2.26}$$

This probability can be taken as the packet blocking probability P_B, i.e., $P_B = P_L(min)$. Thus the system designer can select a desired $P_L(min) \ll 1$ by an appropriate choice of b_0 and b_1. Typical values of $P_L(min)$ may be in the range 10^{-3} to 10^{-6}.

2.3.4 Two-level threshold for initial acquisition

At high SNR, correlation sidelobes of the first PN sequence may cause false acquisition at an incorrect position prior to the correct position because the threshold b_0 is determined independent of the received signal power. [1] Thus P_L will have a minimum value at some SNR, and will increase for higher as well as lower values of SNR. This effect has been observed for $N_h = 1$ in [29], and was called the *masking effect* in [11].

One technique to eliminate this effect is to use the hardlimiting receiver presented in [1] with the cost of some degradation in performance in low SNR for AWGN channel. Another choice is to construct a maximum likelihood receiver which can compare all the samples in a whole period of PN correlations and pick up the largest one as the main correlation peak. A simple way is to apply the two-level

[1] Automatic gain control (AGC) schemes are not used in the system because the SNR before the despreading is usually low so that the AGC may not work fine. Besides, if we consider a CDMA system, the estimated energy may not represent the real signal's energy due to other users interference.

threshold [29] to the present case. The priority in the sync decision is given to the higher level. Whenever an acquisition detection by a decision device with the lower threshold level b_0 is followed by the crossing of a higher threshold $b_{0h} = b_0 + \Delta$, within one PN period, the latter is taken for the correct sync detection [29]. By this method, enough dynamic range may be obtained. In appendix C, the computation of $P_{acq}(i,k)$ for the two-level threshold is completed by using the technique of signal flow graph.

2.4 Numerical results

In this sec. .1, the performance of the receiver is illustrated for $L = 8$ and $L_D = 1000$ with 255 Kasami sequence as the PN code. b_0 and b_1 are selected to get the required $P_L(min)$. The optimal pair of b_0 and b_1 is obtained by maximizing the dynamic range of P_L at low SNR. Performance comparison with the TL acquisition method is made at low SNR.

For $L = 8$, figure 2.6 shows P_L versus SNR for different N_h and N_s, respectively. The two-level threshold method of [29] is used with $\Delta = 4$ dB. For each value of N_h, h_e and h_x are selected for the widest dynamic range. The best overall performance is obtained with $(N_h, N_s) = (5,3)$. From these curves, we can see that almost 3 dB improvement can be achieved at low SNR compared to the method of [29] where $(N_h, N_s) = (1,7)$, with only a slight reduction at high SNR.

Figure 2.7 shows P_L versus SNR with thresholds chosen to obtain $P_L(min) = 10^{-3}$ to 10^{-6} and parameters $(N_h, N_s) = (5,3)$ and (1,7). Lower values of $P_L(min)$ are obtained by raising the threshold b_0 and accepting a slight reduction in performance at low SNR. The amount of improvement at low SNR obtained with the proposed sync technique is essentially independent of the choice of $P_L(min)$.

Performance comparisons between the proposed acquisition scheme and the TL

acquisition scheme [35][58] are made in the case of low SNR where the effect of correlation sidelobes can be ignored. In this situation the average rate of false code start signals when a packet comes is the same as that when no signals show up. The analysis for high SNR will be difficult for the TL scheme because the false code start rate when a packet is present will be different from that when a packet is absent.

All the comparisons are made under the assumption that the two schemes use the preamble of the same length and the same matched filter which processes 255 PN chips. Thus we have $(N_h + N_s)m = N_{pc}(m + M)$, where N_{pc} is the number of prefixes in the preamble for the TL scheme. The optimal sync performance of the proposed scheme for a given preamble length is obtained by appropriately selecting the parameters N_h, N_s, b_0, b_1, h_e and h_x. The sync performance of the TL scheme for the same preamble length is computed for all the possible number of prefixes and several different number of active correlators. A modified performance analysis of the TL scheme with a consideration of blocking probability is given in appendix D.

Figures 2.8 to 2.10 show performance calculations given the preamble length of 2040 chips or equivalently 8 bits long for the proposed method. The proposed scheme has been found to be optimal with $N_h = 5, N_s = 3, h_e = 0$ and $h_x = 1$. In figure 2.8 performance of the TL method for single prefix preamble is plotted with several different c as parameter. The length of the active correlators is 1785 chips. b_0' and b_1' are selected in the way that the performance for each c is optimized. From this figure we see that the proposed method yields better performance than the TL one does, with a slight reduction in very low SNR. For the same preamble length, performance with two prefixes is plotted in figure 2.9. The length of the active correlators is correspondingly shortened to 765 chips. It can be seen that the proposed scheme is almost equivalent in performance to the TL scheme of 2-prefix with 3 active correlators. To further increase c, the performance cannot be significantly improved. The maximum improvement over the proposed scheme

is limited to within 1.3 dB in this case with $c = 32$. Figure 2.10 illustrates the comparison of the proposed method and the TL method with 3-prefix preamble where the length of the active correlators is further reduced to 425 chips. Since the sequence length of the active correlators is not long enough for the reliable coincidence detection, no curves by the TL method, which yield better performance than that by the proposed method, can be found. These figures indicate that the 2-prefix preamble is the best choice for the TL method in this case. The performance with more prefixes will saturate more quickly as c increases. Lower values of $P_{B_{TL}}$ can be achieved by raising b_0 and b'_0. The performance relation between the two schemes is about the same as before. This is shown in figures 2.11 and 2.12. If the receiver complexity were not under consideration, the TL scheme would have a little better performance than the proposed scheme. However, receiver complexity is indeed an important factor in practical applications. More comparisons between the proposed scheme and the TL scheme are given in the next chapter.

2.5 Summary

For burst mode DS spread spectrum communications, where a fixed length preamble is used at the beginning of each data packet for synchronization, and noncoherent matched filters are used for detection, the new acquisition technique shows advantages over the previous schemes in either sync performance or receiver complexity.

The probability of packet loss is lower bounded by the probability of receiver blocking caused by false alarms. The system designer can determine this lower bound by selecting appropriate decision thresholds. For a fixed preamble length, the proposed acquisition scheme is equivalent in performance to the multiple-prefix TL scheme with less active correlators. At the same time, it yields a much simpler receiver structure. The TL method has the potential to improve the sync performance

in low SNR by adding more active correlators, although the hardware complexity may not be acceptable.

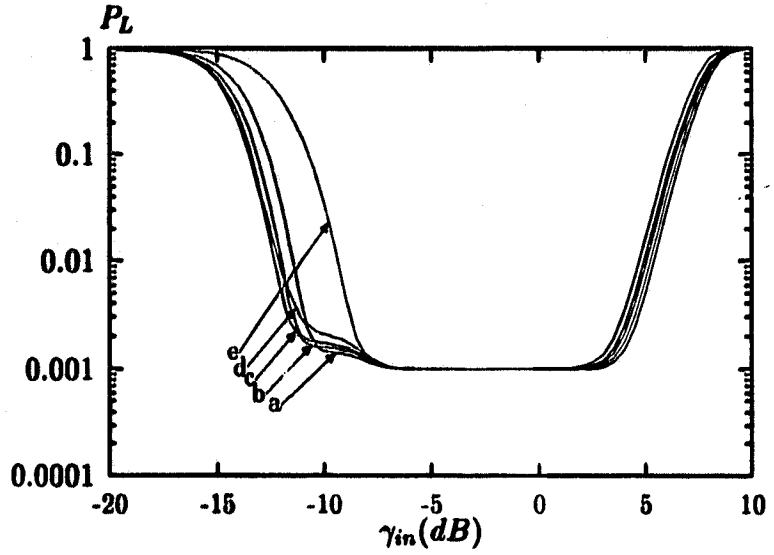

Figure 2.6: P_L **versus SNR for different parameters of** N_h **and** N_s**.**
a. $(N_h, N_s) = (3, 5)$;
b. $(N_h, N_s) = (4, 4)$;
c. $(N_h, N_s) = (5, 3)$;
d. $(N_h, N_s) = (6, 2)$;
e. $(N_h, N_s) = (1, 7)$.

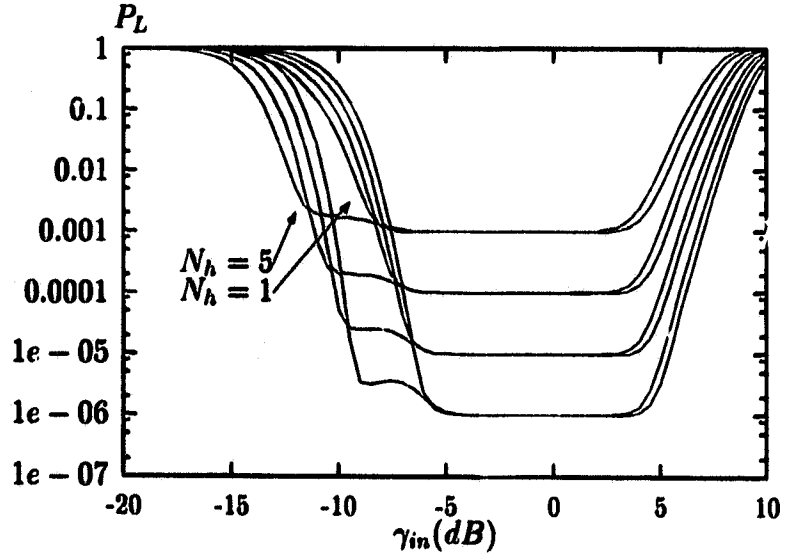

Figure 2.7: Comparison of the new scheme and the conventional scheme with $N_h = 1$.

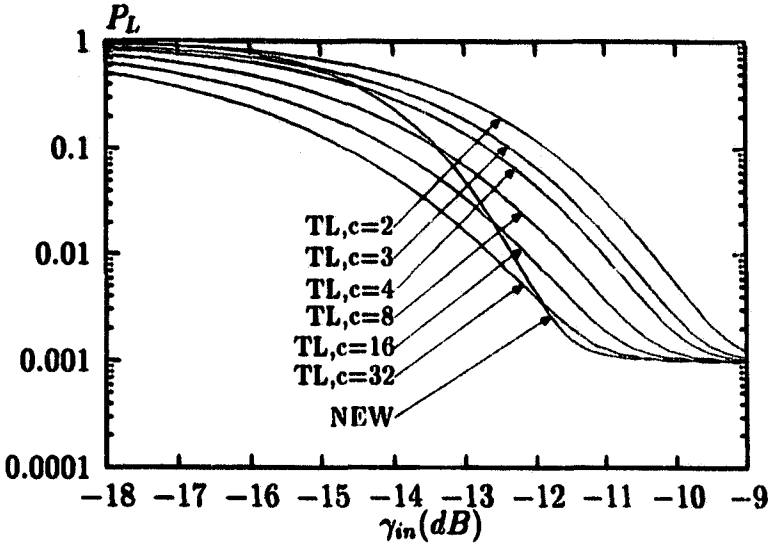

Figure 2.8: Performance comparison of the new method and the TL method with 1 prefix at $P_B = 10^{-3}$.
Preamble length=2040 chips, M=1785 for the TL method, $(N_h, N_s) = (5, 3)$ for the new method.

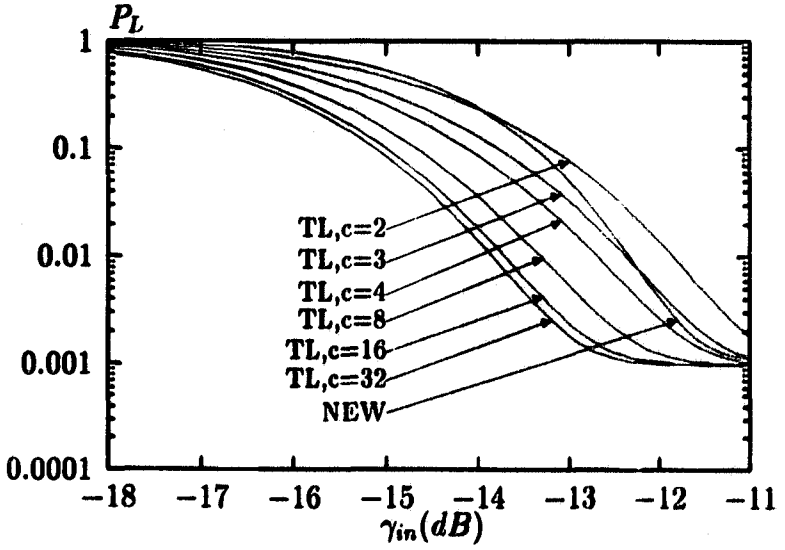

Figure 2.9: Performance comparison of the new method and the TL method with 2 prefixes at $P_B = 10^{-3}$.
Preamble length=2040 chips, M=765 for the TL method, $(N_h, N_s) = (5, 3)$ for the new method.

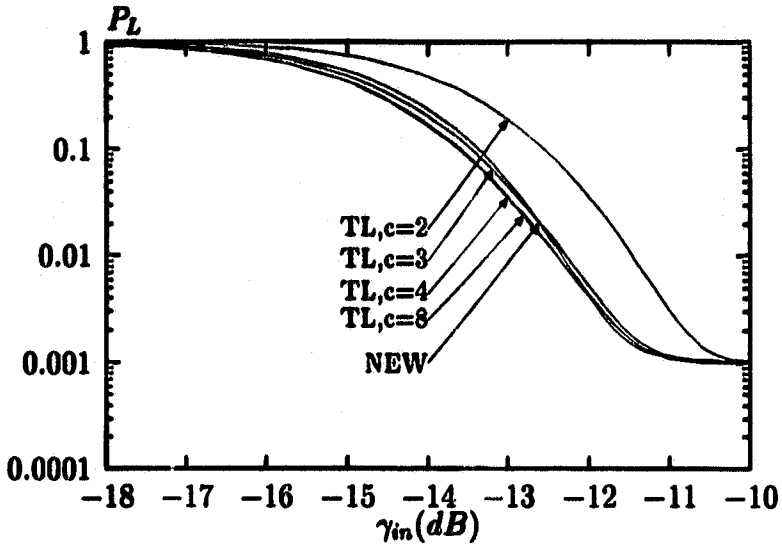

Figure 2.10: Performance comparison of the new method and the TL method with 3 prefixes at $P_B = 10^{-3}$.

Preamble length=2040 chips, M=425 for the TL method, $(N_h, N_s) = (5, 3)$ for the new method.

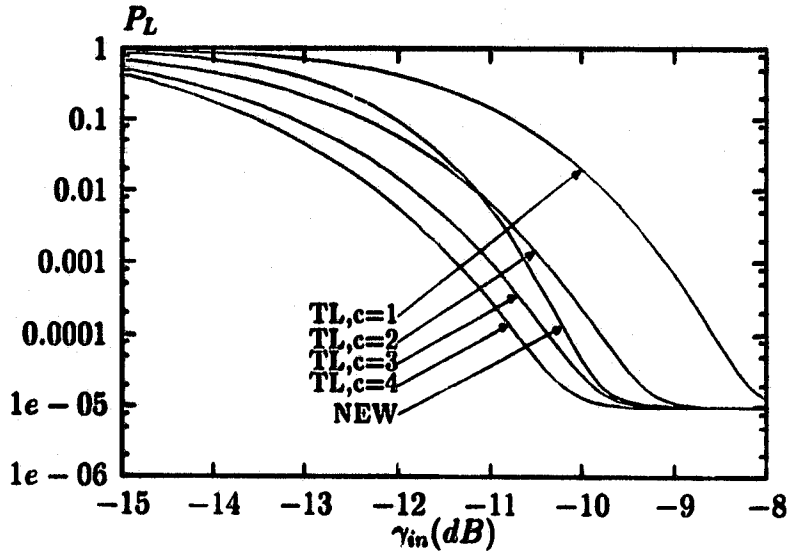

Figure 2.11: Performance comparison of the new method and the TL method with 2 prefixes at $P_B = 10^{-5}$.

Preamble length=2040 chips, M=765 for the TL method, $(N_h, N_s) = (5, 3)$ for the new method.

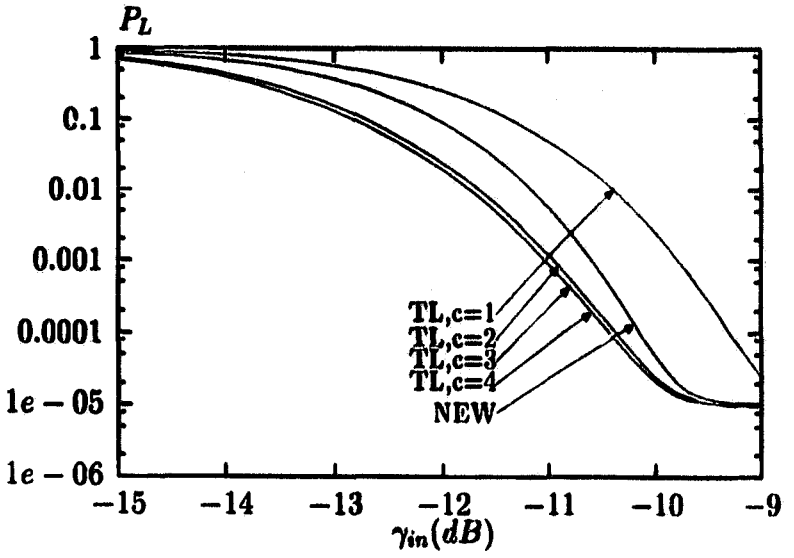

Figure 2.12: Performance comparison of the new method and the TL method with 3 prefixes at $P_B = 10^{-5}$.

Preamble length=2040 chips, M=425 for the TL method, $(N_h, N_s) = (5, 3)$ for the new method.

Chapter 3

Acquisition Using Hardlimiting Matched Filter

3.1 Introduction

The acquisition scheme discussed in chapter 2 can be also applied to the hardlimiting matched filter receiver. As we mentioned in section 2.3.4, the masking effect during acquisition can be eliminated by using hardlimiting matched filters. This is shown in figures 3.1 to 3.4, where the correlation outputs from a linear matched filter and a hardlimiting matched filter are plotted respectively. The linear matched filter is seen to be sensitive to the dynamic range of the received signal power and thus vulnerable to false acquisitions prior to the main correlation peak, while the HL receiver preserves good acquisition performance in a large range of SNR. Furthermore, the HLMF implemented in VLSI has advantages over the analog (linear) MF in terms of flexibility, reliability, speed, compactness, and cost efficiency [2].

In this chapter, we analyze the acquisition performance of a HL receiver. Since the acquisition system model is basically the same as that in chapter 2, we will skip those similar analyses and focus on the decision statistics and the numerical results.

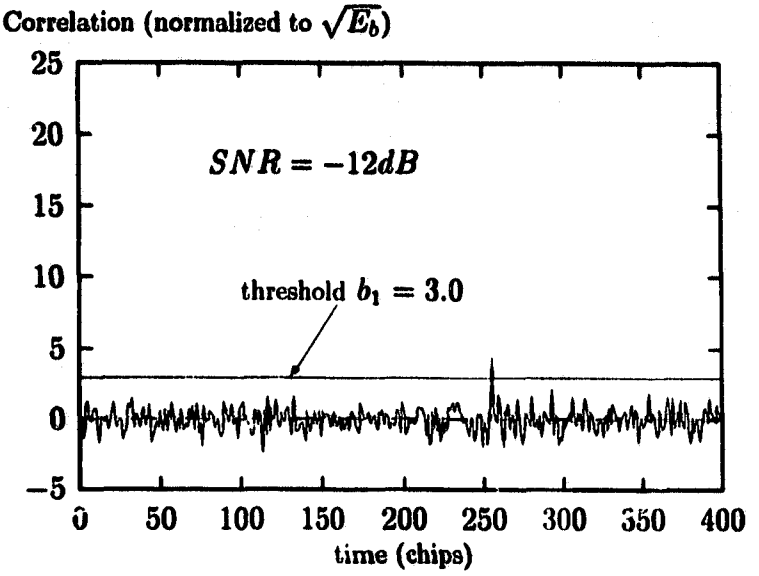

Figure 3.1: Outputs from a linear matched filter. $SNR = -12dB$

PN sequence length $m = 255$, E_b = bit energy.

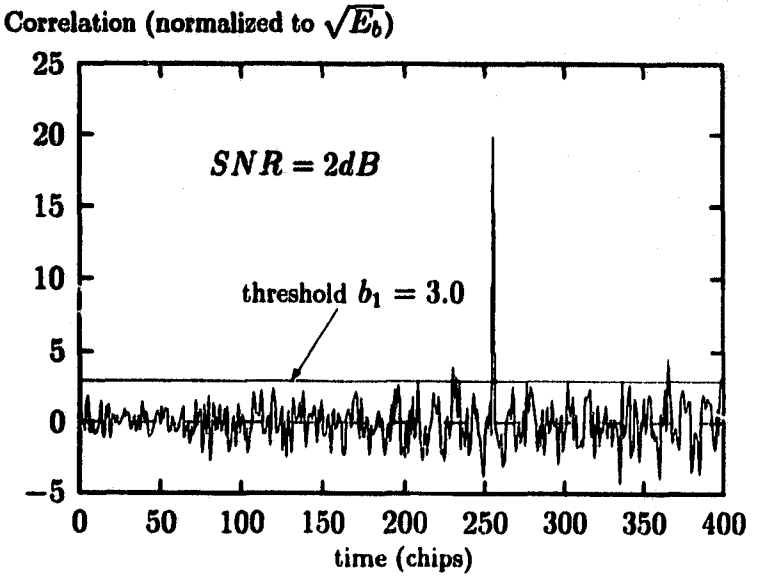

Figure 3.2: Outputs from a linear matched filter. $SNR = 2dB$

PN sequence length $m = 255$, E_b = bit energy.

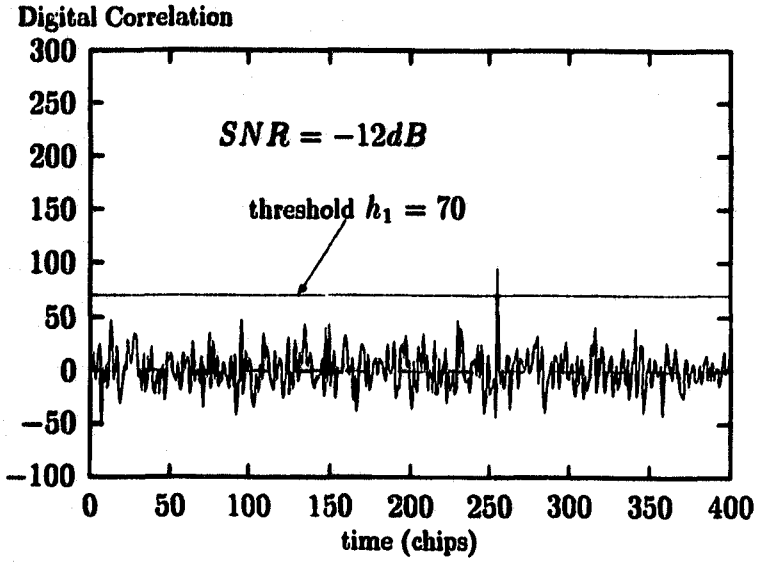

Figure 3.3: Outputs from a hardlimiting matched filter. $SNR = -12dB$ PN sequence length $m = 255$.

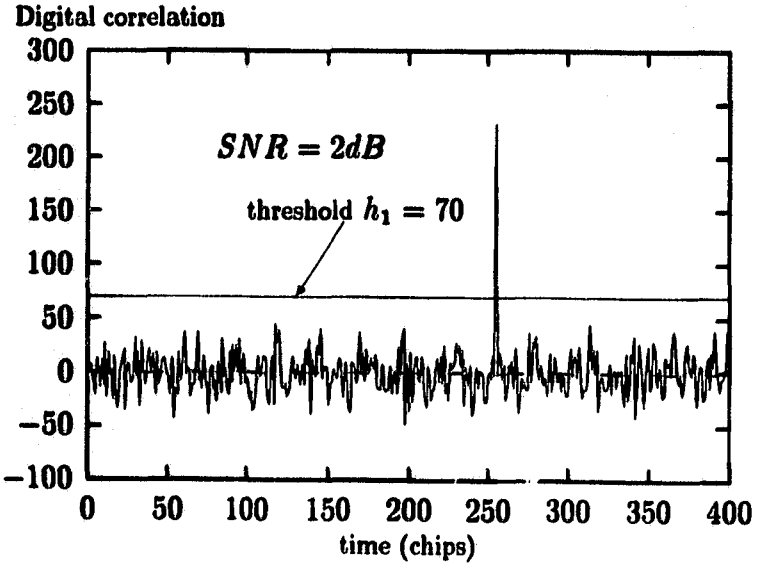

Figure 3.4: Outputs from a hardlimiting matched filter. $SNR = 2dB$ PN sequence length $m = 255$.

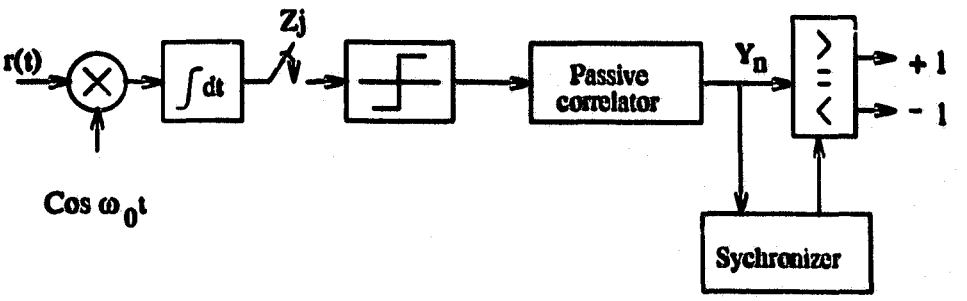

Figure 3.5: Receiver structure with hardlimiting matched filter.

3.2 System description

The proposed receiver structure with a hardlimiting matched filter is shown in figure 3.5. This receiver is similar to that of [1] except that the active correlator is replaced by a passive correlator/matched filter. Coherent receiver reception is assumed for simplicity of analysis, since the comparative performance of the new scheme with other schemes is expected to be similar for the more practical non-coherent receiver of [48]. However, the principle of the proposed acquisition technique is the same for both the coherent and non-coherent receivers. Bit decisions are made by comparing the output of the correlator with appropriate thresholds to obtain $+1$, -1 or erasure decisions.

The preamble format and the synchronization process are exactly the same as those described in the last chapter.

3.3 Performance analysis

The purpose of this section is to obtain the probability of P_L when a hardlimiting matched filter is used. The derivations of P_L, $P_{acq}(i,k)$, $P_c(i)$ and P_{fcn} are the same as those in chapter 2 except P_d, P_{fan}, $P_{fd}(n)$, q, p, s, q_n, p_n and s_n. Therefore we will mainly focus on the derivations of these terms. Besides, in order to apply the

analysis given in chapter 2, we must also show that successive samples from the HL matched filter are approximately Gaussian and are mutually independent.

3.3.1 Probabilities of false and correct acquisitions

In this subsection, we derive P_d, P_{fan} and $P_{fd}(n)$ for HL receiver. A binary PSK direct-sequence spread-spectrum is considered. The received signal is written as

$$r(t) = Ab(t)a(t)\cos(\omega_0 t + \phi) + n(t) \tag{3.1}$$

where

$$b(t) = \sum_j b_j P_T(t - jT) \tag{3.2}$$

with $b_j \epsilon \{-1, +1\}$ is the jth information symbol, A is the amplitude of the received signal, and $P_T(\cdot)$ is the unit rectangular pulse of duration T. The data signal $b(t)$ is modulated onto a phase-coded carrier, where the code waveform or spectrum spreading signal $a(t)$ may be written

$$a(t) = \sum_{j=-\infty}^{\infty} a_j P_{T_c}(t - jT_c) \tag{3.3}$$

where $a_j \epsilon \{-1, +1\}$ and $a_j = a_{j+m}$ for all j and for some integer m which is the period of the spreading sequence $\{a_j\}$. The chip length T_c relates to the symbol length T via $T = mT_c$, so that there is one code period per data symbol. $n(t)$ is AWGN with power spectral density $N_0/2$. For coherent receiver, we assume $\phi = 0$ in the analysis.

To calculate the system performance in terms of packet loss probability, we need to compute the probabilities of false and correct acquisitions at every test instant.

During the process of acquisition where $b_i = 1$ $(i = 1, 2, ..., N_h)$, the test statistics from the digital matched filter (as illustrated in figures 3.3 and 3.4) are given by the inner product of the two sequences $\{a_j\}$ and $\{sgn(Z_{n-j})\}$

$$Y_n = \sum_{j=0}^{m-1} a_j \cdot sgn(Z_{n-j}) \tag{3.4}$$

where Z_{n-j} is the input sample to the hardlimiter at the $(n-j)$th sampling instant. Note that the $m-n$ samples $Z_0, Z_{-1}, ..., Z_{-(m-n-1)}$ in case of $n < m$ represent $m-n$ random data generated by noise alone. Z_{n-j} for $j < n$ contains the information $a_{[m-[n-j]_m]_m}$ plus the noise, where the modular function $[X]_m$ of an integer X is defined as $[X]_m = X \ MOD[m]$. Thus the synchronization epoch is at any of $n = im$, where $i = 1, 2, ..., N_h$. We use H^0 to represent the test when $n \neq im$ and H^1 to represent the test when $n = im$.

The probability of acquisition at each test epoch n from the matched filter was derived in [9]. First, if $n \leq m$, i.e. the binary sequence coming into the matched filter consists of $m-n$ random data contributed by noise alone followed by n binary samples of the real signal plus the noise, then the probability that the output of the matched filter exceeds the threshold h_1 is written as

$$P_{fd}(n) = \sum_{j=0}^{min(n,h)} \sum_{l=max(0,j-h_0(n))}^{min(j,n-h_0(n))} \binom{n-h_0(n)}{l} \binom{h_0(n)}{j-l}$$
$$(1-p_e)^{n-h_0(n)+j-2l} p_e^{h_0(n)-j+2l} \{(0.5)^{m-n} \sum_{k=0}^{min(h-j,m-n)} \binom{m-n}{k}\}, \quad n \leq m \tag{3.5}$$

where $p_e = 0.5\,\mathrm{erfc}\,(\gamma_{in})$ is the chip error rate, γ_{in} is the input SNR. Even though γ_{in} is usually very small, which results in relatively large p_e, the probability of acquisition detection at the right sync-epoch is usually high enough because of the use of digital correlator. In the above equation, h is the error tolerance of the acquisition detection, with $h_1 = m-2h$. h_1 or h is usually determined by a specified given false alarm rate in the absence of signal.

$h_0(n)$ is the contribution of the received samples to the Hamming distance test measure at the nth test [41], in the absence of transmission and detection errors. $h_0(n)$ for $n < m$ is expressed as

$$h_0(n) = H((a_0 a_1 \cdots a_{n-1}), (a_{m-n} a_{m-n+1} \cdots a_{n-1})) \qquad n < m \tag{3.6}$$

where $H(x,y)$ is the hamming distance between vectors x and y.

Second, when $n \geq m$, i.e. the binary sequence coming into the matched filter consists of m data samples of the real signal plus the noise, the probability that the output of the matched filter exceeds the threshold h_1 is written as

$$P_{fd}(n) = \sum_{j=0}^{h} \sum_{l=max(0,j-h_0(n))}^{min(j,m-h_0(n))} \binom{n-h_0(n)}{l} \binom{h_0(n)}{j-l} (1-p_e)^{m-h_0(n)+j-2l} p_e^{h_0(n)-j+2l} \qquad n \geq m \tag{3.7}$$

Similar to (3.6), $h_0(n)$ for $n \geq m$ is written as

$$h_0(n) = H((a_0 a_1 \cdots a_{m-1}), (a_{[m-[n]_m]_m} a_{[m-[n-1]_m]_m} \cdots a_{[m-[n-m+1]_m]_m})) \tag{3.8}$$

The probability of false acquisition in noise alone is obtained from (3.5) by specializing the parameters $p_e = 0.5$, $n = 0$, and $h_0(n) = 0$

$$P_{fan} = (0.5)^m \sum_{k=0}^{h} \binom{m}{k}, \tag{3.9}$$

and the probability of acquisition at the correct position, i.e. $n = m$, $h_0(m) = 0$, is

$$P_d = \sum_{j=0}^{h} \binom{m}{j} p_e^j (1-p_e)^{m-j} \tag{3.10}$$

In the next section, it will be shown that the statistic Y_n in (3.4) can be very well approximated by a Gaussian variable, with mean

$$\bar{Y}_n = [\min\{n,m\} - 2h_0(n)](1-2p_e), \tag{3.11}$$

and variance

$$\sigma^2_{Y_n} = 4\min\{n,m\}p_e(1-p_e) + m - \min\{n,m\} \tag{3.12}$$

Thus (3.5) and (3.7) can be approximated by

$$P_{fd}(n) = 0.5\,\mathrm{erfc}(\frac{h_1 - \bar{Y}_n}{\sqrt{2\sigma^2_{Y_n}}}), \qquad n \neq im \tag{3.13}$$

For $p_e = 0.5$, $n = 0$ and $h_0(n) = 0$, the approximation of (3.9) is

$$P_{fan} = 0.5\,\mathrm{erfc}(\frac{h_1}{\sqrt{2m}}) \tag{3.14}$$

For $n = m$ and $h_0(m) = 0$, (3.10) may be approximated by

$$P_d = 0.5\,\mathrm{erfc}(\frac{h_1 - (1-2p_e)m}{\sqrt{8mp_e(1-p_e)}}) \tag{3.15}$$

The derivations of q, p, s, q_n, p_n and s_n are given in appendix E for the hardlimiting receiver.

The Gaussian approximation makes it possible for us to show that those Gaussian statistics of the HLMF can be considered to be approximately mutually independent. As described for the case of linear MF in [32], this is not immediately obvious from the system description since, by virtue of the shift register employed, overlapping segments of received data are used repeatedly in many subsequent H^0 tests. The independence among all the H^0 test statistics for the linear matched filter was shown in [32]. For the hardlimiting case, this is shown in section 3.3.3.

3.3.2 Gaussian approximation

In this subsection, we will show that, by the Central Limit Theorem [36], the statistics at the output of the matched filter can be very well approximated by Gaussian variables, provided that the length of the PN code is long enough. By this approximation, the calculation of false alarms and detection will be very simple.

At the nth test, the received sequence in the matched filter consists of $\min\{n, m\}$ signal plus noise samples and $m - \min\{n, m\}$ noise samples.

First of all, the products of those noise samples multiplied by the replica sequence can be taken as $m - \min\{n, m\}$ independent Bernoulli trials, each of them having two possible values ± 1 with probability $1/2$ for each value. From the Central Limit Theorem, the summation of those i.i.d. random variables, denoted as Y_{n_1}, can be approximated as a Gaussian variable, with mean $\bar{Y}_{n_1} = (m - \min\{n, m\})\bar{y}_1 = 0$, and variance $var(Y_{n_1}) = (m - \min\{n, m\})\sigma_1^2 = m - \min\{n, m\}$, where $\bar{y}_1 = 0$ and $\sigma_1^2 = 1$, respectively, are the mean and the variance of the Bernoulli random variable of value ± 1 with probability $1/2$ for each value.

Then the products made by those signal plus noise samples with the replica sequence are further divided into two types. One of them is from the predetermined $h_0(n)$ disagreements corresponding to "-1", without interference or noise. The other is from the $\min\{n, m\} - h_0(n)$ agreements corresponding to "+1", without interference or noise. The products from the first type are i.i.d. random variables of two values ± 1, with probability $1 - p_e$ for the value "-1" and p_e for "+1". Similarly the products from the second type are also i.i.d. random variables of two values, with probability $1 - p_e$ for "+1" and p_e for "-1". The summation, denoted as Y_{n_2}, from the products of the first type, can be approximated by a Gaussian variable with mean $\bar{Y}_{n_2} = h_0(n)\bar{y}_2 = h_0(n)(2p_e - 1)$, and variance $var(Y_{n_2}) = h_0(n)\sigma_2^2 = 4h_0(n)p_e(1 - p_e)$, where $\bar{y}_2 = 2p_e - 1$ and $\sigma_2^2 = 4p_e(1 - p_e)$, respectively, are the mean and the variance corresponding to the first type product. The summation Y_{n_3} from the products of the second type is approximated by a Gaussian variable with mean $\bar{Y}_{n_3} = [\min\{n, m\} - h_0(n)]\bar{y}_3 = [\min\{n, m\} - h_0(n)](1 - 2p_e)$, and variance $var(Y_{n_3}) = [\min\{n, m\} - h_0(n)]\sigma_3^2 = 4[\min\{n, m\} - h_0(n)]p_e(1 - p_e)$, where $\bar{y}_3 = 1 - 2p_e$ and $\sigma_3^2 = \sigma_2^2 = 4p_e(1 - p_e)$, respectively, are the mean and the variance of the second type product.

Y_n, as the statistic at the output of the matched filter, is given by the summation of these three independent Gaussian variables (by construction), which is also a

Gaussian variable with its mean and variance computed as follows

$$\begin{aligned} \bar{Y}_n &= \bar{Y}_{n_1} + \bar{Y}_{n_2} + \bar{Y}_{n_3} \\ &= [\min\{n,m\} - 2h_0(n)](1-2p_e) \end{aligned} \tag{3.16}$$

and

$$\begin{aligned} \sigma^2_{Y_n} &= var(Y_{n_1}) + var(Y_{n_2}) + var(Y_{n_3}) \\ &= 4\min\{n,m\}p_e(1-p_e) + m - \min\{n,m\} \end{aligned} \tag{3.17}$$

At H^1 tests where $h_0(im) = 0$, the mean and the variance are simply

$$\bar{Y}_{im} = m(1-2p_e) \qquad i = 1,2,...,N_h \tag{3.18}$$

and

$$\sigma^2_{Y_{im}} = 4mp_e(1-p_e) \qquad i = 1,2,...,N_h \tag{3.19}$$

Thus the probability density function of Y_n at the nth test is written as

$$f_{Y_n}(y) = \frac{1}{\sqrt{2\pi\sigma^2_{Y_n}}} \exp(-\frac{(y-\bar{Y}_n)^2}{2\sigma^2_{Y_n}}) \tag{3.20}$$

From (3.20), the probability of false acquisition at H^0 test will be

$$\begin{aligned} P_{fd}(n) &= \int_{h_1}^{\infty} \frac{1}{\sqrt{2\pi\sigma^2_{Y_n}}} \exp(-\frac{(y-\bar{Y}_n)^2}{2\sigma^2_{Y_n}})dy \\ &= 0.5\,\mathrm{erfc}(\frac{h_1 - \bar{Y}_n}{\sqrt{2\sigma^2_{Y_n}}}), \qquad n \neq im \end{aligned} \tag{3.21}$$

The probability of acquisition detection at H^1 is written as

$$\begin{aligned} P_d &= \int_{h_1}^{\infty} \frac{1}{\sqrt{8\pi mp_e(1-p_e)}} \exp[-\frac{(y-m(1-2p_e))^2}{8mp_e(1-p_e)}]dy \\ &= 0.5\,\mathrm{erfc}(\frac{h_1 - (1-2p_e)m}{\sqrt{8mp_e(1-p_e)}}) \end{aligned} \tag{3.22}$$

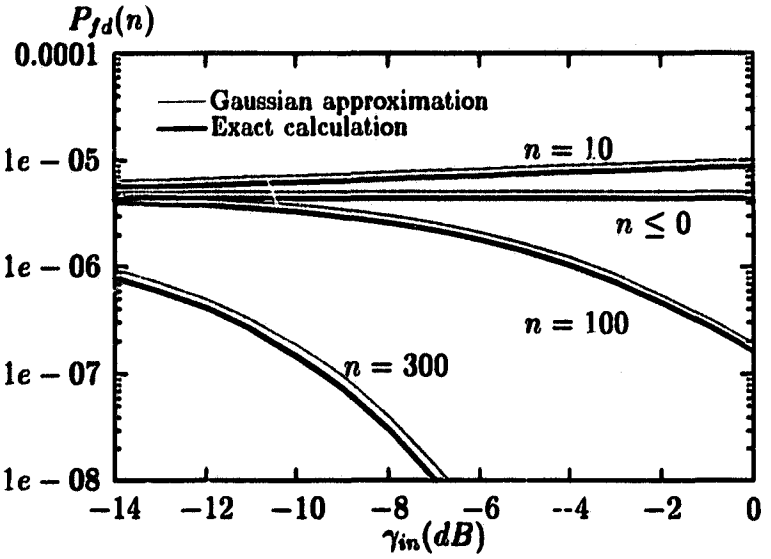

Figure 3.6: Gaussian approximation to the probability of false detection at n. $h_1 = 71$.

Figure 3.6 illustrates the comparison between the exact computation of (3.5) or (3.7) and the Gaussian computation of (3.21) when the received sequence and the replica are not in alignment. In this figure, $P_{fa}(n)$ versus SNR are shown for $n = 0$ (noise samples alone), $n = 10$, $n = 100$ and $n = 300$ with 255 Kasami sequence as the PN code in a data bit. From the four pairs of curves, we can see that the exact or the complicated computation of false acquisition probability can be very well approximated by the simple Gaussian computation. The same conclusion can be drawn for the calculation of the probability P_d of acquisition detection. The comparison between the two computations is shown in figure 3.7

It is interesting to see that, with the larger n, $P_{fd}(n)$ tends to decrease as SNR increases. The reason for this is that, as the SNR becomes higher, Y_n tends to be a determined value defined by the partial correlation of the PN sequence at the corresponding position, and the value of this partial correlation, by the design of the PN sequence, will be far less than the assigned threshold. This may mean that

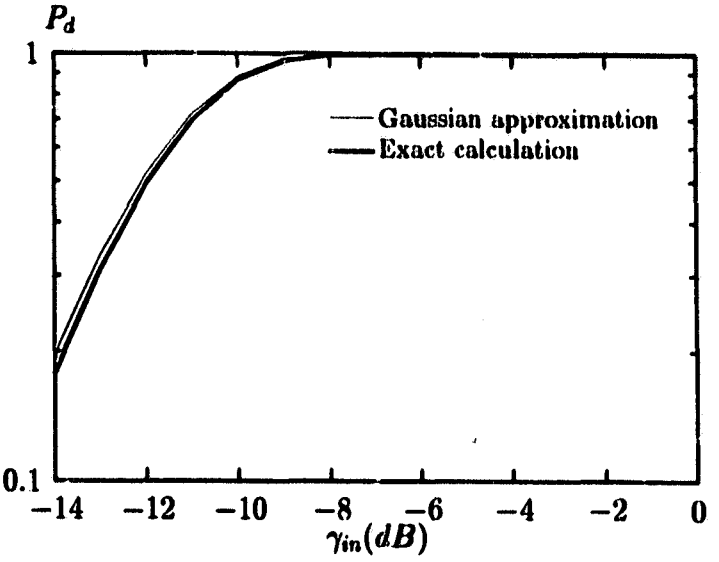

Figure 3.7: Gaussian approximation to the probability of acquisition at H^1 tests. $h_1 = 71$.

the partial correlations or sidelobes with a large amount of signal samples in the correlator can be neglected in the performance analysis at high SNR. The influence on Y_n by noise will be smaller for larger n at high SNR. This is not true for smaller n since the contribution on Y_n by noise can not be neglected. And for $\bar{Y}_n > 0$ or $n > 2h_0(n)$, $P_{fa}(n)$ will even go a little higher as SNR goes up. This is shown in figure 3.6 for $n = 10$ where $h_0(10) = 3$.

3.3.3 Independence at HLMF output

The Gaussian approximation in section 3.3.2 makes it possible to show that the statistics at the output of HLMF are approximately mutually independent. This is done by showing that the statistics are almost uncorrelated instead of highly correlated as they appear to be with a large amount of chips overlapped in the shift register.

Denote $\hat{Z}_n$ as the input sequence vector of m elements in the HLMF, and $\hat{Z}_n =$

$[\hat{z}_n\ \hat{z}_{n-1}\ \ldots\ \hat{z}_{n-m+1}]^T$, where $\hat{z}_n$ represents the most recent signal plus noise sample. It is noted that the input sequence consists only of noise samples when $n \leq 0$. The replica sequence is expressed by the vector $a = [a_0\ a_1\ \ldots\ a_{m-1}]^T$. The output given by the inner product of the two vectors can be written as

$$Y_n = a^T \hat{Z}_n \tag{3.23}$$

where the superscript T denotes the transpose of the corresponding vector. The covariance between the two outputs Y_n and Y_{n+k} is given by

$$\begin{aligned} cov(Y_n, Y_{n+k}) &= E\{(Y_n - \bar{Y}_n)(Y_{n+k} - \bar{Y}_{n+k})\} \\ &= a^T E\{(\hat{Z}_n - \bar{\hat{Z}}_n)(\hat{Z}_{n+k} - \bar{\hat{Z}}_{n+k})^T\} a \\ &= a^T C a \end{aligned} \tag{3.24}$$

where $\bar{Y}_n = a^T E\{\hat{Z}_n\}$ is the statistic mean of Y_n. And the $m \times m$ matrix

$$C = E\{(\hat{Z}_n - \bar{\hat{Z}}_n)(\hat{Z}_{n+k} - \bar{\hat{Z}}_{n+k})^T\} \tag{3.25}$$

is the covariance matrix of the input sequence $\hat{Z}_n$ and $\hat{Z}_{n+k}$. The element C_{ij} of C, where $i, j = 0, 1, 2, \ldots, m-1$, is given by

$$C_{ij} = E\{(\hat{z}_{n-i} - \bar{\hat{z}}_{n-i})(\hat{z}_{n+k-j} - \bar{\hat{z}}_{n+k-j})\} \tag{3.26}$$

Since $\hat{z}_{n-i}$ and $\hat{z}_{n+k-j}$ for $j \neq i + k$ are independent, we have

$$\begin{aligned} C_{ij} &= E\{\hat{z}_{n-i} - \bar{\hat{z}}_{n-i}\} E\{\hat{z}_{n+k-j} - \bar{\hat{z}}_{n+k-j}\} \\ &= 0 \qquad\qquad j \neq i + k \end{aligned} \tag{3.27}$$

When $j = i + k \leq m - 1$,

$$C_{ij} = E\{(\hat{z}_{n-i} - \bar{\hat{z}}_{n-i})^2\} \tag{3.28}$$

If the sample $\hat{z}_{n-i}$ contains only noise, we simply get $\bar{\hat{z}}_{n-i} = 0$ and $C_{ij} = 1$. If $\hat{z}_{n-i}$ contains signal plus noise, C_{ij} can be calculated by assuming the test sample to be

equal to $x_{n-i}\epsilon\{+1,-1\}$ without the interference or noise. Thus $\bar{\hat{z}}_{n-i}$ will be

$$\begin{aligned}\bar{\hat{z}}_{n-i} &= x_{n-i}(1-p_e) - x_{n-i}p_e \\ &= x_{n-i}(1-2p_e)\end{aligned} \tag{3.29}$$

And the random variable $\hat{z}_{n-i} - \bar{\hat{z}}_{n-i}$ will be

$$\hat{z}_{n-i} - \bar{\hat{z}}_{n-i} = \begin{cases} 2x_{n-i}p_e & \text{with probability } 1-p_e \\ -2x_{n-i}(1-p_e) & \text{with probability } p_e \end{cases} \tag{3.30}$$

Then C_{ij} for $j = i + k$ is

$$\begin{aligned}C_{ij} &= 4p_e^2(1-p_e) + 4(1-p_e)^2p_e \\ &= 4p_e(1-p_e)\end{aligned} \tag{3.31}$$

which is not bigger than 1. It is interesting to notice that the variance of a signal plus noise sample from a linear sampler is always equal to the noise variance, no matter how large the SNR is. But this is not true for HL sampler from the above derivations, where we have shown that the variance from a hardlimiter will depend on the SNR of the signal or p_e.

With the C_{ij} calculated above, C can be written as

$$C = \begin{array}{c} \begin{matrix} j=0 & & j=k & & & & \end{matrix} \\ \begin{matrix} \downarrow & & \downarrow & & & & \end{matrix} \\ \begin{bmatrix} 0 & \cdots & 0 & r & 0 & \cdots & 0 \\ \vdots & & & \ddots & \ddots & & \\ & & & & r & & \vdots \\ & & & & & 1 & \\ & & & & & \ddots & \ddots \\ & & & & & & 0 & 1 \\ & & & & & & & 0 \\ \vdots & & & & & & & \vdots \\ 0 & \cdots & & & & \cdots & 0 & 0 \end{bmatrix} \end{array} \begin{array}{l} \\ \\ \leftarrow \text{i=0} \\ \\ \leftarrow \text{i=min\{n,m-k\}-1} \\ \\ \\ \leftarrow \text{i=m-k-1} \\ \\ \\ \leftarrow \text{i=m-1} \end{array} \tag{3.32}$$

where $r = 4p_e(1-p_e)$. It is to be noted that there are $min\{n, m-k\}$ common samples in the sequences $\hat{Z}_n$ and $\hat{Z}_{n+k}$, which contain signal components, and there are $m-k-n$ common samples (when $n < m-k$) which contain noise components alone.

Substituting C in (3.32) into (3.24), the covariance becomes

$$cov(Y_n, Y_{n+k}) = r \sum_{i=0}^{min\{n,m-k\}-1} a_i a_{i+k} + \sum_{i=n}^{m-k-1} a_i a_{i+k} \tag{3.33}$$

Since

$$\begin{aligned} var(Y_n) &= m - min\{n,m\} + min\{n,m\}r \\ &= m - min\{n,m\}(1-r) \end{aligned} \tag{3.34}$$

and

$$var(Y_{n+k}) = m - min\{n+k, m\}(1-r) \tag{3.35}$$

The normalized covariance or the correlation coefficient between the two tests is written as

$$\begin{aligned} \rho(Y_n, Y_{n+k}) &= \frac{cov(Y_n, Y_{n+k})}{\sqrt{var(Y_n) \cdot var(Y_{n+k})}} \\ &= \frac{r\sum_{i=0}^{min\{n,m-k\}-1} a_i a_{i+k} + \sum_{i=n}^{m-k-1} a_i a_{i+k}}{\sqrt{[m - min\{n,m\}(1-r)][m - min\{n+k,m\}(1-r)]}} \end{aligned} \tag{3.36}$$

We notice that this correlation coefficient depends on r or SNR of the received signal as well as the construction of the PN sequence. As pointed out in section 3.3.2, the influence of the sidelobes can be neglected at high SNR when the correlator contains a large number of signal plus noise samples. Thus we may only need to concern the values of $\rho(Y_n, Y_{n+k})$ at relatively low SNR when signal samples are dominant in the correlator.

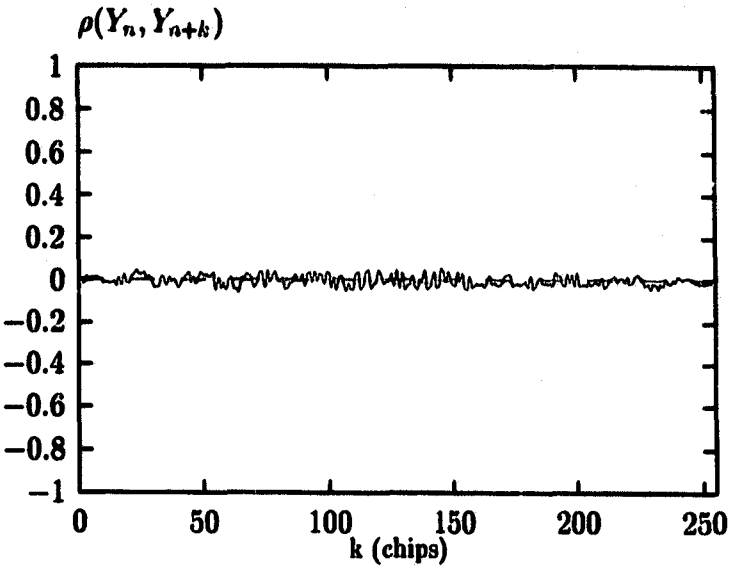

Figure 3.8: Correlation coefficient $\rho(Y_n, Y_{n+k})$ versus k. $n = 50$ chips, $\gamma_{in} = -5dB$.

Several plots concerning values of $\rho(Y_n, Y_{n+k})$ versus the shift k are drawn in figures 3.8 to 3.10 with n and input SNR as parameters. From these figures, we can say that, for the selected 255 Kasimi sequence, $\rho(Y_n, Y_{n+k})$ is usually very small, and the successive statistic tests from the HLMF are almost uncorrelated instead of highly correlated as they appear to be with a large amount of chips overlapped. With the Gaussian approximation, they are also mutually independent.

3.3.4 Thresholds selection for desired performance characteristics

From (2.16) and (2.18), since $P_{syn}(k) \leq 1$ for $k = 0, 1, ..., N_h N - 1$, P_L can never be less than

$$P_L(min) = 1 - \frac{1}{1+\rho} - \frac{P_{fan}}{1+\rho}(N_h N - 1) \tag{3.37}$$

This probability can be taken as the exact packet blocking probability P_B, i.e., $P_B = P_L(min)$ and is more accurate than the approximation $\rho/(1+\rho)$ used in [29].

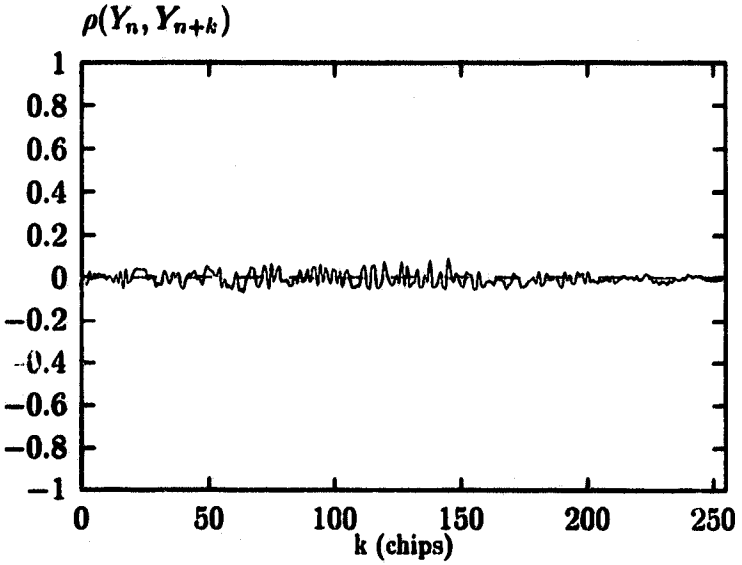

Figure 3.9: Correlation coefficient $\rho(Y_n, Y_{n+k})$ versus k. $n = 50$ chips, $\gamma_{in} = 0dB$.

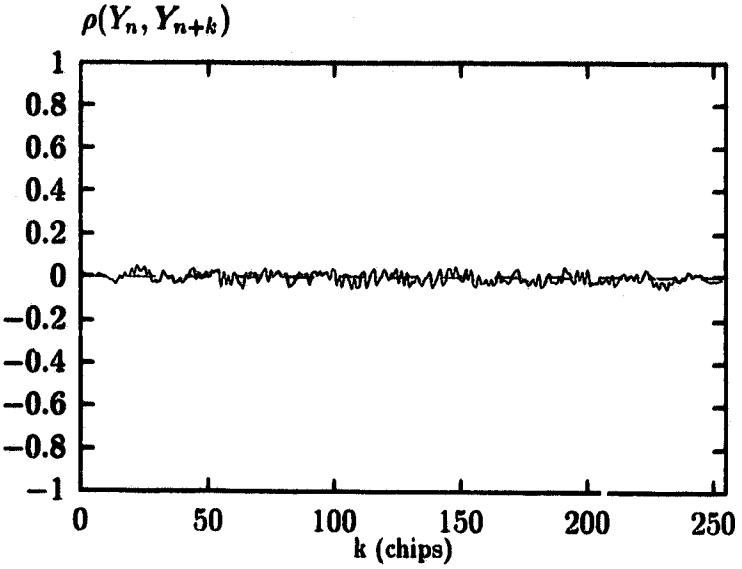

Figure 3.10: Correlation coefficient $\rho(Y_n, Y_{n+k})$ versus k. $n = 200$ chips, $\gamma_{in} = -5dB$.

The system designer can select a desired $P_L(min) \approx 10^{-b}$ (b is an integer) by an appropriate choice of h_1, h_2, h_e and h_x, while the overall performance or the dynamic range is optimized. The approximation sign means that generally $P_L(min)$ cannot be exactly equal to a given constant because the thresholds are not continuous. Typical values of $P_L(min)$ may be in the range 10^{-3} to 10^{-6}. Practically, h_1, h_2, h_e, and h_x can be easily determined by comparing the values of the objective functions of all the candidates (h_1, h_2, h_e, h_x) which satisfy the constraint.

For this problem, the parameters N_h and N_s are assumed to be given such that $N_h + N_s = L$, L is a constant integer. Thus for different pairs (N_h, N_s), a different solution can be found. Then the best combination of N_h and N_s can be determined.

3.4 Numerical results

In this section, the acquisition performance of the receiver is illustrated for $L = 8, 16$ and $L_D = 1000$ with 255 Kasami sequence as the PN code. (h_1, h_2) and (h_e, h_x) are selected to approximately get the required $P_L(min)$. The optimal combination of h_1, h_2, h_e and h_x is obtained by maximizing the dynamic range of P_L at low SNR. A performance comparison is made with the TL acquisition method.

For $L = 8$, figure 3.11 shows P_L versus SNR for different pairs of N_h and N_s with $P_L(min) \approx 10^{-3}$. The best overall performance is obtained with $(N_h, N_s) = (5, 3)$. Similar to the linear receiver, almost 3 dB improvement can be achieved compared to the method of [29] where $(N_h, N_s) = (1, 7)$. However, the performance will not degrade when SNR goes up, which is different from the linear receiver.

Figure 3.12 shows P_L versus SNR with thresholds chosen to obtain $P_L(min) \approx 6 \times 10^{-4}$ and 8×10^{-6} and parameters $(N_h, N_s) = (5, 3)$. Lower values of $P_L(min)$ are obtained by raising the threshold h_1 and accepting a slight reduction in performance at low SNR. For each pair of (h_1, h_2), three curves for P_L are calculated. The lowest

one is obtained by neglecting the blocking probability, i.e. $P_L = 1 - P_{syn}(0)$. The middle one represents the exact P_L from (2.16) and (2.18). And the highest one corresponds to the approximation from (2.7). Simulation of the lowest curve for the lower threshold h_1 is shown to be consistent with the theoretical result.

Performance comparisons between the proposed acquisition scheme and the TL acquisition scheme [35][58] are made in the case of low SNR such that the average rate of false code start signals for the TL method is unchanged whether or not a packet is present. The performances of the two methods at high SNR are limited by the given $P_L(min)$ or the blocking rate. It is noted that, due to the hardlimiter, the effect of false starts can be neglected at high SNR (this is the difference from the linear matched filter), and the performance will mainly depend on the detection of the main correlation peaks.

All the comparisons are made under the assumption that the two schemes use the same length of preamble and the same matched filter which processes 255 PN chips. The optimal sync performance of the proposed scheme for a given preamble length is obtained by selecting the parameters N_h, N_s, h_1, h_2, h_e and h_x according to section 3.3.4. The modified performance analysis of the TL scheme in appendix D is still applicable to the hardlimiting receiver. The optimal sync performance of the TL scheme for the same preamble length is computed for all the possible number of prefixes and different numbers of active correlators.

Figures 3.13 to 3.15 show the comparison between the two schemes with the preamble length equal to 2040 chips or equivalently 8 bits long for the proposed method. The blocking rates for both methods are approximately 8×10^{-4}. We have seen that the proposed scheme is found to be optimal with $N_h = 5, N_s = 3$. In figure 3.13, the performance of the TL method for a single prefix preamble is plotted with c (the number of active correlators) as a parameter. The length of the active correlators is 1785 chips. h_1' and h_2' are selected so that the performance for each c

is optimized. From this figure we see that the proposed method yields better performance than the TL one does, with a slight reduction in very low SNR, unless more than 32 active correlators are employed in the TL receiver. For the same preamble length, the performance with two prefixes (active correlators reduced to 765 chips) is plotted in figure 3.14. It can be seen that the proposed scheme is almost equivalent in performance to the TL scheme with 2 prefixes and 3 active correlators. By further increasing c, the performance of the TL method cannot be significantly improved. The maximum improvement over the proposed scheme is limited to within 1.3 dB in this case with $c = \infty$. Figure 3.15 illustrates the comparison of the proposed method and the TL method with 3-prefix preamble where the length of the active correlators is further reduced to 425 chips. Since the length of the active correlators is not long enough for reliable coincidence detection, the TL method cannot yield a significant performance improvement over the proposed method. From these figures, we can see that the TL method with fewer prefixes or longer active correlators has the potential to improve the performance over that of the new proposed method, but only if an impractically large number of active correlators are used. For example, in figure 3.13, even using 32 active correlators, the performance of the TL method is just about the same as the proposed method which has a much simpler receiver construction. The performance with more prefixes will saturate more quickly as c increases. If the receiver complexity were not under consideration, the TL scheme would have a little better performance than the proposed scheme.

Similar results are obtained for longer preamble. In figure 3.16 performance with 3-prefix and longer preamble of 4080 chips is plotted when the blocking rate is about 8.5×10^{-4}. The proposed method is found to be optimal with $(N_h, N_s) = (10, 6)$. For the TL method, more prefixes with the same preamble cannot give any better performance no matter how many active correlators are used. A preamble with one or two prefixes is able to yield a little better performance at the cost of using many

active correlators. The maximum amount of improvement by the TL scheme with the 3-prefix preamble over the proposed scheme is about 1.6 dB by using more than 16 active correlators. The proposed scheme is performance equivalent to the TL scheme with a 3-prefix preamble and 3 or 4 active correlators.

Lower values of $P_L(min)$ and $P_{B_{TL}}$ can also be achieved by raising h_1 and h_1'. The performance relation between the two schemes is about the same as before. This is shown in figure 3.17 for a 2-prefix case.

Thus for packet radio communication where the preamble of the packet is usually short, the proposed scheme provides an equivalent performance to the TL scheme with a small number of active correlators. At the same time, the receiver is significantly reduced in its complexity. The TL scheme has the potential to improve the sync performance but at the cost of increased (possibly unacceptable) hardware complexity.

3.5 Summary

The proposed acquisition scheme in chapter 2 is shown to be also effective for the hardlimiting receiver. In spite of the difference between the linear and hardlimiting receivers, the performance comparisons of the scheme with the conventional and the TL schemes are essentially the same for the two types of receivers.

The reason of studying the hardlimiting receiver is its simplicity of implementation and its insensitivity to amplitudes of received signals.

Gaussian and independence approximations for the decision statistics of the matched filter have been shown to be appropriate. Thus the computation of the performance becomes simple and explicit. The correctness of the approximations is verified by means of simulation.

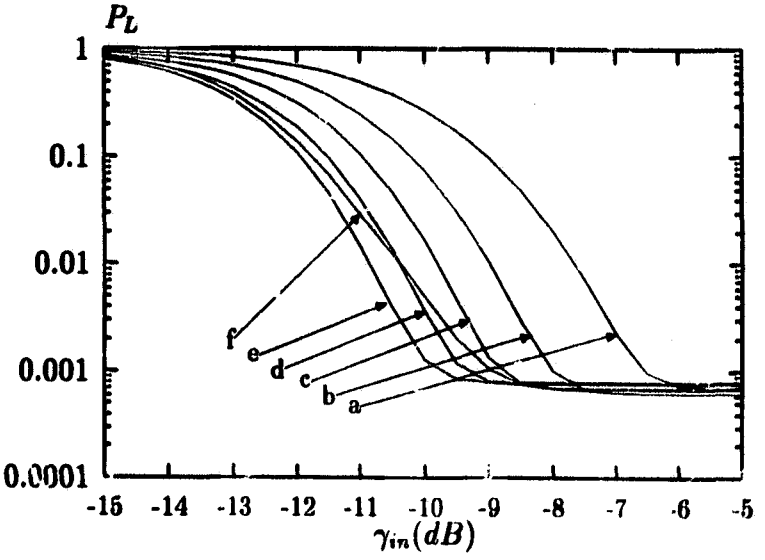

Figure 3.11: P_L versus SNR for different parameters.

a. $(N_h, N_s, h_1, h_2, h_e, h_x) = (1, 7, 79, 25, 1, 2)$;
b. $(N_h, N_s, h_1, h_2, h_e, h_x) = (2, 6, 79, 35, 1, 3)$;
c. $(N_h, N_s, h_1, h_2, h_e, h_x) = (3, 5, 78, 35, 0, 2)$;
d. $(N_h, N_s, h_1, h_2, h_e, h_x) = (4, 4, 77, 35, 0, 1)$;
e. $(N_h, N_s, h_1, h_2, h_e, h_x) = (5, 3, 76, 45, 0, 1)$;
f. $(N_h, N_s, h_1, h_2, h_e, h_x) = (6, 2, 76, 45, 0, 0)$;

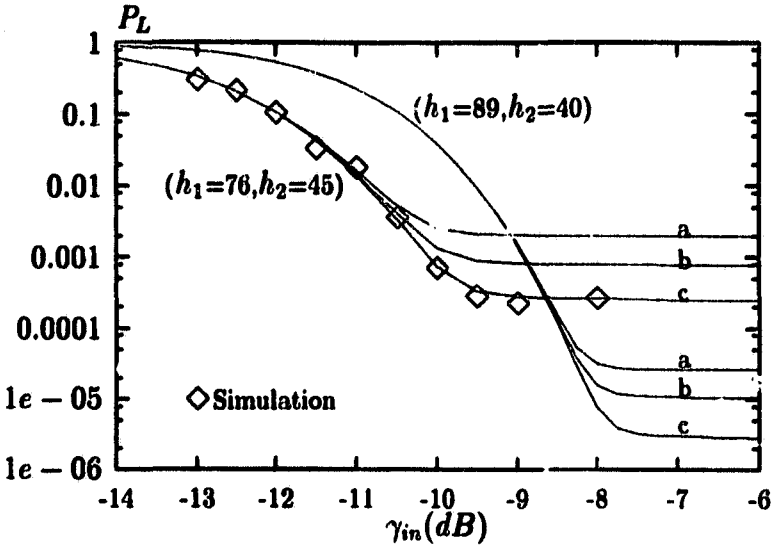

Figure 3.12: P_L versus SNR for different thresholds.

$(N_h, N_s, h_e, h_x) = (5, 3, 0, 1)$; a. approximation from (2.7); b. exact result from (2.16) and (2.18); c. $1 - P_{syn}(0)$.

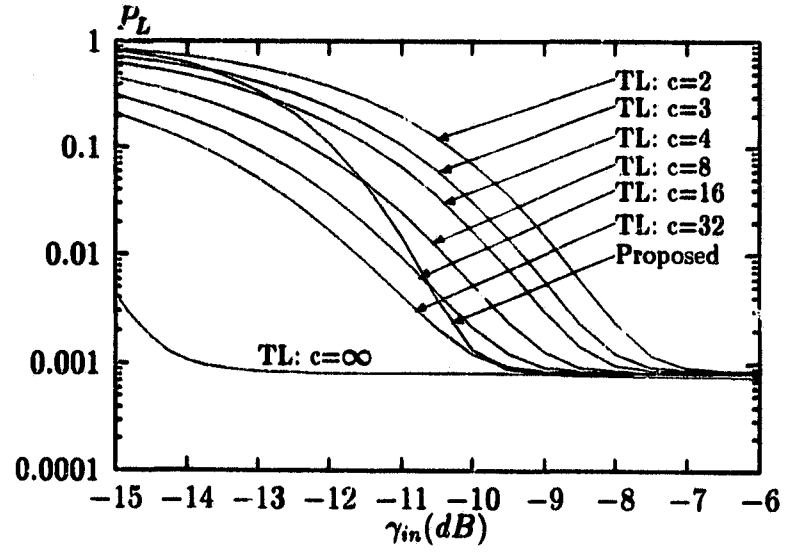

Figure 3.13: Performance comparison of the new method and the TL method with 1 prefix at $P_B \approx 8.5 \times 10^{-4}$.

Preamble length=2040 chips, M=1785 for the TL method, $(N_h, N_s, h_e, h_x) = (5, 3, 0, 1)$ for the new method.

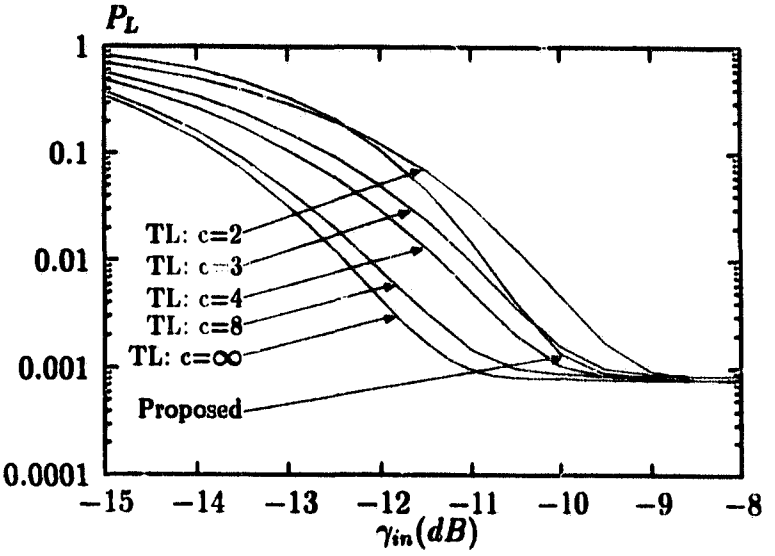

Figure 3.14: Performance comparison of the new method and the TL method with 2 prefixes at $P_B \approx 8.5 \times 10^{-4}$.

Preamble length=2040 chips, M=765 for the TL method, $(N_h, N_s, h_c, h_x) = (5, 3, 0, 1)$ for the new method.

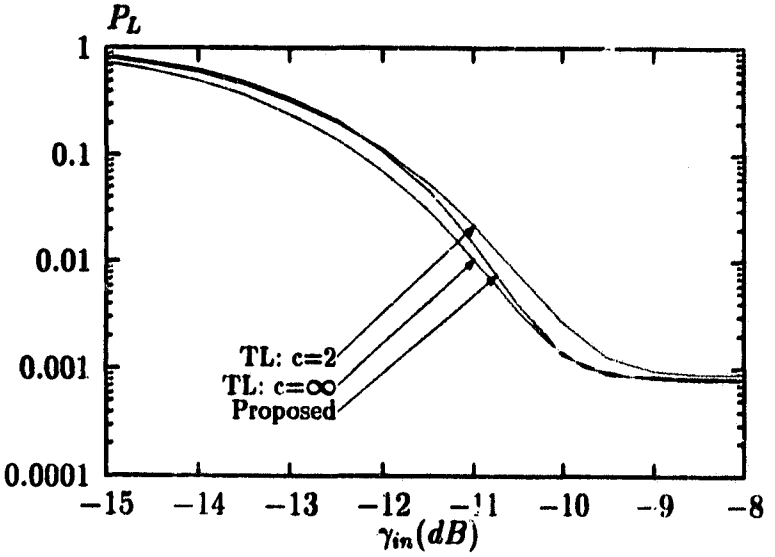

Figure 3.15: Performance comparison of the new method and the TL method with 3 prefixes at $P_B \approx 8.5 \times 10^{-4}$.

Preamble length=2040 chips, M=425 for the TL method, $(N_h, N_s, h_c, h_x) = (5, 3, 0, 1)$ for the new method.

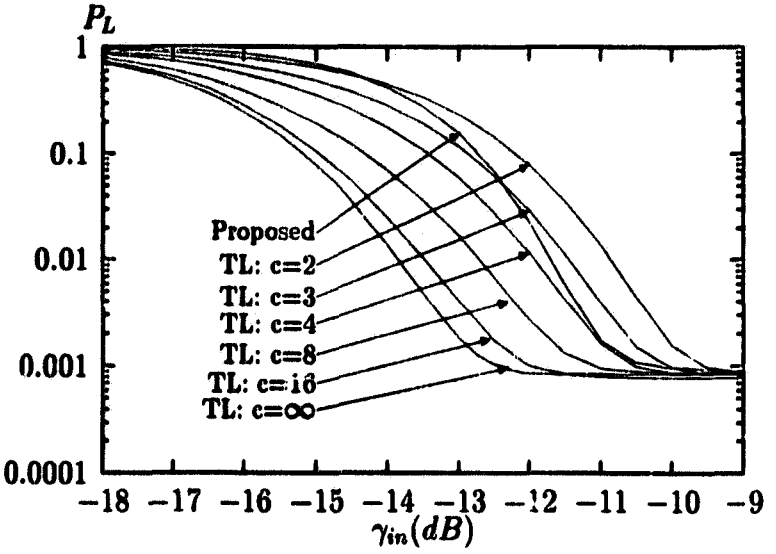

Figure 3.16: Performance comparison of the new method and the TL method with 3 prefixes for preamble length=4080 chips.

$P_B \approx 8.5 \times 10^{-4}$, M=1105 for the TL method, $(N_h, N_s) = (10, 6)$ for the proposed method.

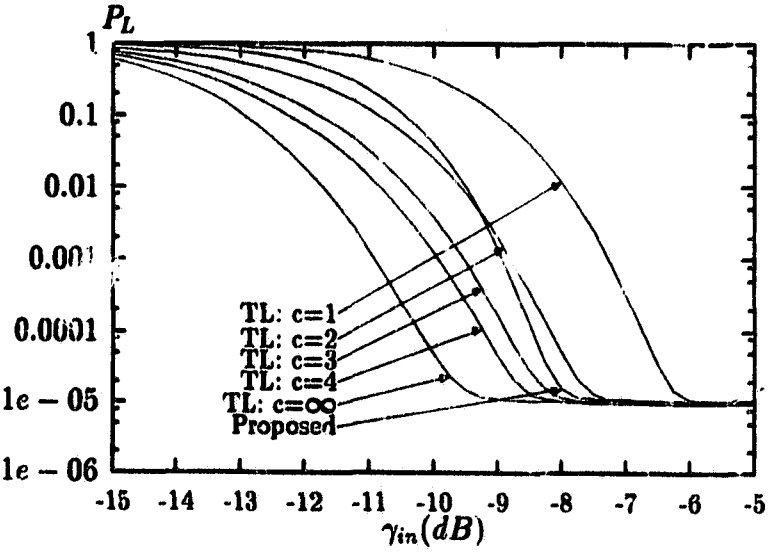

Figure 3.17: Performance comparison of the new method and the TL method with 2 prefixes at $P_B \approx 10^{-5}$.

Preamble length=2040 chips, M=765 for the TL method, $(N_h, N_s, h_e, h_x) = (5, 3, 0, 1)$ for the new method.

Chapter 4

Automatic Threshold Control in Acquisition

4.1 Introduction

In chapter 2 and chapter 3, a fast acquisition scheme using multiple sequences was analyzed. The main purpose of using more than one acquisition sequences is to increase the acquisition probability for weak signals. A few dB improvement can be obtained by the scheme at the low SNR range. However, the dynamic range has been limited at the high SNR range due to the partial auto-correlations. Two-level threshold may be used for the linear detector, which is still not applicable to receiving signals with a large dynamic range, especially in CDMA environment. Hardlimiting detector can be used to deal with a large dynamic range signal with a very simple receiver structure. Unfortunately, it may be only useful in the point to point data communications. In a code division random access system, signals from different users are added together linearly (the channel is assumed to be approximately linear additive), a lot of information from the received signal will be cut out by a hardlimiter due to its nonlinearity. In addition, as pointed out in [47], a

linear modulation process and the principle of superimposition will prove to be quite important when dealing with multipath reception. In this chapter, we will study a new type of acquisition scheme which uses a linear matched filter with its decision threshold being adjusted by the input signal. Although it is extremely useful for acquisition of CDMA signals, as we will see in chapter 7, for simplicity we will still assume that a single packet is present. Furthermore, the acquisition scheme presented in this chapter can be also combined with the method using multiple copies of correlation word to improve performance at low SNR.

For a packet with the DS modulated signal, the received PN waveform plus noise is convolved with a replica PN waveform, the output is tested against a normalized threshold b to determine when acquisition has occurred. Once the threshold is exceeded, which corresponds to a declaration of an acquisition, a coincidence detector is initiated to confirm the acquisition test. The operation of the coincidence detector (CD) was described in [44]. The performance of the acquisition technique will strongly depend upon the setting of the threshold b. In practical situations, a receiver has no prior knowledge about the SNR of any received packet, thus b is often determined by applying the well-known Neyman-Pearson criterion [36], i.e. the receiver sets its acquisition threshold according to a false alarm rate P_{fan} it can afford when no packets are present [1]. For a receiver based on the Neyman-Pearson criterion or a constant threshold (CT) criterion, if the acquisition threshold b is set relatively low in favor of receiving weak signals, the false acquisition probability will be too high when strong level packets show up, because the partial correlation side-lobes are likely to exceed the threshold before the main correlation peak is detected. On the other hand, if b is set relatively high in favor of large signals, the probability that receivers miss those relatively weak packets will be increased.

[1] P_{fan} can be easily related to the minimum packet loss probability, which is a more convenient parameter for evaluation of the system performance.

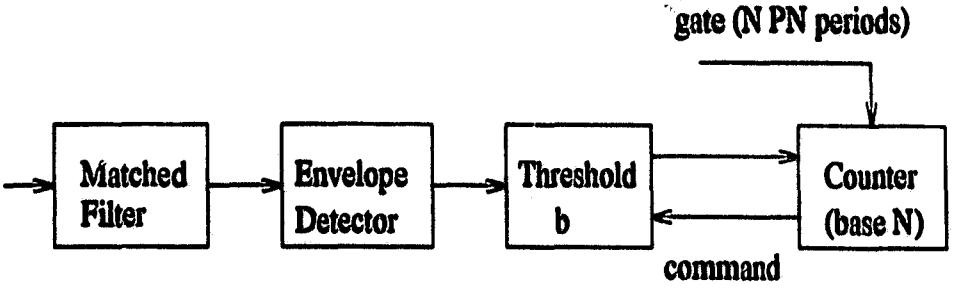

Figure 4.1: ADTLC circuit block diagram.

Both cause losses of many packets. Such phenomena become more serious in CDMA environment because the signals including both sidelobes and main peaks are more likely to fluctuate with the random number of active users in the system. Thus it is necessary to design an acquisition threshold with its value being set according the effective SNR of the main correlation peak and the strengths of sidelobes.

In [12], a method called automatic decision threshold level control (ADTLC) was presented. Using this method, the detection threshold will be changed as the input signal SNR varies. The ADTLC diagram is shown in figure 4.1. The sampling rate at the output of the envelope detector (ED) is assumed to be equal to the chip rate of the PN sequences. If the threshold is too high for a given SNR, the number of pulses collected at the output of the threshold detector in an observation interval of N PN periods will be less than N, otherwise, if the threshold is too low for the SNR, the number will be greater than N. The desired threshold is obtained when the number is equal to N. The threshold selected in this way is trying to make a receiver pick up the N largest samples in the observation interval as the real decision samples. If the method is used for the acquisition, the instants corresponding to the selected samples will be taken as the sync-state epochs since these are the most likely moments that the received PN code and its replica are synchronized. It has been shown in [12] that the average acquisition time is very sensitive to the step size Δb for updating b. Some modifications for the ADTLC searching strategy may

be applied to speed up the approaching to the desired threshold. For example, Δb can be designed nonlinearly with the number of positive pulses in the observation interval, such that Δb is large when the current threshold b is far away from the desired threshold, and Δb is small when b is close to the threshold. However, the acquisition time for the ADTLC scheme is a random variable which cannot be less than N PN periods. Therefore the method cannot be directly used for the acquisition in packet radio system, because the system usually requires that the acquisition be achieved in a given number of PN periods.

In this chapter, a new automatic threshold control (ATC) scheme for the acquisition of DS spread spectrum packets is proposed. This method guarantees that the acquisition threshold b be set right below the largest correlation peak in a PN period when a packet is present. Thus the threshold will be equivalent to the steady-state threshold approached by the ADTLC method, because the number of pulses which exceed b of the ATC scheme will be equal to N in an observation interval of N PN periods. However, this threshold can be obtained automatically in one PN period. The proposed acquisition scheme is found to be useful in receiving packets with a large amplitude dynamic range. A potential application with this scheme is for CDMA systems where the equivalent SNRs of received packets fluctuate according to the number of simultaneous transmitted packets.

The chapter is organized as follows. In the next section, the description of the ATC acquisition process is presented. The corresponding circuit implementation is given in section 4.3. The performance analysis is carried out in section 4.4 followed by numerical examples in section 4.5 and summary in section 4.6.

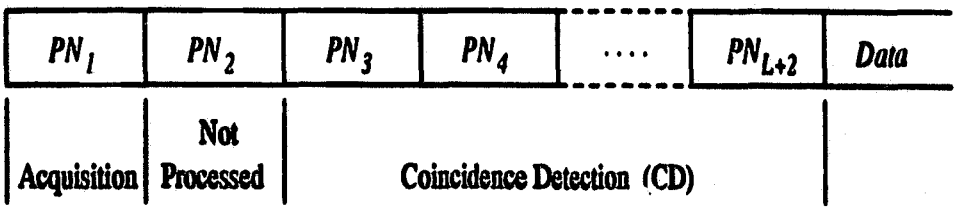

Figure 4.2: Packet format.

4.2 Description of acquisition process

The packet format is shown in figure 4.2, where the preamble consists of $L+2$ different m-chip PN codes. The first PN code PN_1 is used for the fast acquisition, the second one, which is not processed, is utilized to provide enough time for the receiver to adjust its local PN code, and the other L PN codes are designed for the coincidence detection. The matched filter is programmable such that, upon any tentative acquisition decision made by PN_1 at $t = t_k$, the local PN code is updated by PN_i at $t = t_k + (i-2)mT_c$ $(i = 3, 4, ..., L+2)$, where T_c is the chip duration. The decision for each PN_i test of the CD is made by comparing the test output with the CD threshold b_c at $t = t_k + (i-1)mT_c$ $(i = 3, 4, ..., L+2)$. At the end of the CD, if l out of L CD tests are larger than b_c, the acquisition is accepted and the data demodulation begins, otherwise the local code returns to PN_1 and the acquisition search continues.

For signals with a large dynamic range, a satisfactory acquisition performance can only be maintained by properly determining the acquisition threshold b according to the SNR of received packets. The goal of the ATC method is to set the threshold to a level such that the largest correlation peak in an observation interval of one PN period is selected. To do this, we design a detection window which is shown in figure 4.3. The initial or minimum value b_0 of b is set according to the Neyman-Pearson criterion for an acceptable false alarm rate when the receiver is in acquisition search state in which the matched filter is waiting at PN_1 for a match

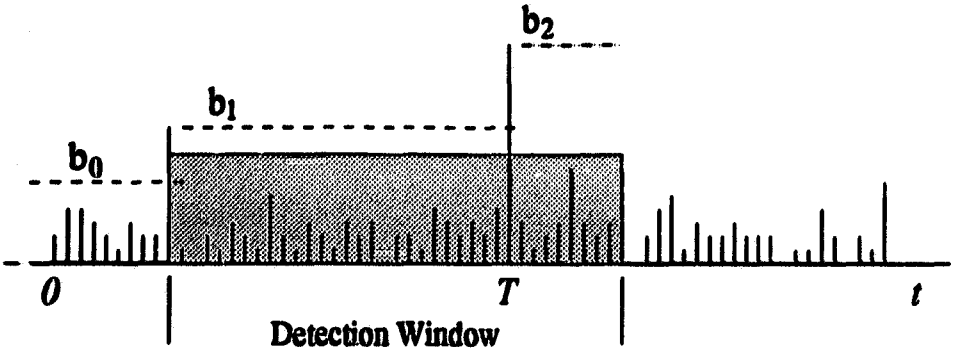

Figure 4.3: Window operation. b_0: initial threshold, b_j: the jth updated threshold.

with an anticipated packet. Once the threshold is exceeded, the detection window opens and will stay open for one PN period. At the same time, the threshold is updated by the value of the correlation peak which exceeds b_0. The epoch corresponding to the correlation is stored. During the following tests in the window, the current threshold and the stored epoch are updated in the same way, whenever the threshold is exceeded. Consequently, the largest correlation in the window is selected as the in-sync peak. It is noted that the window may start at any sampling epoch of the preamble, but only the window initiated by the first PN code of the received preamble can lead to the successful acquisition. If no packets are present, a false acquisition impulse due to noise may also start a window. In this case, the CD test will be initiated, and the receiver will be busy for $L+1$ PN periods. Furthermore, if a false coincidence occurs, the receiver will not be available for another interval equal to the length of a packet.

4.3 ATC implementation

In this section, a simple implementation of the ATC algorithm is described. The ATC circuit block diagram is illustrated in figure 4.4. The programmable matched filter scanning one PN period is loaded with PN_1 at the acquisition search state. The

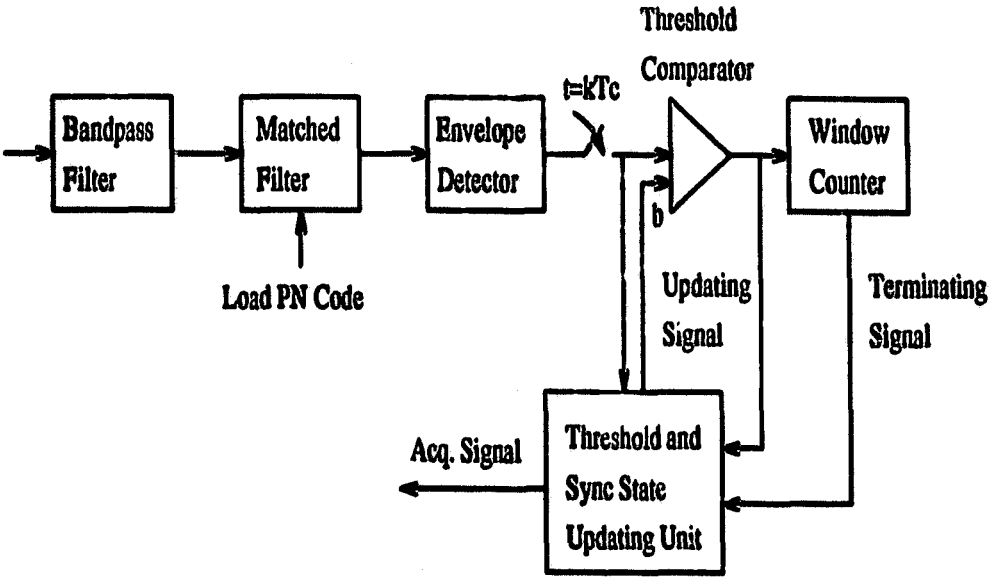

Figure 4.4: ATC circuit block diagram.

correlation pulses after the envelope detector are sampled every T_c second. With the receiver front end bandpass filter of bandwidth $B = 2/T_c$, these samples were shown to be mutually independent [32]. The number of samples in the detection window is equal to m, i.e. the number of chips in every single PN code. When the receiver is in the standby state or acquisition search state, the threshold for the comparator is b_0. Once b_0 is exceeded, the comparator will output an updating signal, and the threshold is updated by the value of the correlation and the position corresponding to the correlation is stored in the threshold sync-state updating unit. In addition, the window counter is immediately started by the positive output from the comparator. During the operation of the window, any positive output from the comparator will lead to an update of b by the new correlation and an update of the sync position. After all m samples have been tested, the window counter will send out a terminating signal to stop the updating and initiate the CD operation.

4.4 Performance analysis

In this section, the synchronization performance of the proposed ATC technique is analyzed in terms of the probability P_L of packet loss versus SNR. The system parameters which determine P_L are the PN sequence length m, the number L of the CD tests, the number L_D of data bits in a packet, the minimum tolerance l in the majority logic decision of the CD, and the initial acquisition threshold b_0. An expression for P_L is determined and each component of this expression is evaluated in terms of the system parameters.

4.4.1 Preliminaries

The received preamble signal at the output of the bandpass filter is written as

$$r(t) = [APN_j(t) + n_I]\cos\omega_0 t - n_Q \sin\omega_0 t \quad j = 1, 2, \ldots L+2. \tag{4.1}$$

where A is the amplitude of the signal, and $PN_j(t)$ represents the jth spreading sequence spanning from $(j-1)T$ to jT of the preamble with $T = mT_c$. n_I and n_Q are the in-phase and quadrature components of the white Gaussian noise with two-sided power spectral density $N_0/2$. The noise power at the output of the bandpass filter of bandwidth $B = 2/T_c$ is $\sigma^2 = N_0/T_c$.

Considering the acquisition procedure in which the detector observes $PN_1(t)$ and $PN_2(t)$ over a period $0 \le t < 2T$. The test statistic at the output of the matched filter is

$$y(t) = \int_0^T r(t)PN_1(T - t + \tau)cos[\omega_0(T - t + \tau)]d\tau \tag{4.2}$$

By doing some manipulations and ignoring the double frequency terms in the integral, we have

$$y(t) = [\frac{AT}{2}\rho(t) + n_I']\cos\omega_0(t - T) - n_Q' \sin\omega_0(t - T) \tag{4.3}$$

where

$$n_I' \triangleq \frac{1}{2}\int_0^T n_I PN_1(T-t+\tau)d\tau \tag{4.4}$$

$$n_Q' \triangleq \frac{1}{2}\int_0^T n_Q PN_1(T-t+\tau)d\tau \tag{4.5}$$

are both Gaussian random variables with zero-mean and variance $T\sigma^2/4$, and

$$\rho(t) \triangleq \begin{cases} \frac{1}{T}\int_0^t PN_1(\tau)PN_1(\tau-t+T)d\tau & t \le T \\ \frac{1}{T}[\int_0^{t-T} PN_2(\tau)PN_1(\tau-t+2T)d\tau & \\ +\int_{t-T}^{T} PN_1(\tau)PN_1(\tau-t+T)d\tau] & T<t<2T \end{cases} \tag{4.6}$$

is the normalized correlation of the PN sequences. The upper equation in (4.6) corresponds to the partial correlation of PN_1 when it has not yet completely come into the matched filter, i.e. only a fraction of it is in the matched filter. The first term of the lower equation represents the partial cross-correlation between PN_1 and PN_2, and the second term represents the partial auto-correlation of PN_1.

The envelope $Z(t)$ of $y(t)$ is given by

$$Z(t) = \sqrt{[\frac{AT}{2}\rho(t) + n_I']^2 + n_Q'^2} \tag{4.7}$$

The probability distribution of $Z(t)$ is known to be Rayleigh distribution when $\rho(t) = 0$ and Rice distribution when $\rho(t) > 0$.

4.4.2 Probabilities of false and correct acquisition

Starting with PN_1, we denote $t_k = kT_c$ as the instant corresponding to the kth ED output sample by PN_1. As we have mentioned, upon any tentative acquisition decision at $t = t_k$, i.e. the largest correlation output occurs at t_k, the local PN code of the matched filter is updated by PN_i at $t = t_k + (i-2)T$ with $i = 3, 4, ..., L+2$.

If the acquisition decision is correct, i.e. $k = m$, each CD test statistic at the output of the ED will be given by (4.7) with $\rho(t) = 1$, otherwise the statistic will be given by (4.7) with $\rho(t) < 1$ depending on the partial cross-correlations of PN_j.

When no packets are present (equivalent to $\rho(t) = 0$), the receiver's threshold is set by b_0. From [57], the probability of the false acquisition P_{fan} in noise alone is

$$P_{fan} = \exp(-\frac{b_0^2}{2}) \tag{4.8}$$

and the probability P_{fc} of the false coincidence detection at each test is written as

$$P_{fc} = \exp(-\frac{b_c^2}{2}) \tag{4.9}$$

The above two equations imply that the receiver may open its detection window falsely due to noise and start the CD operation even though no packets show up. In such a situation, the receiver will not be available for at least $L + 1$ PN periods.

Let $Z_k = Z(kT_c)$ denote the correlation output from ED at t_k, where Z_m corresponds to the actual correlation peak and Z_k $(k \neq m)$ are the correlation sidelobes, then any Z_k could start a detection window w_k which contains samples $(Z_k, Z_{k+1}, \ldots, Z_{k+m-1})$, but only those windows with $1 \leq k \leq m$ can lead to the successful acquisition. Since the ATC circuit is designed to pick up the largest correlation in a detection window, the correct correlation Z_m can only be selected when all the sidelobes in the window are less than Z_m. Thus the probability of correct detection for the acquisition is

$$\begin{aligned} P_d &= \sum_{k=1}^{m} P_{w_k} Pr\{Z_m > \text{all } m-1 \text{ sidelobes in } w_k\} \\ &= \sum_{k=1}^{m} P_{w_k} \prod_{i=k, i\neq m}^{k+m-1} Pr\{Z_i < Z_m\} \end{aligned} \tag{4.10}$$

where P_{w_k} is the probability that the window w_k is initiated. P_{w_k} can be written as

$$P_{w_1} = Pr\{Z_1 \geq b_0\} \tag{4.11}$$

and

$$\begin{aligned} P_{w_k} &= Pr\{Z_1,\ Z_2,\ \ldots,\ Z_{k-1} < b_0,\ \ Z_k \geq b_0\} \\ &= \prod_{j=1}^{k-1}(1 - Pr\{Z_j \geq b_0\})Pr\{Z_k \geq b_0\},\ k \geq 2 \end{aligned} \tag{4.12}$$

in (4.11) and (4.12) $Pr\{Z_j \geq b_0\}$ can be expressed as [57]

$$Pr\{Z_j \geq b_0\} = Q(\sqrt{2\gamma_o\rho^2(jT_c)},\ b_0) \tag{4.13}$$

where $\gamma_o = m\gamma_i = mA^2/(2\sigma^2) = m(E_c/N_0)$ ($E_c = A^2T_c/2$ is the chip energy) is the SNR at the output of the MF, and Q(a,b) is the Marcum-Q function.

The probability $Pr\{Z_i < Z_m\}$ in (4.10) can be written as [42]

$$Pr\{Z_i < Z_m\} = \frac{1}{2}[1 - Q(\sqrt{c}, \sqrt{a}) + Q(\sqrt{a}, \sqrt{c})] \tag{4.14}$$

where $a = \gamma_o$ and $c = \gamma_o\rho^2(iT_c)$.

The probability P_f of the false acquisition, when signal is present and the selected correlation peak in any detection window corresponds to a sidelobe, is given by

$$\begin{aligned} P_f &= \sum_{k=1}^{m} P_{w_k} Pr\{\text{at least one of the } m-1 \text{ sidelobes} \\ &\quad \text{in } w_k > Z_m\} \\ &= \sum_{k=1}^{m} P_{w_k}(1 - Pr\{\text{no sidelobes in } w_k > Z_m\}) \\ &= \sum_{k=1}^{m} P_{w_k} - P_d \end{aligned} \tag{4.15}$$

Thus we have

$$P_d + P_f = \sum_{k=1}^{m} P_{w_k} \tag{4.16}$$

Note that $\sum_{k=1}^{m} P_{w_k}$ is just the probability that at least one of the possible windows which contain the main lobe at $k = m$ is opened, and can be written as

$$\begin{aligned}\sum_{k=1}^{m} P_{w_k} &= 1 - Pr\{Z_1 < b_0,\ Z_2 < b_0,\ \ldots,\ Z_m < b_0\} \\ &= 1 - \prod_{j=1}^{m}[1 - Q(\sqrt{2\gamma_o\rho^2(jT_c)},\ b_o)] \end{aligned} \tag{4.17}$$

As SNR goes up, $\sum_{k=1}^{m} P_{w_k} \to 1$, and $P_d \to 1$ because $Pr\{Z_i < Z_m\} \to 1$, i.e. the probability that the main correlation is larger than any of the sidelobes approaches unity. From (4.16), $P_f \to 0$.

For the constant threshold (CT) receiver, the probability P_d' of the correct acquisition is written as [22]

$$\begin{aligned} P_d' &= Pr\{Z_1,\ Z_2,\ \ldots,\ Z_{m-1} < b_0,\ Z_m \geq b_0\} \\ &= \prod_{i=1}^{m-1}(1 - Pr\{Z_i \geq b_0\})Pr\{Z_m \geq b_0\} \\ &= P_{w_m} \end{aligned} \tag{4.18}$$

and the probability P_f' of the false acquisition is expressed as

$$\begin{aligned} P_f' &= 1 - Pr\{Z_1,\ Z_2,\ \ldots,\ Z_{m-1} < b_0\} \\ &= 1 - \prod_{i=1}^{m-1}(1 - Pr\{Z_i \geq b_0\}) \end{aligned} \tag{4.19}$$

It is easy to verify that

$$P_d' + P_f' = P_d + P_f \tag{4.20}$$

which means that the two receivers have an equal acquisition probability (false and correct), but the distribution of the false and correct probabilities at each given SNR are different for the two schemes. For the CT receiver, $P_d' \to 1$ and $P_f' \to 0$ are no longer true at high SNR. This is the disadvantage of the CT scheme.

4.4.3 Performance calculation

We neglect the probability that an arrived packet is lost due to the collision with another earlier arrived packet at the receiver. From [22], the probability P_L of packet

loss is given by

$$P_L = 1 - (1 - P_B)P_d P_{cd} \tag{4.21}$$

where P_B is the probability of the receiver being blocked by the earlier occurred false alarms caused by noise, P_{cd} is the probability of the successful coincidence detection. P_d for the ATC scheme is given by (4.10). For the CT scheme P_d is replaced by P_d' in (4.18).

P_B can be estimated as

$$\begin{aligned} P_B &= \bar{F}/(\bar{A} + \bar{F}) \\ &= \frac{\alpha}{1+\alpha} \end{aligned} \tag{4.22}$$

where $\alpha = \bar{F}/\bar{A}$, $\bar{F}$ is the average receiver blocking time, in which an arrived packet will be blocked and lost, and $\bar{A}$ is the average idle time between two consecutive false alarms, in which the receiver is available for packets.

From section 4.2, we see that the receiver will be busy for $L+1$ PN periods after a false acquisition provided that no false coincidence occurs subsequently. If a false coincidence occurs, the receiver will be unavailable for a time period equal to the packet length. Thus the receiver blocking time is at least $L+1$ PN periods. The average blocking time $\bar{F}$ can be determined from

$$\begin{aligned} \bar{F} &= (1 - P_{fcn})(L+1)T + P_{fcn}(L+1+L_D)T \\ &= (L+1)T + P_{fcn}L_D T \end{aligned} \tag{4.23}$$

where the probability of the false coincidence detection P_{fcn} is given by

$$P_{fcn} = \sum_{k=l}^{L} \binom{L}{k} P_{fc}^k (1 - P_{fc})^{L-k} \tag{4.24}$$

The false alarm by noise alone is modeled as a Poisson process with arrival rate $\lambda_f = P_{fan}/T_c$. Since the inter-arrival times of a Poisson process are i.i.d. exponential, the

average idle time can be obtained from

$$\bar{A} = 1/\lambda_f = \frac{T_c}{P_{fan}} \tag{4.25}$$

Substitute $\bar{F}$ and $\bar{A}$ into α, we have

$$\alpha = P_{fan}(L + 1 + P_{fcn}L_D)m \tag{4.26}$$

Finally, the probability P_{cd} of the successful CD test is simply

$$P_{cd} = \sum_{k=l}^{L} \binom{L}{k} P_c^k (1 - P_c)^{L-k} \tag{4.27}$$

where the probability P_c that the ED output at each correct CD test epoch exceeds the threshold b_c is given by

$$P_c = Q(\sqrt{2\gamma_o},\ b_c) \tag{4.28}$$

4.4.4 Thresholds selection for desired performance characteristics

From (4.21), since P_d (or P_d'), $P_{cd} \leq 1$, P_L can never be less than P_B, i.e. P_L is lower-bounded by P_B. The system designer can select a desired $P_B \ll 1$ by an appropriate choice of b_0 and b_c, while the overall performance or the dynamic range is optimized. Typical values of P_B may be in the range 10^{-3} to 10^{-6}. Practically b_0 and b_c can be easily determined by observing the performance curves of P_L versus SNR for different pairs of $(b_0,\ b_c)$, and selecting the pair corresponding to the best P_L.

Ideally, at each SNR there exists a pair of thresholds (b_0, b_c) which would produce minimum packet loss probability: the larger the SNR, the larger the optimal thresholds. The problem can be taken as the following unconstrained optimization form

$$\min\ P_L(b_0, b_c), \quad b_0 \text{ and } b_c \geq 0 \tag{4.29}$$

at the given SNR. For situations in which the SNR of received packets cannot be easily estimated or obtained, the ATC scheme for a fixed P_B would be the best choice. However, the minimum P_L evaluated from (4.29) serves as a benchmark for performance comparisons. The procedure used to solve the stated minimization problem is described in the appendix F.

4.5 Numerical results

In this section, we illustrate the performance of the proposed acquisition scheme for $L = 8$ and $L_D = 1000$ with a set of $m = 127$ chip Gold sequences as the preamble PN codes. First we show how to determine b_0 and b_c to achieve the best overall performance for the ATC acquisition scheme. Second, since P_d, P'_d, P_f and P'_f are the key parameters which dominate the overall performances of both the ATC and the CT schemes, the performance comparison of the two schemes is shown by plotting P_d, P'_d, P_f and P'_f versus SNR. This is followed by the performance comparison given by P_L. Finally, the optimal thresholds for both schemes are calculated and the corresponding optimal performances are shown.

Figure 4.5 shows results of P_L for various values of input SNR γ_{in} from -10 to $-2dB$ with l_3 and b_c as parameters. b_0, b_c and l are selected such that $P_B = 10^{-3}$. The best choice of b_0 and b_c can be determined from the figures for each given l. For example, $b_0 = 5.28$ and $bc > 2.0$ yield the best performance for $l = 6$. It is noted that b_c is not sensitive to P_L as long as it is large enough to make the false coincidence detection probability P_{fc} small enough so that $L + 1 \gg P_{fcn} L_D$. In such a case, α given by (4.26) will reduce to $\alpha = P_{fan}(L + 1)m$, and P_B will only depend on b_0. Further increasing b_c will not reduce b_0 anymore, but may lessen P_c in (4.28) and, therefore, raise P_L. Also note that the lower bound P_3 cannot be reached at any point by the conventional CT scheme due to the false acquisitions.

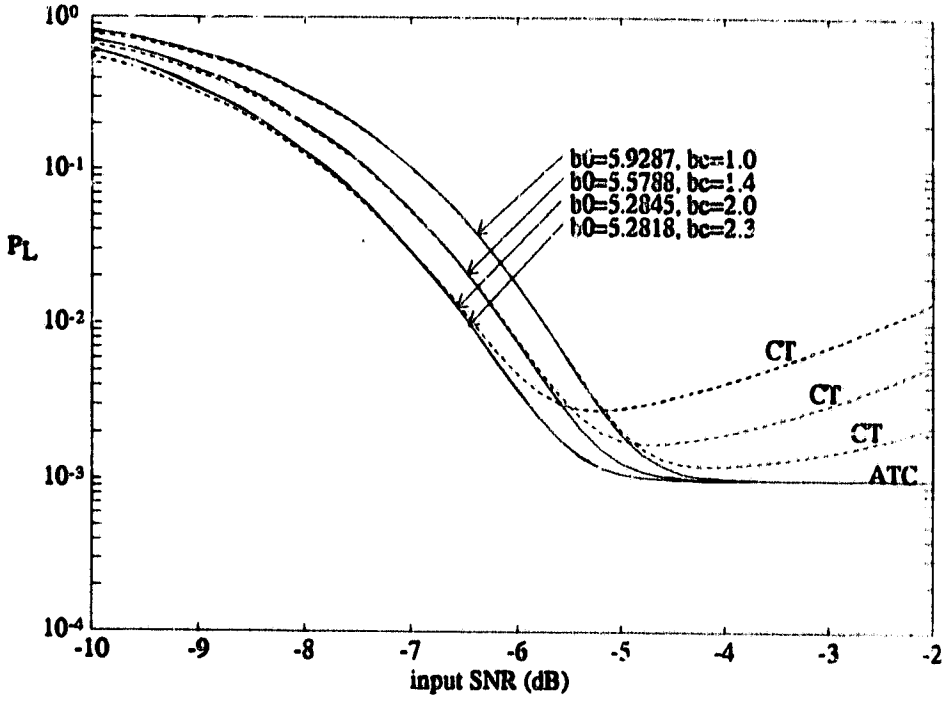

Figure 4.5: Probability of packet loss versus SNR for different thresholds b_0 and b_c. $P_B = 10^{-3}$, $L_D = 1000$, $L = 8$, and $l = 6$.

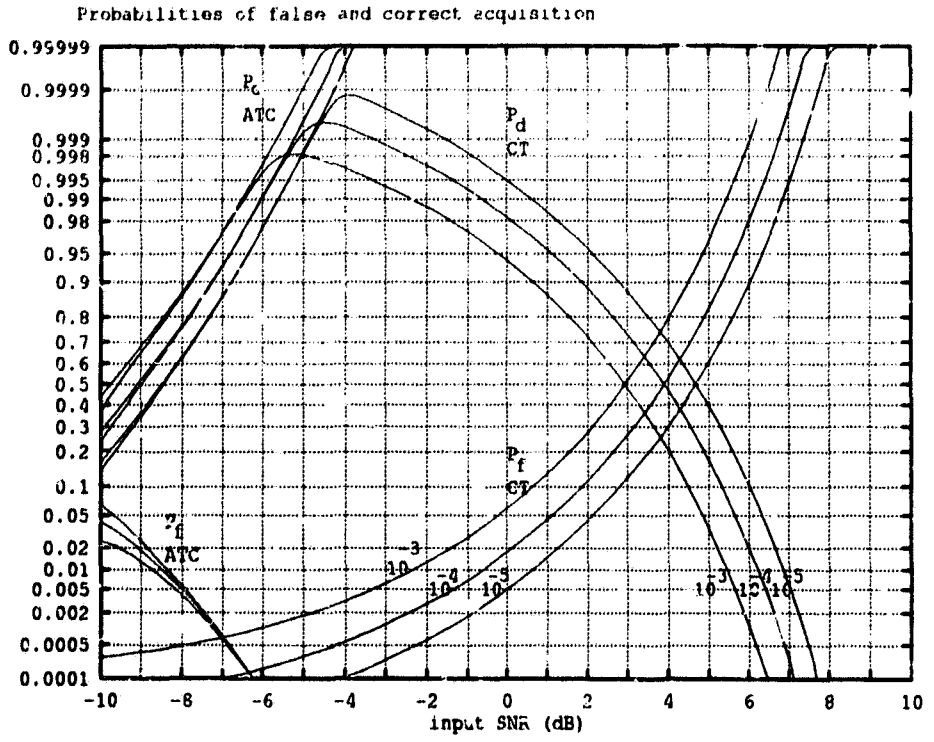

Figure 4.6: Probabilities of false and correct acquisition for ATC and CT with P_B as a parameter.

Figure 4.6 shows the false and correct acquisition probabilities for the ATC and CT systems with parameter P_B equal to $10^{-3}, 10^{-4}$ and 10^{-5}. The acquisition threshold b_0 for the calculations of P_d and P_f is determined by using the procedure described in the previous paragraph for each given P_B. From figure 4.6, we can see that, at very low SNR, P_f for CT is smaller than that for ATC. This is probably due to the fact that the ATC algorithm is able to compare $2m-1$ correlation samples ($m-1$ samples each before and after the actual correlation peak Z_m) and the CT algorithm actually chooses the first sample which exceeds b_0 from the first m correlation samples. At very low SNR, the sidelobes are more likely to be larger than the mainlobe, thus the ATC algorithm has a larger probability that a sidelobe is larger than the mainlobe. More specifically, if $Z_m > b_0$ is larger

than $Z_i < b_0, i = 1, 2, ..., m-1$, the CT algorithm will be successful with the acquisition in this case, but the ATC algorithm will continue to compare Z_m with $Z_i, i = m+1, m+2, ..., 2m-1$, and choose the largest one which may not be Z_m. As SNR goes up, P_f for ATC will drop down sharply since Z_m is more likely to be larger than the sidelobes around it, while P_f for CT will rise gradually since the absolute values of the sidelobes before Z_m are more likely to exceed b_0. Many packets will be lost due to this behavior of P_f for the CT scheme. On the other hand, the proposed ATC acquisition scheme maintains the ideal feature which is $P_d \to 1$ and $P_f \to 0$, even for signals with a large dynamic range of SNR.

The difference between the two acquisition schemes can also be seen by comparing the overall performance in terms of P_L for the two schemes. Figure 4.7 shows P_L for $P_B = 10^{-3}, 10^{-4}$, and 10^{-5} for the ATC scheme as well as the CT scheme.

A significant difference between the two schemes can be seen from this figure. At low but practical values of SNR such that $P_L < 10^{-2}$, performances of the two schemes are almost the same, which are dominated by the probability of missing acquisition. For the ATC receiver, this means that no detection windows were opened after the whole PN_1 has passed through the matched filter. At high SNR, the ATC performance is dominated by P_B, since $P_d \to 1$ and $P_{cd} \to 1$, whereas the performance of the CT scheme highly depends on the partial correlations of the preamble sequences. Since the absolute values of the partial correlations go up as SNR increases, the probability of the acquisition at any incorrect position before the right one rises, which results in poor performance (small P_d') at high SNR and makes it impossible for practical applications.

As described in section 4.4, if energies or SNR of received packets can be estimated quickly enough, the optimal performances can be achieved by using the optimal thresholds which are obtained by minimizing P_L with respect to b_0 and b_c. Optimal P_L of the ATC and CT schemes versus SNR are drawn in figure 4.7. Their

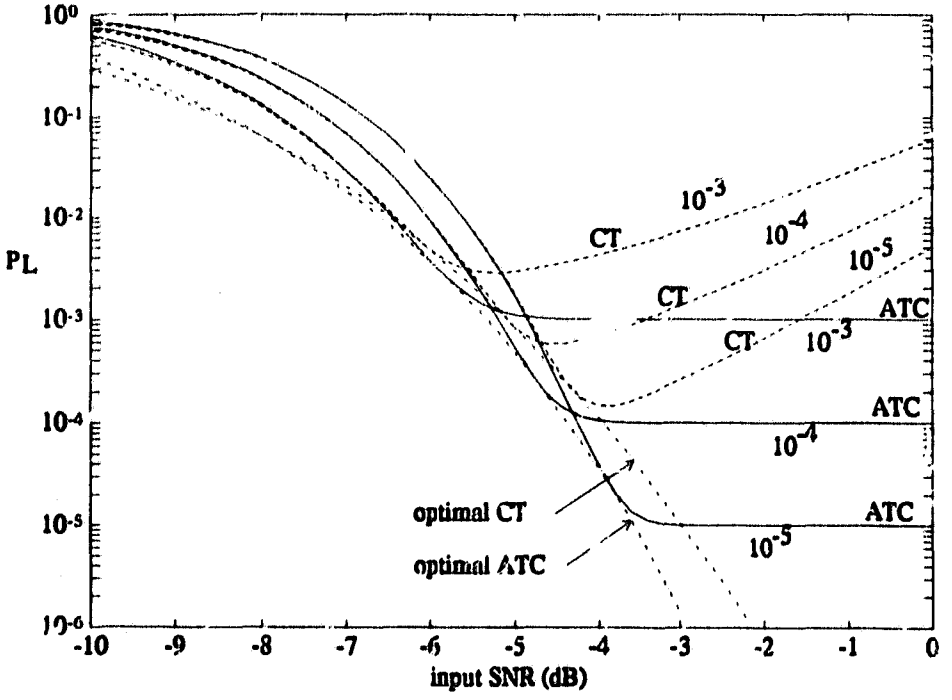

Figure 4.7: Performance comparison of ATC, CT and their optimal versions with P_B as a parameter

performances serve as the lower bounds of their own nonoptimal counterparts. It is seen that the optimal ATC scheme also yields better performance than the optimal CT scheme.

4.6 Summary

In spread spectrum packet radio communications, fast and reliable acquisition is highly desirable. For this purpose, the acquisition threshold must be controlled in such a way that the false acquisition probability is minimized and the correct acquisition probability is maximized, especially in the case of large input signal dynamic range. This is critical for the short preambles in packet radio systems,

where not many PN periods are available for the threshold adjustment. In this chapter, a simple automatic threshold control (ATC) scheme for the acquisition is proposed and analyzed. The ATC algorithm guarantees the perfect threshold setting in one PN period by means of a properly designed detection window, thus the method is suitable for packet radio systems. The analysis shows that the acquisition performance by the ATC algorithm remains a constant value no matter how large the input signal is. Using the conventional constant threshold (CT) scheme, the performance will degrade when input signal amplitude goes up.

In this chapter, we make the analysis for the single acquisition code case. In practice, the ATC scheme can be also combined with the scheme using multiple acquisition codes to improve performance at low SNR.

The proposed method also has potential to improve acquisition performance in CDMA systems, where the effect of the multiuser interference can be minimized as long as the interference-contaminated auto-correlation values of the desired packet is not less than the values of the cross-correlation sidelobes caused by those interfering packets.

Chapter 5

Multiuser Detection in Synchronous CDMA

5.1 Introduction

In the previous chapters, we discussed acquisition techniques by assuming that AWGN is the only noise or interference to the transmitted packet. In practice, a common transmission media is often shared by many users. The three commonly used methods for users to share a given frequency band are Frequency Division Multiple Access (FDMA) , Time Division Multiple Access (TDMA) and Code Division Multiple Access (CDMA). CDMA is the natural product of using spread spectrum modulation and demodulation. It has been found useful in many communication applications such as satellite networks, mobile and indoor communications, and optical networks, because it has the ability to resist a variety of interference and the potential to allow a larger number of users to share a common frequency band [39]. In such a system, each user is assigned an identification code, from which the user's message can be extracted. On the other hand, a packet will more or less suffer interference from other simultaneously transmitted packets because the assigned

codes are often non-orthogonal. In this situation, the acquisition and demodulation of a packet will be more difficult. The conventional acquisition and demodulation schemes often fail when a large number of users are sharing a single channel. In the following three chapters, we will study the detection and acquisition methods in CDMA systems. In this chapter and the following chapter, we will focus on the multi-user detection problem by assuming that acquisitions for all active users have been obtained. In the last chapter, acquisition methods will be presented and analyzed.

In spread spectrum CDMA systems, the detection of a user's message from the mixture of all users' waveforms can be classified into three types. The first one is the conventional approach which only uses one specific user's code to correlate with the received signal. In this approach, information about the mutual interference among users is ignored. Thus the method is vulnerable to the near-far effects and is only useful for the case of low bandwidth efficiency [50] where the identification codes can be designed such that the inter-user interference is negligible. The second type of detection is the optimal approach in which each user's message can be extracted by solving a maximization problem [25]. Although a significant performance improvement can be obtained by this method, the associated computational complexity increases exponentially with the number of users, thus making it impractical. The last type of detection consists of those suboptimal approaches which can yield better performance than the conventional one, especially in the sense of near-far resistance. Although their performance cannot be better than the optimal one, the computational complexity is significantly reduced. One of the suboptimal linear approaches is the so-called decorrelating detector [40] which has been proved to be optimal (near-far resistant) when energies for the users are unknown to the receiver [25].

From chapter 7 , we will see that a real time estimation of energies of all signals

received is possible by our acquisition schemes. With the information of energies of the received signals, the optimal detector will significantly outperform the decorrelating detector. Therefore, it is worthwhile to study the suboptimal detectors in this case. Furthermore, since the synchronous system is a special case of the asynchronous system [50], the study of suboptimal detectors in the synchronous system is essential for further studies of suboptimal detectors in asynchronous systems. In the next chapter, multiuser detection problem in asynchronous systems will be studied.

In [50] it is indicated that the linear approaches hinder the achievement of near-optimal performance for the demodulation of relatively weak signals, and thus a nonlinear approach called multistage detector was proposed. A significant improvement is obtained by this method compared to the linear detectors in [25]. In addition, the computational complexity grows linearly with the number of users. For this method, the maximization of an integer (-1,1) quadratic problem with K dimensions is approximated by K unidimensional maximization problems at each stage or iteration. Thus the maximization simply turns out to be a comparison of the objective function values with a single variable or element equal to 1 and -1. In many cases, the final decisions from the unidimensional optimization cannot be guaranteed to converge to the optimal solution. Furthermore, the performance cannot be improved by increasing the number of stages or iterations.

In this chapter, a new nonlinear multistage approach is proposed. Better performance can be obtained by the new scheme with only a slight increase in the computational complexity compared to the method in [50]. In the next section, the optimal detector is reviewed. The basic transformations are presented in section 5.3. A continuous approach for the optimal 0-1 solution is presented in section 5.4 followed by two algorithms developed from this approach in sections 5.5, 5.6 and 5.7. In section 5.8, some numerical results are illustrated for the new method and other methods. The summary of the chapter is provided in section 5.9.

5.2 Optimal detector

In this section, we briefly describe the optimum solution of the multiuser detection problem in CDMA. Based on the optimal detector, the suboptimal detector can be developed in the followed sections.

For a K-user synchronous CDMA system, at each receiver, the received signal in a symbol duration can be written as

$$r(t) = \sum_{k=1}^{K} b_k s_k(t) + n(t) \tag{5.1}$$

where $s_k(t)$ denotes the signature waveform for the kth packet and is time limited to a bit duration T, $b = [b_1\ b_2\ ...\ b_K]^T \in \{-1,1\}^K$ contains all the users' bits for the symbol, i.e. $b_k = -1$ or 1 represents the kth user's bit, and $n(t)$ represents the additive white Gaussian noise with a spectral density equal to σ^2. It is more convenient to express the above signal using the following discrete form

$$r = \bar{H}b + n \tag{5.2}$$

where $\bar{H} = [s_1\ s_2\ ...\ s_K] \in R^{m\times K}$ contains the amplitudes and the identification codes of all the received signals with s_k being the kth user's signature waveform. The number of chips m in a symbol or the number of elements in each column vector s_k must be greater than K with $m \approx K$ representing high bandwidth efficiency cases. $n = [n_1\ n_2\ ...n_m]^T \in R^{m\times 1}$ is a sample vector from the AWGN $n(t)$.

The optimal decision for the K user's data bits b is obtained by solving the problem [50] [25]

$$\min_{\hat{b}\in\{-1,1\}^K} f(\hat{b}) = \|r - \bar{H}\hat{b}\|^2 \tag{5.3}$$

Although this problem is similar to the well-known Least-Squares (LS) problem, the solution with the constraint $\hat{b} \in \{-1,1\}^K$ will be different from that of the LS problem in general. The quadratic form of the above problem is

$$\min_{\hat{b}\in\{-1,1\}^K} f(\hat{b}) = \frac{1}{2}\hat{b}^T C\hat{b} - y^T\hat{b} \tag{5.4}$$

where vector $y = \bar{H}^T r$ represents K decisions from K conventional receivers, $C = \bar{H}^T \bar{H}$ is the correlation matrix of the K users, which is a $K \times K$ positive definite matrix.

While the above problem is known to be NP-hard [25], the computational load for some suboptimal approaches is only linear with the number of users. In what follows, we present our new suboptimal scheme.

5.3 Basic transformations

To better understand the theorem in the following sections for the development of the new multistage detector, we describe two basic transformations in this section.

First we transfer the problem in (5.4) into an equivalent 0-1 optimization problem, in which 0 and 1 in the transferred function correspond to -1 and 1, respectively, in the original problem.

Letting $x = \frac{\hat{b}+e}{2}$, where K-dimensional vector $e = [1\ 1\ ...\ 1]^T$, the ith element of x is then

$$x_i = \begin{cases} 0 & \hat{b}_i = -1 \\ 1 & \hat{b}_i = +1 \end{cases} \tag{5.5}$$

It is easy to verify that the minimization problem (5.4) is equivalent to

$$\min_{x \in \{0,1\}^K} \{f(x) = \frac{1}{2} x^T Q x + z^T x\} \tag{5.6}$$

where $z = -2(Ce + y)$, and $Q = 4C$. Q is often called Hessian matrix of $f(x)$ [1].

Furthermore, for any given diagonal matrix

$$\Phi = \text{diag}\{\phi_1\ \phi_2\ ...\ \phi_K\} \tag{5.7}$$

[1]The Hessian matrix of $f(x)$ is defined as $Q(x) = \nabla\{\nabla f(x)\}$, if $f(x)$ has continuous second-order partial derivatives.

and a vector made up of the diagonal elements

$$\phi = [\phi_1 \ \phi_2 \ ... \ \phi_K]^T \tag{5.8}$$

it can be shown that the problem

$$\min_{x \in \{0,1\}^K} \{f(x) = \frac{1}{2} x^T \} \bar{Q} x + \bar{z}^T x \tag{5.9}$$

is equivalent to (5.6), where $\bar{Q} = Q - \Phi$ and $\bar{z} = z + \frac{1}{2}\phi$. The equivalence holds because the transformation does not affect the function values at any of the zero-one solutions. It should be noted that the continuous minimum (or the LS solution without the constraint) of the transformed quadratic function is changed.

5.4 Continuous approach to the 0-1 solution

Carter [3] proposed an iterative method to find a basic transformation, such that the continuous minimum solution of the transformed quadratic function can draw nearer to the zero-one minimum solution after each iteration.

The idea is based on the fact that the transformed continuous function minimum $f(\hat{x})$ is bounded by the function value $f(x^I)$, where $\hat{x}$ and x^I are the solutions for the continuous and 0-1 minima, provided that $\bar{Q}$ is positive definite. If the two minima are equal, the continuous solution will be the 0-1 solution. As the continuous minimum $f(\hat{x})$ approaches to the 0-1 one $f(x^I)$, the continuous solution $\hat{x}$ should tend to approach x^I. Figure 5.1 shows such a situation with a one dimensional quadratic function as the objective function. The parameters $q = 2$ and $z = 1.5$ are scalers in this case. From this figure, it is clearly shown that the original function is modified by different values of the parameter ϕ. The continuous minimum is changed whenever a new ϕ is assigned. However, all the continuous minimum values are upper-bounded by the 0-1 minimum which is zero in this case provided that

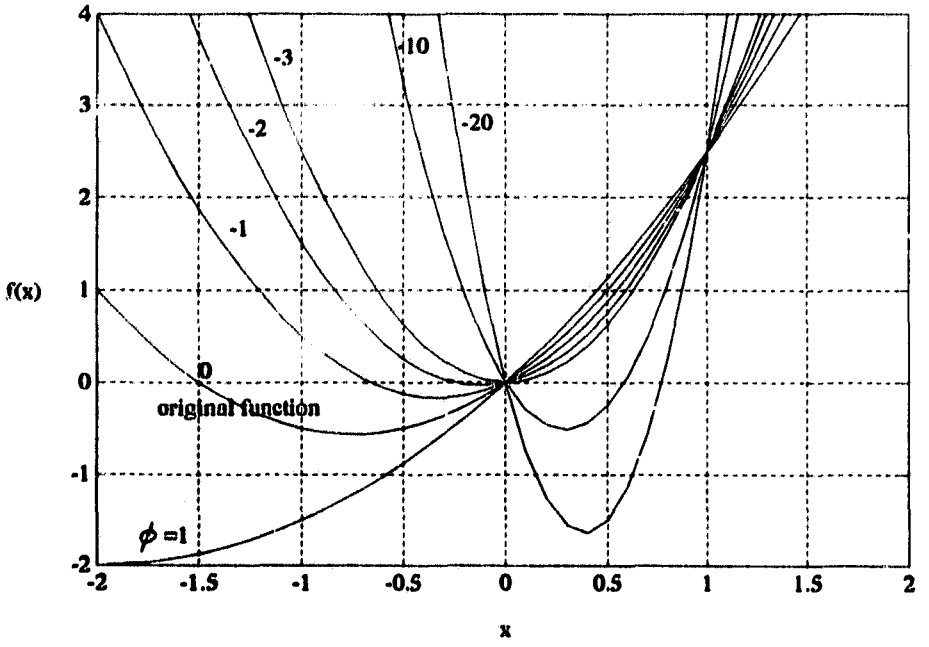

Figure 5.1: One dimensional quadratic function with q=2 and z=1.5

$\bar{q} = q - \phi \geq 0$. When ϕ approaches -3, the continuous solution is getting closer to the 0-1 solution.

An immediate question for this idea is how to find a transformation such that the distance between the corresponding continuous minimum $f(\hat{x})$ and the optimal 0-1 minimum $f(x^I)$ is minimized, while maintaining the transformed Hessian matrix $\bar{Q}$ positive definite.

One answer can be found with the help of the following theorem [3].

Theorem 1. Let Q be the positive definite Hessian matrix of a function f and $\hat{x}$ be the real-valued unconstrained minimum of f. Suppose the ith diagonal element of Q is decreased by ϕ_i; then the unconstrained minimum of the new function will change by [3]

$$\Delta f = \frac{\phi_i}{2}\left[\frac{(\frac{1}{2} - \hat{x}_i)^2}{(\phi_i g_{ii} - 1)} + \frac{1}{4}\right] \tag{5.10}$$

where g_{ii} represents the ith diagonal term of Q^{-1}. The theorem assumes that ϕ_i is

chosen properly such that the new function is still positive definite.

Proof: Given the system

$$Q\hat{x} = -z \text{ or } \hat{x} = -Q^{-1}z \tag{5.11}$$

the modified system is written as

$$\bar{Q}\bar{x} = -\bar{z} \text{ or } \bar{x} = -\bar{Q}^{-1}\bar{z} \tag{5.12}$$

where $\bar{Q} = Q - \phi_i e_i e_i^T$ and $\bar{z} = z + \frac{1}{2}\phi e_i$. The unit vector e_i has a '1' in the ith position and '0' elsewhere.

The two minima for the two systems are $-\frac{1}{2}z^TQ^{-1}z$ and $-\frac{1}{2}\bar{z}^T\bar{Q}^{-1}\bar{z}$. Therefore,

$$\Delta f = -\frac{1}{2}\bar{z}^T\bar{Q}^{-1}\bar{z} + \frac{1}{2}z^TQ^{-1}z \tag{5.13}$$

From the Householder [15] identities for a rank-one update of a matrix, we get

$$\begin{aligned}\bar{Q}^{-1} &= Q^{-1} - \psi Q^{-1}e_i e_i^T Q^{-1} \\ &= Q^{-1} - \psi g_i g_i^T \end{aligned} \tag{5.14}$$

where

$$\psi = \phi_i/(\phi_i g_{ii} - 1) \tag{5.15}$$

and g_i represents column i of the inverse of Q. Substitute $\bar{Q}^{-1}$ and z into 5.13 and performing some manipulations, we get

$$\Delta f = -\frac{1}{2}[\phi_i g_i^T z + \frac{1}{4}\phi_i^2 g_{ii}] + \frac{\psi}{2}[z^T g_i g_i^T z + \phi_i g_{ii} g_i^T z + \frac{1}{4}\phi_i^2 g_{ii}^2] \tag{5.16}$$

Since $g_i^T z = z^T g_i = -\hat{x}_i$, the above equation can be further simplified

$$\begin{aligned}\Delta f &= \frac{\psi}{2}[\hat{x}_i^2 - \phi_i g_{ii}\hat{x}_i + \frac{1}{\psi}\phi_i\hat{x}_i + \frac{1}{4}\phi_i^2 g_{ii}^2 - \frac{1}{4\psi}\phi_i^2 g_{ii}] \\ &= \frac{\psi}{2}[\hat{x}_i^2 - \phi_i(g_{ii} - \frac{1}{\psi})\hat{x}_i + \frac{\phi_i^2}{4}(g_{ii} - \frac{1}{\psi})g_{ii}] \\ &= \frac{\psi}{2}[(\frac{1}{2} - \hat{x}_i)^2 + \frac{\phi_i g_{ii} - 1}{4}] \\ &= \frac{\phi_i}{2}[\frac{(\frac{1}{2} - \hat{x}_i)^2}{\phi_i g_{ii} - 1} + \frac{1}{4}] \qquad \square \end{aligned} \tag{5.17}$$

The parameters for the modified system are summarized as follows

$$\bar{Q} = Q - \phi_i e_i e_i^T \tag{5.18}$$

$$\bar{z} = z + \frac{1}{2}\phi_i e_i \tag{5.19}$$

$$\bar{Q}^{-1} = Q^{-1} - \psi g_i g_i^T \tag{5.20}$$

$$\hat{x} = \hat{x} + \chi \tag{5.21}$$

ψ and χ are computed by

$$\psi = \frac{\phi_i}{(\phi_i g_{ii} - 1)} \tag{5.22}$$

$$\chi = \psi g_i (\frac{1}{2} - \hat{x}_i) \tag{5.23}$$

The following corollary gives the condition for the new Hessian $\bar{Q}$ to be positive definite.

Corollary: In the theorem above, the new Hessian matrix $\bar{Q}$ will always be positive definite provided ϕ_i is less than $1/g_{ii}$.

Proof: The proof of this corollary relies on the assumption that the eigenvalues of a matrix are a continuous function of the changes in the diagonal elements. Consider the Householder identity in (5.14) and observe that the new inverse exists if and only if ψ exists. From (5.15) $\psi = \phi_i/(\phi_i g_{ii} - 1)$ and ψ is undefined only when $\psi = 1/g_{ii}$.

Furthermore, ψ is undefined if and only if at least one eigenvalue is zero. Consequently, for $\psi < 1/g_{ii}$, all eigenvalues must still be positive. □

By maximizing Δf with respect to ϕ_i, the function minimum $f(\hat{x})$ will approach $f(x^I)$ at the fastest rate. The following theorem describes the 'optimum' strategy for choosing ϕ.

Theorem 2: The increase in the function value at the minimum of the new function is maximized when

$$\phi_i = \begin{cases} 2\hat{x}_i/g_{ii} & \text{for } \hat{x}_i \leq \frac{1}{2} \\ 2(1-\hat{x}_i)/g_{ii} & \text{for } \hat{x}_i > \frac{1}{2} \end{cases} \tag{5.24}$$

In the case of $\hat{x}_i = 1/2$, the function is maximized when ϕ_i equals infinity. But, in order to maintain positive definiteness, ϕ_i must be chosen less than $1/g_{ii}$.

The corresponding increase in the minimum function value is given by

$$\Delta f = \begin{cases} \hat{x}_i^2/(2g_{ii}) & \text{for } \hat{x}_i \leq \frac{1}{2} \\ (1-\hat{x}_i)^2/(2g_{ii}) & \text{for } \hat{x}_i > \frac{1}{2} \end{cases} \tag{5.25}$$

and the ith component of the new function minimum will be

$$\hat{x}_i = \begin{cases} 0 & \text{for } \hat{x}_i < \frac{1}{2} \\ 1 & \text{for } \hat{x}_i > \frac{1}{2} \\ 1/2 & \text{for } \hat{x}_i = \frac{1}{2} \end{cases} \tag{5.26}$$

The new function will always be positive definite.

Proof: The result is obtained by computing the value of ψ which maximizes Δf in (5.13) with the condition $\psi < 1/g_{ii}$. □

5.5 Multistage detector

Based on the theorem in the previous section, a new multistage detection algorithm is proposed. Let $\hat{x}$ be the continuous minimum at stage i, the corresponding 0-1 solution denoted as $\hat{x}^I$ is obtained by taking the binary quantization of $\hat{x}$. $\hat{x}^I$, which has the smallest function value $f(\hat{x}^I)$ in up to i iterations, is stored in x_m. The

corresponding function value $f(\hat{x}^l)$ is stored in f_m. At the $(i+1)$st stage, $\hat{x}^l$ is updated using the following algorithm.

Algorithm 1. Multistage detection.

1. For $j = 1$ to K,

$$\text{Let} \quad t_j = \begin{cases} \hat{x}_j & \text{if } \hat{x}_j \leq 0.5 \\ (1 - \hat{x}_j) & \text{if } \hat{x}_j > 0.5 \end{cases}$$

2. Find the index p such that $|t_p| = \max_{j=1}^{K} |t_j|$, i.e. $\hat{x}_p$ is the component of the current minimum which is furthest away from a 0-1 value.

3. Compute

$$\phi_p = 2t_p/g_{pp}$$

$$q_{pp} = q_{pp} - \phi_p; \quad z_p = z_p + \frac{1}{2}\phi_p$$

$$\psi = \phi_p/(\phi_p g_{pp} - 1)$$

$$\hat{x} = \hat{x} + \psi g_p(0.5 - \hat{x}_p)$$

$$\hat{x}^l = \frac{sign(\hat{x} - 0.5) + 1}{2}$$

$$Q^{-1} = Q^{-1} - \psi g_p g_p^T$$

$$f(\hat{x}^l) = \frac{1}{2}(\hat{x}^l)^T Q \hat{x}^l + z^T \hat{x}^l$$

4. if $f(\hat{x}^l) < f_m$, $f_m = f(\hat{x}^l)$ and $x_m = \hat{x}^l$. Repeat from 1 until the L_1th stage.

For this algorithm, there is no need to compute the inverse of Q at each iteration. Thus the dominant operation is given by the computation of $f(\hat{x}^l)$ for each iteration or stage. For a L_1-stage detector, the algorithm needs at most L_1 evaluations of the objective function value under each 0-1 solution. Because some of the solutions at different stages may be the same, there is no need to evaluate their function values every time.

For some sufficient statistics y or z, algorithm 1 will quickly converge to the optimal 0-1 point. For some other cases of y, the optimal 0-1 point is often among the quantized solutions at different stages. And the point is selected by comparing $f(\hat{x}^l)$ at all the stages.

5.6 Convergence of the multistage detector

By simulation trials with different input data y containing information bits from each user and Gaussian noise, we have found that the improvement in terms of bit error rate for a specific user is significant with the new multistage detector compared to the one in [50]. However, the performance difference between the new detector and the optimal one is usually not small. This implies that in many cases the algorithm cannot bring the continuous minima close enough to the integer solution. In these situations, the continuous minimum $\hat{x}$, as the iteration continues, will oscillate among a few points and never converge to the optimal integer point, no matter how many iterations are conducted. In this section, we will explain why the algorithm sometimes does not converge to a 0-1 solution. Based on the analysis, a modified multistage algorithm is proposed.

From section 5.3, we know that the basic transformation by Φ and ϕ cannot affect the function values at any of the 0-1 points. An observation in [13] can

be used to explain why the algorithm sometimes is not convergent. In [13], it is shown that for any $x^* = \{x_1^* \; x_2^* \; ... \; x_K^*\} \in \{0,1\}^K$, we can construct a unique $\phi^* = \{\phi_1^* \; \phi_2^* \; ... \; \phi_K^*\} \in R^K$, such that $x^* = -(\bar{Q}^*)^{-1}\bar{z}^*$, where $\bar{Q}^* = Q - \Phi^*$, and $\bar{z}^* = z + \frac{1}{2}\phi^*$. ϕ^* is given by

$$\phi_i^* = 2(2x_i^* - 1)(z_i + \sum_{j \in I_1(x^*)} q_{ij}) \qquad i = 1, \; 2, \; ... \; K. \tag{5.27}$$

where $I_1(x^*) = \{i | x_i^* = 1\}$. If $\bar{Q}^*$ for a specific x^* is positive semi-definite, the x^* will be the continuous minimum for the unimodular function $f(x) = \frac{1}{2}x^T\bar{Q}^*x + (\bar{z}^*)^T x$. Thus the continuous minimum is the optimal 0-1 minimum. It can be proved that any of the unique transformed matrices $\bar{Q}^*$ derived from (5.27) for the other $2^K - 1$ x^* must be indefinite. The algorithm in the last section is performed to maximize the function minimum at each iteration and, at the same time, the new Hessian $\bar{Q}$ remains positive definite, thus the value of the maximized function minimum cannot decrease. Since the minima are upper bounded by the $f(x^*)$, the algorithm is bound to converge to the unique solution $f(x^*)$, or $\bar{Q} \rightarrow \bar{Q}^*$.

However, if no $\bar{Q}^* \geq 0$ can be found for all $x^* \in \{0,1\}^K$, no such a global minimum exists, and the transformed function is no longer unimodular. The unique 0-1 solution cannot be exactly approached by the algorithm because the transformed Hessian matrix at every stage cannot be indefinite. Rounding off the continuous minimum and selecting the best among all of the iterations will sometimes cause errors.

Whether or not $\bar{Q}^*$ corresponding to the 0-1 minimum, is positive semi-definite, will highly depend on the noise component contained in y or z as well as the structure of Q. When noise is zero, it is easy to verify that $\phi_i^* = 0$ for all $i = 1, 2, ..., K$, and $\bar{Q}^* = Q$ which is positive definite. As noise increases, the possibility for the $\bar{Q}^*$ being indefinite is increased. Q itself depends on the cross-correlations of the users' id codes and the distribution of all the received signal powers. It is found that Q with larger cross-correlations will more likely cause the $\bar{Q}^*$ for the 0-1 minimum to

be indefinite.

5.7 Modified multistage detector

A modified algorithm is proposed to obtain successful convergence when Q^* for the 0-1 minimum is indefinite. The objective of the algorithm is to single out some elements of z which cause the $\bar{Q}^*$ to be indefinite. Such elements may be excluded from the consideration in the algorithm, and the $\bar{Q}^*$ for the reduced problem will often become positive definite. Then the problem can be solved by the continuous approach again. To find such elements, we present the following example for a five-user CDMA system.

Example: For the problem defined by (5.9) with $Q = 4C$, let

$$Q = \begin{bmatrix} 50.48 & -5.11 & 15.32 & 15.32 & -25.53 \\ -5.11 & 25.30 & -3.61 & 10.84 & -3.61 \\ 15.32 & -3.61 & 25.30 & -3.61 & -3.61 \\ 15.32 & 10.84 & -3.61 & 25.30 & -3.61 \\ -25.53 & -3.61 & -3.61 & -3.61 & 25.30 \end{bmatrix}$$

$$z = [-26.18 \ -8.69 \ -35.20 \ -14.54 \ \ 4.18]^T$$

Then $\bar{\phi}^*$ computed from (5.27) with the optimal 0-1 solution $x^* = [1 \ 1 \ 1 \ 0 \ 1]$ is

$$\bar{\phi}^* = [17.97 \ \ 8.56 \ -3.63 \ -8.79 \ -6.55]^T$$

Table 5.1: Results for the example (j = number of a stage)

j	$\hat{x}$					$f(\hat{x})$
0	(-0.45	0.02	1.79	1.06	-0.21)	-33.86
1	(0.48	0.55	1.00	0.27	0.58)	-30.86
2	(0.00	0.25	1.15	0.65	0.13)	-30.11
3	(-0.44	-0.03	1.28	1.00	-0.28)	-30.09
4	(0.00	0.25	1.15	0.65	0.13)	-30.08
5	(-0.43	-0.03	1.28	1.00	-0.28)	-30.07

and

$$\bar{Q}^* = \begin{bmatrix} 32.50 & -5.11 & 15.32 & 15.32 & -25.53 \\ -5.11 & 16.74 & -3.61 & 10.84 & -3.61 \\ 15.32 & -3.61 & 28.93 & -3.61 & -3.61 \\ 15.32 & 10.84 & -3.61 & 34.08 & -3.61 \\ -25.53 & -3.61 & -3.61 & -3.61 & 31.85 \end{bmatrix}$$

which is indefinite with the eigenvalues as $\{40.43\ 15.11\ 24.19\ -3.09\ 67.46\}$. The results for five iterations by algorithm 1 is illustrated in table 5.1.

The algorithm is not convergent, because $\hat{x}$, as the iteration goes on, will jump back and forth around two points $[0.00\ \ 0.25\ \ 1.15\ \ 0.65\ \ 0.13]$ and $[-0.43\ \ -0.03\ \ 1.28\ \ 1.00\ \ -0.28]$. The elements 1 and 4 are the most unstable elements because, whenever they are forced to be 0 and 1, they will go farthest away from 0 and 1 at the next iteration. Let $\hat{x}^0$ denote the element bumping with 0 and $\hat{x}^1$ with 1. In this example, $\hat{x}^0$ is the first element of $\hat{x}$ and $\hat{x}^1$ the fourth element. Often the correct decisions for $\hat{x}^0$ and $\hat{x}^1$ are 1 and 0, respectively instead of 0 and 1. If we force $\hat{x}^0$ to be 1 in $\hat{x}$, or $\hat{x}^1$ to be 0, and substitute it into the original function $f(x)$, the reduced function may have a positive definite $\bar{Q}^*$ corresponding the 0-1

minimum. Using the same continuous approach, the algorithm will converge to the unique 0-1 solution. Assuming that the jth element $\hat{x}_j$ of $\hat{x}$ is $\hat{x}^0$ or $\hat{x}^1$, $\hat{x}_j$ is forced to be 1 or 0, and substituted into $f(x)$. And letting Q_r, x_r and z_r denote the reduced Hessian matrix, the function variable vector, and the data vector, respectively, Q_r, x_r and z_r can be easily formed by deleting the jth row and column of Q, the jth element of x, and the jth element of z, respectively. The new function $f(x_r)$ will be

$$f(x_r) = \frac{1}{2}x_r^T Q_r x_r + (z_r + \hat{x}_j q_j')x_r + z_j\hat{x}_j + \frac{1}{2}q_{jj}\hat{x}_j^2 \tag{5.28}$$

where q_j' is the jth column of Q with the jth element deleted. The constant terms $z_j\hat{x}_j$ and $\frac{1}{2}q_{jj}\hat{x}_j^2$ have nothing to do with the optimization and this can be ignored. Then the original minimization problem becomes

$$\min_{x_r \in \{0,1\}^{K-1}} \{f(x_r) = \frac{1}{2}x_r^T Q_r x_r + (z_r + \hat{x}_j q_j')x_r\} \tag{5.29}$$

If the assignment of the $\hat{x}_j$ is correct and the reduced $\bar{Q}_r^*$ is positive semidefinite, the result will be the optimal solution. However, we will always choose the best candidate from these two tests and the previous L_1 tests.

This heuristic method is shown to be very effective for this particular communication problem. Some numerical results are shown in the next section.

The modified algorithm is summarized as

Algorithm 2. Modified Multistage Detection.

1. Run algorithm 1 for L_1 stages.
2. Find out the indexes of $\hat{x}^0$ and $\hat{x}^1$ from step 1, denote them as index0 and index1.
3. - Let $x_{index0} = 1$,
   - Pick up the new Hessian $Q = Q_r$.
   - Compute $z = z_r + q'_{index0}$

- Run algorithm 1 with the new Q and z for L_2 iterations without evaluating the function values at each iteration except the last one. Compare with the one from 1 and choose the best one.

4. • Repeat 3 with the $index0$ replaced by $index1$, and $x_{index1} = 0$ and $z = z_r$. Choose the best from the comparison with the one obtained in 3.

5.8 Numerical results

In this section, bit error rates of algorithm 1 and 2 are obtained by simulations. For comparison, simulation results from the previous multistage algorithm [50], conventional, decorrelating, and optimal detectors are also presented.

First we consider a five-user CDMA system. Each user is assigned a different id code which is the same as that used in [50]. The largest correlation coefficient among the id codes is 5/7. Figure 5.2 shows the bit error rate of the first user with its $SNR_1 = 8dB$, versus the ratio of the user's signal strength to the strength of the other four signals. As shown in the figure, the multistage detectors proposed in this chapter and in [50] yield much better performance than the conventional and the decorrelating detectors, particularly in the worse near-far effects case. Also note that, while algorithm 1 shows a clear improvement over the previous multistage algorithm, algorithm 2 almost achieves the same performance as the optimal one.

Figure 5.3 illustrates the same performance comparison in the case of a ten-user system with the id code length of 15. The largest correlation coefficient is 3/5. From this figure, we see that the performance of the decorrelating detector is improved because of the smaller cross-correlation or higher *asymptotic efficiency* [52] [53]. The proposed modified multistage detector is observed to significantly improve the performance over the one in [50].

If we select the id codes with all the normalized cross-correlations equal to $-1/15$

for a ten-user system, the performance of the decorrelating detector is further improved, and the performance by the multistage detectors proposed in this chapter and [50] will be very close to that of the decorrelating detector. This is shown in figure 5.4. In this case, there is no need to design the nonlinear multistage detectors. This implies that a simple decorrelating detector would be good enough for detecting messages from a synchronous CDMA channel since the design of a set of orthogonal codes is possible in a synchronous CDMA channel. A system which uses a set of orthogonal codes for users in a micro-cell was proposed and developed by CYLINK Corporation [30]. Note that conventional matched filters were used instead of a decorrelating detector in the system because the codes are assumed to be orthogonal. In practical situation, although the intra-cell interference is zero by utilizing orthogonal codes, the inter-cell interference from the adjacent cells cannot be neglected due to undesirable partial correlation property of the orthogonal codes (generated from the Hadamard matrices). Error control coding must be used to deal with the inter-cell interference. The system may be improved by employing a decorrelating detector and assigning each user with a near-orthogonal code such as the Gold sequence. The intra-cell interference is minimized by the decorrelating detector, and the inter-cell interference is not significant due to the good partial correlation property of Gold sequences.

It should be noted that the number of iterations in algorithm 1 and 2 is independent of the number of users in the system. Increasing L_1 and L_2, little improvement can be achieved. This is important because the computational complexity of the algorithms will not increase much as the number of users goes up.

5.9 Summary

A new multistage detector is proposed in this chapter to detect synchronous CDMA signals. The algorithms are based on the continuous approach to the optimal 0-1 solution. By modifying a single diagonal element of the Hessian matrix of the quadratic function, all the elements of the estimated vector are modified in one stage. The convergence of the algorithms is studied. The algorithms are shown to achieve more reliable signal detection than the multistage algorithm of [50], especially in the case of higher cross-correlations between any pair of the users' id codes. The computational complexity of the proposed schemes is dominated by a few of quadratic function value evaluations, which are independent of the number of users in the system.

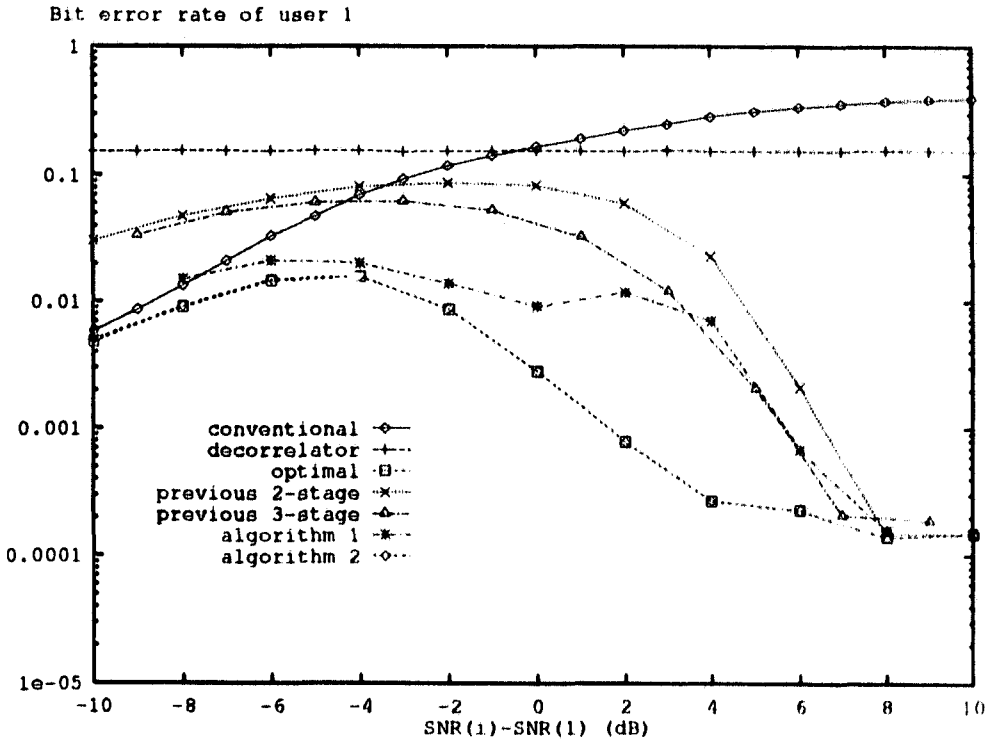

Figure 5.2: Bit error rate of user 1 for a five-user system. The largest cross-correlation is 5/7, $SNR(1) = 8dB$, $L_1 = 4$, $L_2 = 3$.

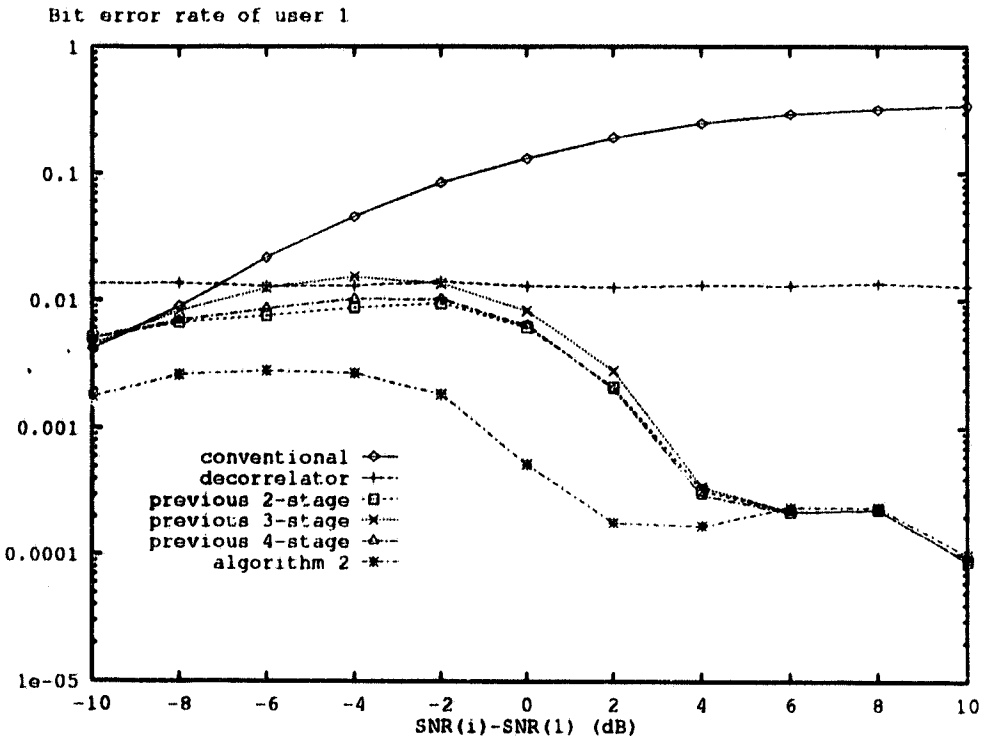

Figure 5.3: Bit error rate of user 1 for a ten-user system. The largest cross-correlation is 3/5, $SNR(1) = 8dB$, $L_1 = 4$, $L_2 = 3$.

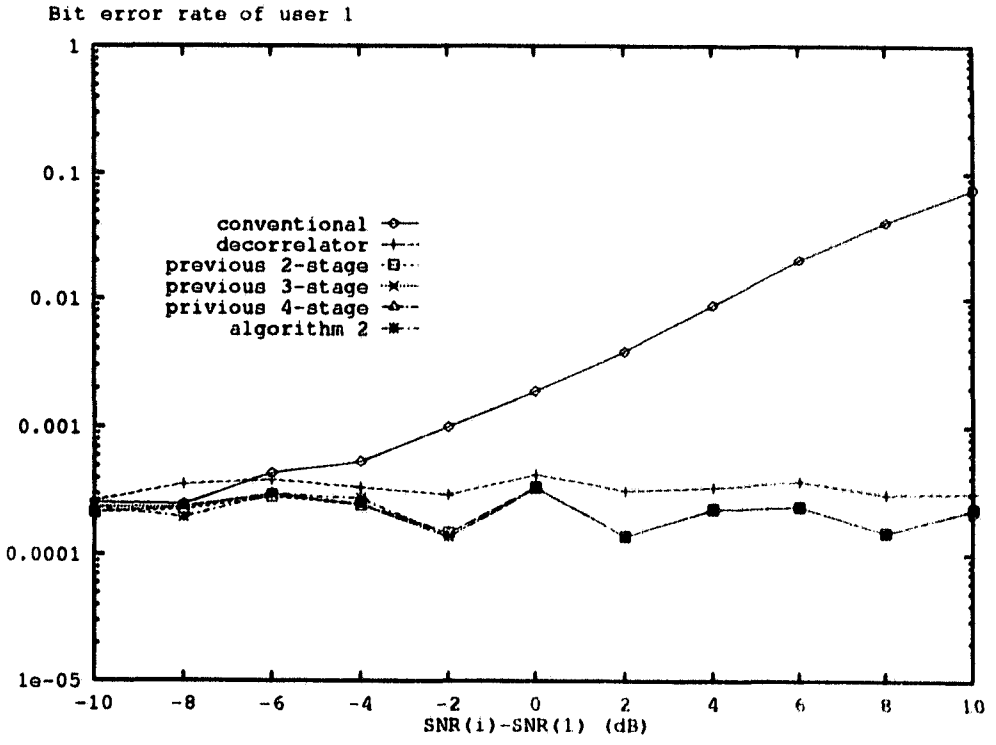

Figure 5.4: Bit error rate of user 1 for a ten-user system. The largest cross-correlation is $-1/15$, $SNR(1) = 8dB$, $L_1 = 4$, $L_2 = 3$.

Chapter 6

Multiuser Detection in Asynchronous CDMA

6.1 Introduction

In chapter 5, we have proposed a non-linear multiuser detector which yields better performance than the linear multiuser detectors when received signal powers are known for synchronous CDMA systems. In this chapter, we will show that the algorithm developed in chapter 5 can be also used for solving the multiuser detection problem of asynchronous CDMA systems. The way we do this is to translate the signal from asynchronous users into an equivalent signal from synchronous users. Two types of detectors will be analyzed. They are one-shot detector and M-shot detector depending on the length of the observation. The detection schemes developed in this chapter may be applied to the reverse link demodulation of the Qualcomm's system [19] such that the vulnerability of the closed-loop power control technique may be alleviated.

The optimal detector in the asynchronous case is a maximum-likelihood sequence detector which requires the sufficient statistics to be obtained in an observation of

the whole received waveform. The associated sub-optimal detectors based on the sequence detection do not lend themselves to practical implementation. Motivation is made to study the more practical detector, the one-shot detector and the M-shot detector which only require the sufficient statistics obtained in a single symbol or several symbols. The advantage of the detectors are the simplicity of implementation as well as the near-far resistance.

The chapter is organized as follows. In section 6.2, a system model for an asynchronous CDMA system is described. In section 6.3, we show that the one-shot detector and M-shot detector are near-far resistant. Numerical results are given in section 4 followed by a brief summary of this chapter.

6.2 System model

Two types of asynchronous CDMA detectors are presented in this section. The first one is called one-shot detector which is based on the detection of signals in an interval of a single symbol. The second type is called M-shot detector which detects signals in an interval of M-symbols.

6.2.1 One-shot detector

For a K-user CDMA system, the received signal at a receiver in a specific symbol which corresponds to the desired user (assumed to be user 1) can be written in the same discrete signal form as (5.2)

$$r = \bar{H}b + n \tag{6.1}$$

However, the b and $\bar{H}$ are different from those variables in (5.2) due to the asynchronous characteristic. In this case, b is expressed as

$$b = [b_1\ b_2(1)\ b_3(1)\ \cdots\ b_K(1)\ b_2(2)\ b_3(2)\ \cdots\ b_K(2)]^T \in \{-1, 1\}^{(2K-1)\times 1}$$

where $b_k(1)$ and $b_k(2)$ represent the kth user's first and second symbols which partially overlap with b_1. $\bar{H}$ in (6.1) is written as

$$\bar{H} = [s_1\ s_2(1)\ s_3(1)\ \cdots\ s_K(1)\ s_2(2)\ s_3(2)\ \cdots\ s_K(2)] \in R^{m\times(2K-1)}$$

where $s_k(1)$ and $s_k(2)$ are the partial signature waveforms corresponding to $b_k(1)$ and $b_k(2)$, respectively. Denote $c_k = [c_{k,1}\ c_{k,2}\ \ldots\ c_{k,m}]^T$ $(c_{k,i} \in \{-1,\ 1\})$ as the unit-amplitude spreading sequence used for the kth user, the signature waveforms can be written as

$$s_1 = (\frac{w_1}{m})^{1/2} c_1 = (\frac{w_1}{m})^{1/2}[c_{1,1}\ \ldots\ c_{1,m}]^T$$

$$s_k(1) = (\frac{w_k^{(0)}}{p_k})^{1/2} c_k(1) = (\frac{w_k^{(0)}}{p_k})^{1/2}[c_{k,m-p_k+1}\ \ldots\ c_{k,m}\ 0\ \ldots\ 0]^T$$

$$s_k(2) = (\frac{w_k^{(1)}}{m-p_k})^{1/2} c_k(2) = (\frac{w_k^{(1)}}{m-p_k})^{1/2}[0\ \ldots\ 0\ c_{k,1}\ c_{k,2}\ \ldots\ c_{k,m-p_k}]^T$$

where the random variable $p_k \in [0, m]$ is the chip phase difference between the PN codes of user k and user 1 [1]. p_k is determined by the synchronization circuit in the receiver. A practical way to acquire p_k for all k is described in chapter 7. In the above equations, $w_1 = \|s_1\|^2$, $w_k^{(0)} = \|s_k(1)\|^2$ and $w_k^{(1)} = \|s_k(2)\|^2$ are the symbol energies for the symbol waveforms s_1, $s_k(1)$ and $s_k(2)$, respectively.

Given the symbol observation for the one-shot detector, the Maximum-Likelihood detector selects the most likely hypothesis $\hat{b}^*$, which corresponds to the solution of the minimization problem

$$\begin{aligned}\min_{\hat{b}\in\{-1,1\}^{(2K-1)}} \{f(\hat{b}) &= \|r - \bar{H}\hat{b}\|^2\} \\ &= \min_{\hat{b}\in\{-1,1\}^{(2K-1)}} \{\frac{1}{2}\hat{b}^T C\hat{b} - y^T\hat{b}\} \qquad (6.2)\end{aligned}$$

[1] For simplicity, we assume that p_k is an integer in [0, m]. In practice, we can increase the resolution of p_k by increasing the sampling rate.

where vector $y = \bar{H}^T r$ represents $2K-1$ decisions from $2K-1$ equivalent conventional receivers, $C = \bar{H}^T \bar{H}$ is a $(2K-1) \times (2K-1)$ positive definite matrix. Thus the K-user asynchronous multi-user detector is equivalent to a $(2K-1)$-user synchronous multi-user detector.

6.4.2 M-shot detector

For the one-shot detector, the observation duration is equal to a one-symbol length. In practice, it is also possible for a receiver to observe signals in more than one symbols and make a decision after a short delay. A multiuser detector is called M-shot detector if the observation duration is equal to M-symbol length. In this case, the number of data bits in the observation interval is $M+1$ in general, and the received signal can still be written as $r = \bar{H}b + n$, where

$$\begin{aligned} b &= [b_1(1)\, b_2(1) \cdots b_K(1)\, b_1(2)\, b_2(2) \cdots b_K(2) \\ &\quad \cdots b_1(M+1)\, b_2(M+1) \cdots b_K(M+1)]^T \end{aligned}$$

$$\begin{aligned} \bar{H} &= [s_1(1)\, s_2(1) \cdots s_K(1)\, s_1(2)\, s_2(2) \cdots s_K(2) \\ &\quad \cdots s_1(M+1)\, s_2(M+1) \cdots s_K(M+1)] \end{aligned}$$

and

$$s_k(1) = \left(\frac{w_k^{(0)}}{p_k}\right)^{1/2} [c_{k,m-p_k+1} \cdots c_{k,m}\, \mathbf{0}^T_{mM-pk}]^T$$

$$s_k(i) = \left(\frac{w_k}{m}\right)^{i/2} [\mathbf{0}^T_{(i-2)m+pk}\, c_{k,1} \cdots c_{k,m}\, \mathbf{0}^T_{m(M-i+1)-pk}]^T \quad i = 2, 3, ..., M$$

$$s_k(M+1) = \left(\frac{w_k^{(1)}}{m-p_k}\right)^{1/2} [\mathbf{0}^T_{(M-1)m+pk}\, c_{k,1} \cdots c_{k,m-p_k}]^T$$

Here we use $w_k^{(0)}$, w_k $w_k^{(1)}$ to denote the energies of the first partial symbol, a whole symbol and the last partial symbol of user k, respectively, in the observation duration. $\mathbf{0}_L$ is a column vector with L zero elements.

Again the ML detector selects the most likely $\hat{b}^*$, which corresponds to the solution of

$$\begin{aligned}&\min_{\hat{b}\in\{-1,1\}^{K(M+1)}}\{f(\hat{b}) = \|r - \bar{H}\hat{b}\|^2\}\\ &= \min_{\hat{b}\in\{-1,1\}^{K(M+1)}}\{\frac{1}{2}\hat{b}^T C\hat{b} - y^T\hat{b}\}\end{aligned} \tag{6.3}$$

where vector y represents $K(M+1)$ decisions from $K(M+1)$ equivalently matched filters, C is a $K(M+1)\times K(M+1)$ positive definite matrix. Thus the K-user asynchronous multiuser detection is translated into a $K(M+1)$-user synchronous multiuser detection. However, not all the elements of $\hat{b}^*$ are picked up for the decisions. Later on, we will show that only those elements which correspond to the largest minimum *asymptotic efficiency* are selected. The M-shot detector is supposed to outperform the one-shot detector because, for the one-shot detector, estimations on interfering signals rely on parts of symbols.

6.2.3 Linear independence assumption

To guarantee that (6.2) and (6.3) have unique solutions, the matrix C must be nonsingular. This is almost true by the Linear Independence Assumption (LIA) of [26]. The LIA simply says that the received signal does not vanish everywhere if at least one of the users has transmitted a symbol independent of the received energies. It was also shown that the violation of the LIA occurs with probability zero if *a priori* unknown delays are uniformly distributed which is the case in the asynchronous channel used by non-cooperating users. In addition to the LIA, a condition of $m \geq 2K-1$ must be satisfied, otherwise C will be singular. In the case that the LIA is violated, there will be more than one solutions for the problems (6.2) (6.3), but the decisions we selected are often unique [2].

[2]For decorrelating detector, pseudoinverse of C is often used. For the multistage detector in chapter 5, a small perturbation to the diagonal elements of the cross-correlation matrix can be

6.3 Near-far resistance

In this section, we show that the M-shot (including $M = 1$) detectors are near-far resistant. Generally speaking, a detector is said to be near-far resistant if the bit-error-rate of any single user goes to zero as background noise (AWGN) disappears. Conversely, a detector is not near-far resistant if there is an irreducible probability of error for a user even in the absence of background noise [26].

We can easily verify that the M-shot detector by (6.3) (including one-shot detector since it is a special case of M-shot detector) is near-far resistant. We do this by checking the bit-error-rate of the solution (decision) of the least-squares problem in (6.3) by removing the constraint $\hat{b} \in \{-1,1\}^{K(M+1)}$. The solution, which corresponds to the decision made by the decorrelating detector [25], is given by

$$\begin{aligned} \hat{b}^* &= sign(C^{-1}y) \\ &= sign(\bar{H}^{\dagger}r) \end{aligned} \tag{6.4}$$

where $\bar{H}^{\dagger} = (\bar{H}^T\bar{H})^{-1}\bar{H}^T$ is the pseudoinverse of $\bar{H}$ [46]. Since $r = \bar{H}b + n$, we get

$$\hat{b}^* = sign(b + \bar{H}^{\dagger}n) \tag{6.5}$$

As the background noise goes to zero (i.e., the vector $n \to \mathbf{0}$), $\hat{b} - b \to \mathbf{0}$, which means that the bit-error-rate for any of the K users goes to zero. The constrained least-squares solution (optimal detector) defined in (6.3) always has better performance than the unconstrained solution. Thus as $\sigma \to 0$, the bit-error-rate of the detector goes to zero. Therefore, it is indeed near-far resistant. The optimum detection in (6.3) is known to be NP hard. Some sub-optimum detectors have been studied in chapter 5. The performance of these detectors are generally better than that of the decorrelating detector, especially in the severe near-far environment. Thus we can conclude that these detectors are also near-far resistant.

---

made. Both efforts guarantee that the detectors work well when C is singular.

A quantitative measure for the near-far resistance is the *asymptotic efficiency* which was defined and thoroughly studied in [52] [53]. Define the *effective* energy of equivalent user i, $e_i(\sigma)$, as the energy that the user would require to achieve bit-error-rate $P_i(\sigma)$ in the same Gaussian channel without interfering users. Thus the ratio $e_i(\sigma)/w_i$, which is a number between 0 and 1, characterizes the performance loss due to the existence of other users in the channel. The *asymptotic efficiency* is defined by

$$\eta_i = \lim_{\sigma \to 0} e_i(\sigma)/w_i \tag{6.6}$$

which measures the slope with which $P_i(\sigma)$ goes to 0 in the high SNR region. Further, the Minimum Asymptotic Efficiency (MAE) over the relative energies of all the other users is defined as

$$\bar{\eta}_i = \inf_{\{w_j \geq 0, j \neq i\}} \eta_i \tag{6.7}$$

which quantifies the robustness of a receiver against the near-far problem. An advantage of introducing MAE is that it is much easier to compute than the *asymptotic efficiency*. More precisely, from [25]

$$\bar{\eta}_i = 1/R^{\dagger}_{ii} \tag{6.8}$$

where $R^{\dagger}$ is the pseudoinverse of the normalized cross-correlation matrix R which relates to C by

$$C = W^{1/2} R W^{1/2} \tag{6.9}$$

where

$$\begin{aligned} W \;=\; & \mathrm{diag}(w_1^{(0)}\, w_2^{(0)} \cdots w_K^{(0)}\, w_1\, w_2 \cdots w_K \\ & \cdots w_1\, w_2 \cdots w_K\, w_1^{(1)}\, w_2^{(1)} \cdots w_K^{(1)}) \end{aligned} \tag{6.10}$$

$\bar{\eta}_i$ gives the worst case of the *asymptotic efficiency* of user i with respect to the energies of the interfering users. Thus it is a lower bound for the *asymptotic efficiencies* of an optimal detector and its sub-optimal detectors. In [25], it was proved that the *asymptotic efficiency* of the decorrelating detector achieves the lower bound exactly, no matter how the users' energies change. Later on, we will compare the proposed multistage detector with the decorrelating detector since its ith user's *asymptotic efficiency* can be easily obtained from (6.8).

To see how the one-shot detector performs in the near-far environment, we compare its MAE with that of the synchronous detector (recall that the one-shot detector for synchronous channels is optimal) and that of the decorrelating detector. The comparisons can be easily made by assuming a two-user system. Therefore, there are 3 equivalent users for the one-shot detector in the asynchronous case.

For the synchronous two-user case, the MAE for user 1 is $\bar{\eta}_1 = 1 - \rho_{12}^2$ [25], where ρ_{12} is the normalized cross-correlation value between the two users. The asymptotic efficiency of the decorrelating detector takes the same value, no matter how the relative energies of other users change.

For the asynchronous two-user case, the normalized cross-correlation matrix R of the one-shot detector is written as

$$R = \begin{bmatrix} 1 & \epsilon^{-1/2}\rho_{12}^{(0)} & (1-\epsilon)^{-1/2}\rho_{12}^{(1)} \\ \epsilon^{-1/2}\rho_{12}^{(0)} & 1 & 0 \\ (1-\epsilon)^{-1/2}\rho_{12}^{(1)} & 0 & 1 \end{bmatrix} \tag{6.11}$$

where $\epsilon = p_2/m$, $\rho_{12}^{(0)} = c_1^T c_2(1)/m$ and $\rho_{12}^{(1)} = c_1^T c_2(2)/m$. The minimum asymptotic efficiency is given by

$$\begin{aligned} \bar{\eta}_1 &= 1/R_{11}^{-1} \\ &= 1 - \frac{\rho_{12}^{(0)2}}{\epsilon} - \frac{\rho_{12}^{(1)2}}{1-\epsilon} \end{aligned} \tag{6.12}$$

When $\epsilon = 0$ or 1, which is the case of synchronous CDMA system, the term $\rho_{12}^{(0)2}/\epsilon$ or $\rho_{12}^{(1)2}/(1-\epsilon)$ in (6.12) will disappear, and the minimum asymptotic efficiency will coincide with that of the synchronous case.

Tables 6.1 to 6.3 list the MAEs of the synchronous and asynchronous channels of 2 users with 3 different pairs of PN sequences. From the table, we see that the MAEs at different phase delays are different. Denoting $\Delta\bar{\eta}$ as the difference (in dB) between the largest and the smallest MAEs, we observe that, in general, $\Delta\bar{\eta}$ will be smaller if longer sequences are used. In the three examples listed in the tables, it is fount that $\Delta\bar{\eta} = 2.73dB$, $\Delta\bar{\eta} = 1.24dB$ and $\Delta\bar{\eta} = 0.86dB$ for sequence lengths of 7, 15 and 31, respectively. $\Delta\bar{\eta}$ can be used to measure the degree of the variation of bit-error-rate for a one-shot detector and a M-shot detector. It is interesting to notice that the MAE obtained by a synchronous one-shot detector ($p_2 = 0$) is not necessarily larger than all of the MAEs of an asynchronous one-shot detector, but is usually larger than the smallest one. This means that an asynchronous one-shot detector sometimes outperforms the synchronous detector. However, the detector must be designed such that it can perform satisfactorily in the worst case. $\Delta\bar{\eta}$ should be made as small as possible. Tradeoff may be made between the $\Delta\bar{\eta}$ and the bandwidth efficiency.

Now we examine $\bar{\eta}_i$ for a M-shot detector. We know that the subscript i of $\bar{\eta}_i$ denotes the number of the user in an equivalent synchronous CDMA system, it actually represents the $\lfloor \frac{i}{K} + 1 \rfloor$th bit of user $i - \lfloor \frac{i-1}{K} \rfloor K$ provided that each user has $M+1$ bits in the observation block. For comparison, we first examine a two-user system and use the same sequences of length 7 as those used for the one-shot

Table 6.1: Minimum asymptotic efficiencies for synchronous and asynchronous 2-user one-shot detectors. PN sequences length=7.

p_2	0 (syn)	1	2	3	4	5	6
MAE	.816	.857	.686	.810	.810	.457	.762

Table 6.2: Minimum asymptotic efficiencies for synchronous and asynchronous 2-user one-shot detectors. PN sequences length=15.

p_2	0 (syn)	1	2	3	4	5	6	7
MAE	.782	.914	.954	.778	.849	.747	.993	.881
p_2	8	9	10	11	12	13	14	
MAE	.957	.889	.880	.994	.956	.749	.857	

Table 6.3: Minimum asymptotic efficiencies for synchronous and asynchronous 2-user one-shot detectors. PN sequences length=31.

p_2	0 (syn)	1	2	3	4	5	6	7
MAE	.999	.963	.946	.989	.871	.819	.915	.909
p_2	8	9	10	11	12	13	14	15
MAE	.949	.944	.986	.916	.861	.990	.837	.914
p_2	16	17	18	19	20	21	22	23
MAE	.998	.900	.990	.826	.901	.999	.996	.931
p_2	24	25	26	27	28	29	30	
MAE	.937	.977	.989	.841	.948	.946	.968	

Table 6.4: Minimum asymptotic efficiencies for asynchronous 2-user 3-shot detector. $p_2 = 5$, PN sequences length=7.

user	Bit No.			
No.	1	2	3	4
1	.640	.684	.510	N/A
2	.713	.684	.640	.641

Table 6.5: Minimum asymptotic efficiencies for asynchronous 2-user 6-shot detector. $p_2 = 5$, PN sequences length=7.

user	Bit No.						
No.	1	2	3	4	5	6	7
1	.640	.691	.693	.693	.685	.510	N/A
2	.713	.685	.693	.693	.691	.640	.641

detector. Table 6.4 shows the MAEs of the two users at different bit positions for a 3-shot detector. Remember that $(p_1, p_2) = (0, 5)$ corresponds to the worst case for the two-user system. Comparing tables 6.1 and 6.4, we can see that the MAE at the worst case has been increased from 0.457 to 0.684 by the 3-shot detector. Similarly, table 6.5 and table 6.6 list the MAEs when 6-shot and 9-shot detectors are employed. Compared to the 3-shot detector, we find that no significant improvement can be achieved by the 6-shot detector. The 6-shot and the 9-shot detector achieve the same maximum MAE. Considering the computational complexity, we should say that the 3-shot detector is the best choice. Table 6.7 lists the first user's maximum MAE achieved by a 3-shot detector at all the possible phase distributions. Compared with table 6.1, we find that MAEs at all phase delays are increased. Furthermore, $\Delta\eta$

Table 6.6: Minimum asymptotic efficiencies for asynchronous 2-user 9-shot detector. $p_2 = 5$, PN sequences length=7.

user	Bit No.									
No.	1	2	3	4	5	6	7	8	9	10
1	.640	.691	.693	.693	.693	.693	.693	.685	.510	N/A
2	.713	.685	.693	.693	.693	.693	.693	.691	.640	.641

Table 6.7: Maximum MAE for synchronous and asynchronous 2-user 3-shot detectors. PN sequences length=7.

p_2	0 (syn)	1	2	3	4	5	6
MAE	.816	.980	.894	.894	.894	.684	.894

is reduced by over 1dB. Also from this table, it is found that the 3-shot detector has similar detection performance at most phase delays. Finally, we compute MAE for a 6-user system using the M-shot detector. The phase distribution of the users' signature sequences are selected randomly. Tables 6.8 and 6.9 give the results for a 3-shot and 5-shot detectors. Again we can see from these two tables that the 3-shot detector would be the best choice.

6.4 Numerical results

In this section, the bit-error-rate (BER) of the one-shot detector is obtained by simulation using the multistage algorithm 1 of chapter 5. The BER of the detector will be upper bounded by the BER of the one-shot decorrelating detector because the MAE of the one-shot detector is equal to the asymptotic efficiency of the one-shot decorrelating detector. The BER of the one-shot decorrelating detector for user

Table 6.8: Minimum asymptotic efficiencies for asynchronous 6-user 3-shot detector. p = [29 26 16 3 20 13], PN sequences length=31.

user No.	Bit No.			
	1	2	3	4
1	.602	.745	.733	.559
2	.788	.889	.861	.507
3	.471	.683	.689	.851
4	.823	.742	.806	.736
5	.633	.792	.789	.557
6	.861	.773	.783	.535

Table 6.9: Minimum asymptotic efficiencies for asynchronous 6-user 5-shot detector. p = [29 26 16 3 20 13], PN sequences length=31.

user No.	Bit No.					
	1	2	3	4	5	6
1	.602	.745	.746	.746	.733	.559
2	.788	.889	.892	.892	.861	.507
3	.471	.683	.697	.697	.690	.851
4	.843	.743	.807	.808	.807	.736
5	.633	.792	.800	.800	.789	.557
6	.861	.773	.787	.787	.783	.535

1 is given by [26]

$$p_{d_1} = \frac{1}{2}\mathrm{erfc}(\sqrt{\frac{\bar{\eta}_1 w_1}{2\sigma^2}}) \tag{6.13}$$

The results are also compared with the BER of a conventional matched filter, which is written as [2?]

$$p_{c_1} = \frac{1}{2^{2(K-1)}} \sum_{b_j(1),b_j(2),j\neq 1} \frac{1}{2}\mathrm{erfc}(\frac{\sqrt{w_1} - \sum_{j=2}^{K}[\rho_{1j}^{(0)} b_j(1) + \rho_{1j}^{(1)} b_j(2)]\sqrt{w_j}}{\sqrt{2\sigma^2}}) \tag{6.14}$$

where $\rho_{1j}^{(0)} = c_1^T c_j(1)/m$ and $\rho_{1j}^{(1)} = c_1^T c_j(2)/m$. At last, all the results of BER are lower-bounded by the BER of a single user detector, i.e., no interfering users exist.

We first study the two-user case. Figure 6.1 shows the bit-error-rates of user 1 versus the interfering energy of user 2. In this figure, we use the same PN sequences of length 7 as those used for the calculation of the MAEs in table 6.1 in section 6.3, and consider the phase delay $p_2 = 5$ (chips) which is the worst case. The actual signal-to-noise ratio of user 1 is 5dB. From the figure, we can see that the multistage detector outperforms the decorrelating detector, and both detectors are near-far resistant. The conventional detector suffers from the near-far problem. Simulation results of the decorrelating and conventional detectors have been shown to match the theoretical values.

We now look at the performance in the best phase delay case, i.e., $p_2 = 1$ for the same codes. Figure 6.2 gives the performance in this case. Since the detectors have a higher MAE which implies the smaller overall cross-correlations, better overall performance is seen from this figure compared to figure 6.1. Meanwhile, the difference between the decorrelating detector and the multistage detector becomes smaller as MAE increases. The same phenomenon was observed in the synchronous case in chapter 5.

Figure 6.3 shows the bit-error-rate of user 1 versus the actual SNR1 with SNR2=SNR1. The performance difference between the best and worst delays can

be seen in the figure. At 10 dB, almost 2 orders of magnitude difference exist between the two extreme cases. The multistage detector can usually improve the performance of the decorrelating detector at the worst delay case. In this example, about 1dB improvement is made by the multistage detector over the decorrelating detector. Figure 6.4 is the same as figure 6.3 except that SNR2 is 5dB higher than SNR1. Because of the larger interfering energy, the performance of the conventional detector becomes poorer, but the decorrelating detector remains the same and the multistage detector obtains even better performance.

Then we use a set of PN sequences of length 31 for CDMA users. Figures 6.5 and 6.6 illustrate the BERs of the conventional and the decorrelating detectors for a 3-user channel. Because of the smaller cross-correlations, the performance difference between the worst and best delays is reduced. However, as the number of users increases, this difference will again increase. This is illustrated in figures 6.7 and 6.8 where 3 more users are added into the system. If longer PN sequences are used, we can expect a reasonably small $\Delta\bar{\eta}$ in a CDMA system with a large number of users.

BER by a M-shot detector is plotted in figure 6.9. For the poor case shown in figure 6.7, a 3-shot decorrelating detector is able to improve the performance up to 2dB. Further increasing the number of symbols in the observation blocks, little improvement can be made at the expense of more computations and longer delay.

All the figures above have demonstrated the attractive property of the near-far resistance of the one-shot and 3-shot multi-user detectors.

6.5 Summary

In this chapter, we have studied the behavior of a type of M-shot (including the one-shot) multi-user detectors in asynchronous CDMA channels. The detectors have been shown to be near-far resistant. The multistage M-shot detector will out-

perform the decorrelating detector, especially when cross-correlations between the desired user and the interfering users are relatively large. As the cross-correlations decrease, the two detectors approach the same performance. A shortcoming of one-shot detectors is that their performance will more or less depend upon the phase delay distributions of the active users in the system. Tradeoff may be made between the performance variation and the bandwidth efficiency to achieve a satisfactory performance if a one-shot detector is used. Alternatively, M-shot detectors can be used to significantly reduce the amount of the variation of bit-error-rate caused by different delays. However, the computational complexity will increase accordingly. It is found that the 3-shot detectors will be efficient enough to reduce the maximum variation between the highest and the lowest minimum asymptotic efficiencies which is represented by $\Delta\bar{\eta}$.

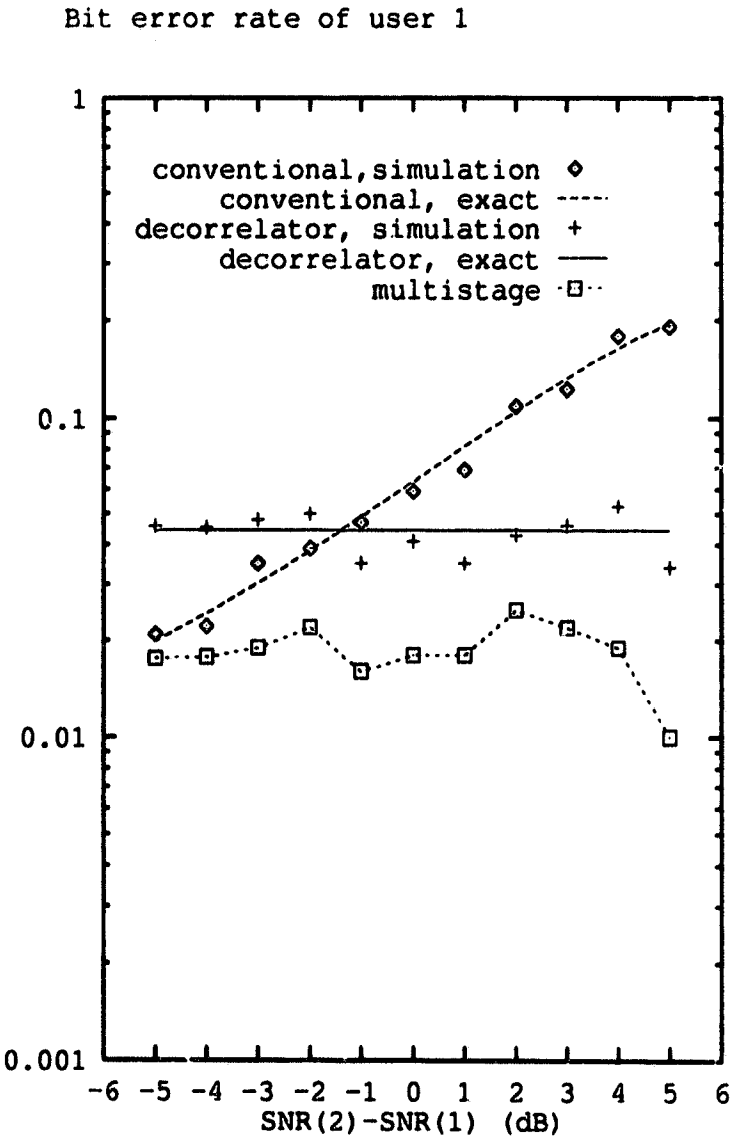

Figure 6.1: Bit error rate of user 1 versus SNR2-SNR1 for a two-user system at SNR1=5dB. PN sequences of length 7 are used. The phase difference between the two sequences is 5 which is found to be the worst case for the codes selected.

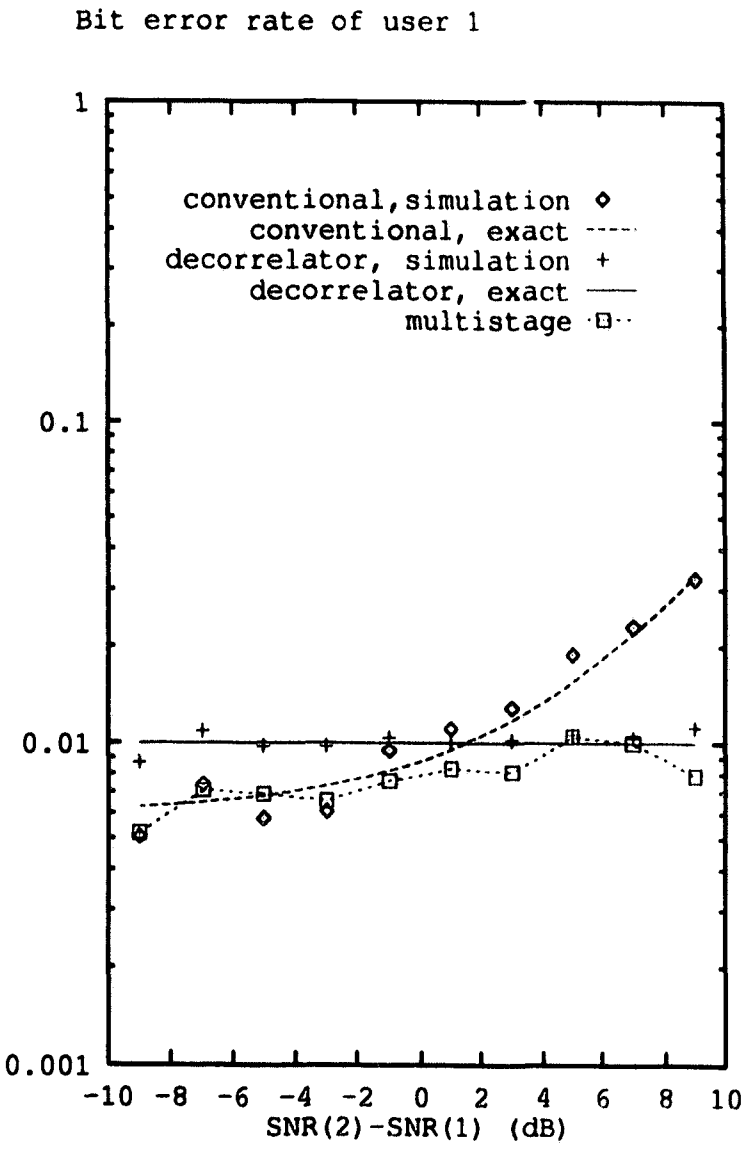

Figure 6.2: Bit error rate of user 1 versus SNR2-SNR1 for a two-user system at SNR1=5dB. PN sequences of length 7 are used. The phase difference between the two sequences is 1 which is found to be the best case for the codes selected.

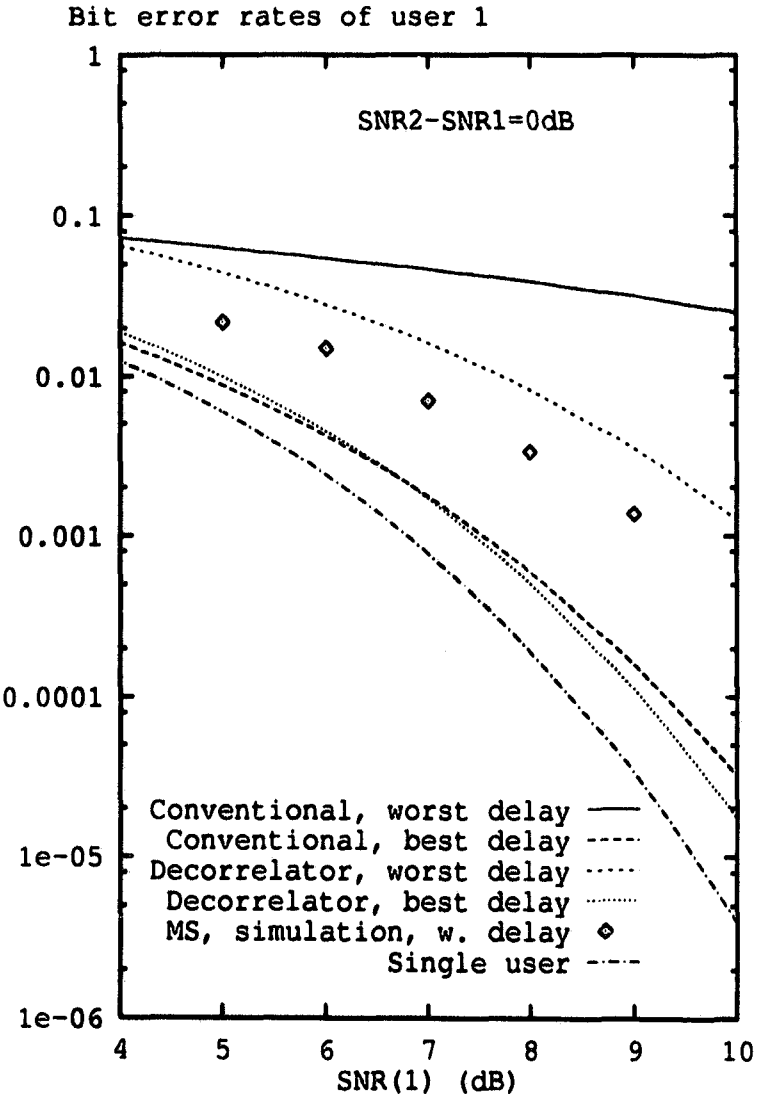

Figure 6.3: Bit error rate of user 1 versus SNR1 for a two-user system. PN sequences of length 7 are used. $\Delta\eta = 2.7$dB.

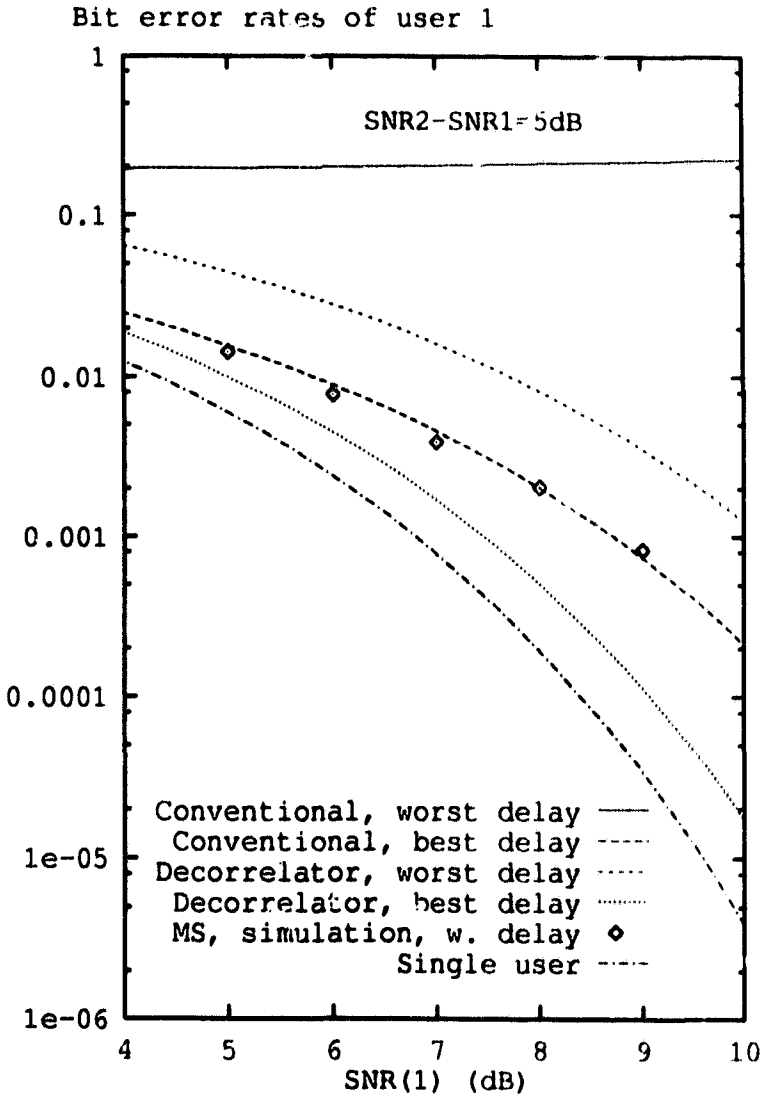

Figure 6.4: Bit error rate of user 1 versus SNR1 for a two-user system. PN sequences of length 7 are used. $\Delta\eta = 2.7$dB.

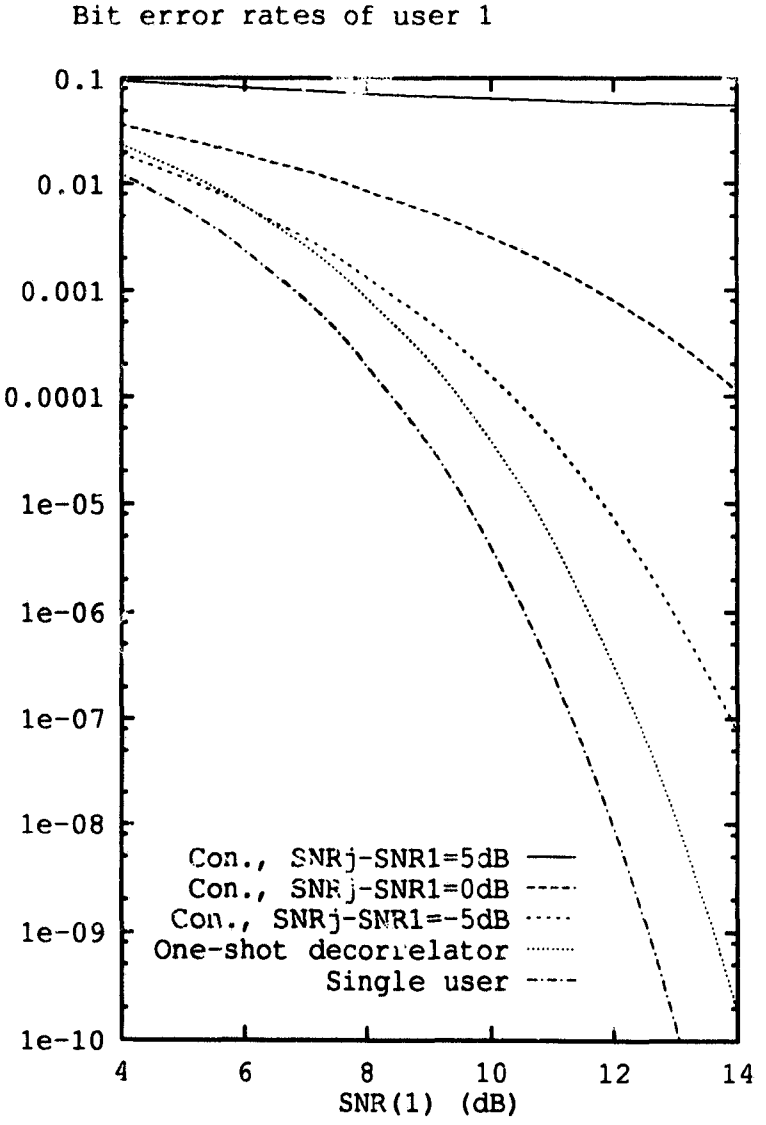

Figure 6.5: Bit error rate of user 1 versus SNR1 for a 3-user system. PN sequences of length 31 are used. This is an example of a poor phase-delay distribution of users.

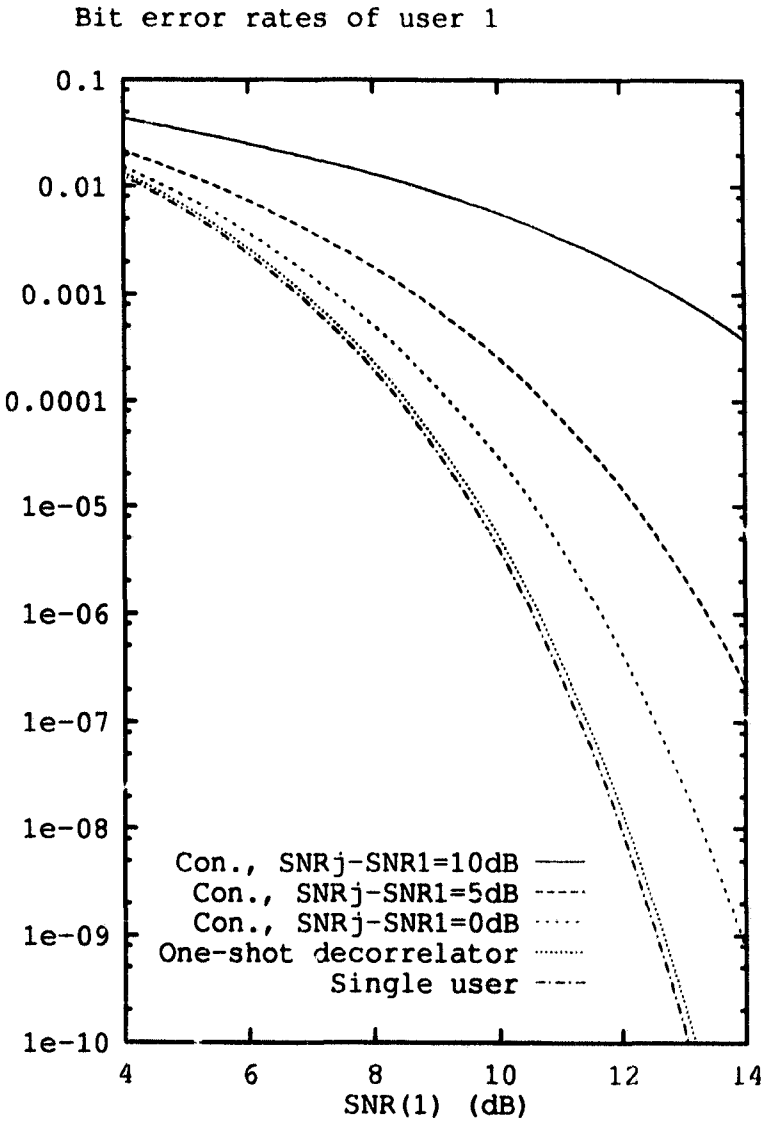

Figure 6.6. Bit error rate of user 1 versus SNR1 for a 3-user system. PN sequences of length 31 are used. This is an example of a good phase-delay distribution of users.

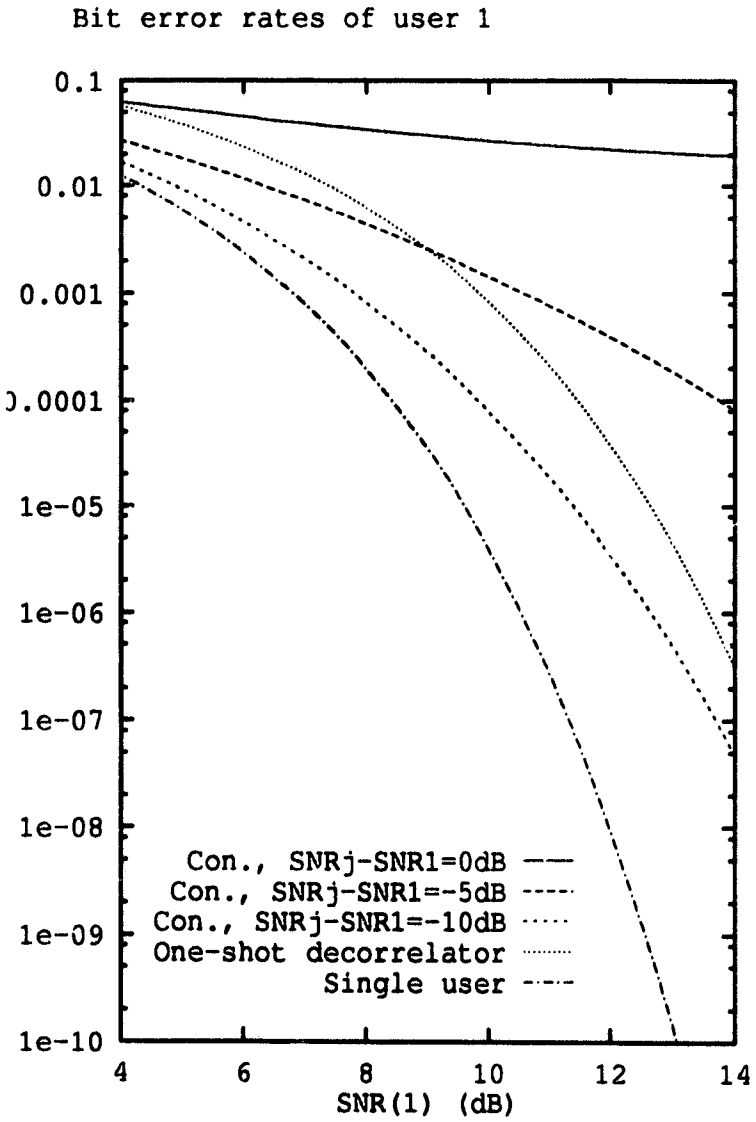

Figure 6.7: Bit error rate of user 1 versus SNR1 for a 6-user system. PN sequences of length 31 are used. This is an example of a poor phase-delay distribution of users.

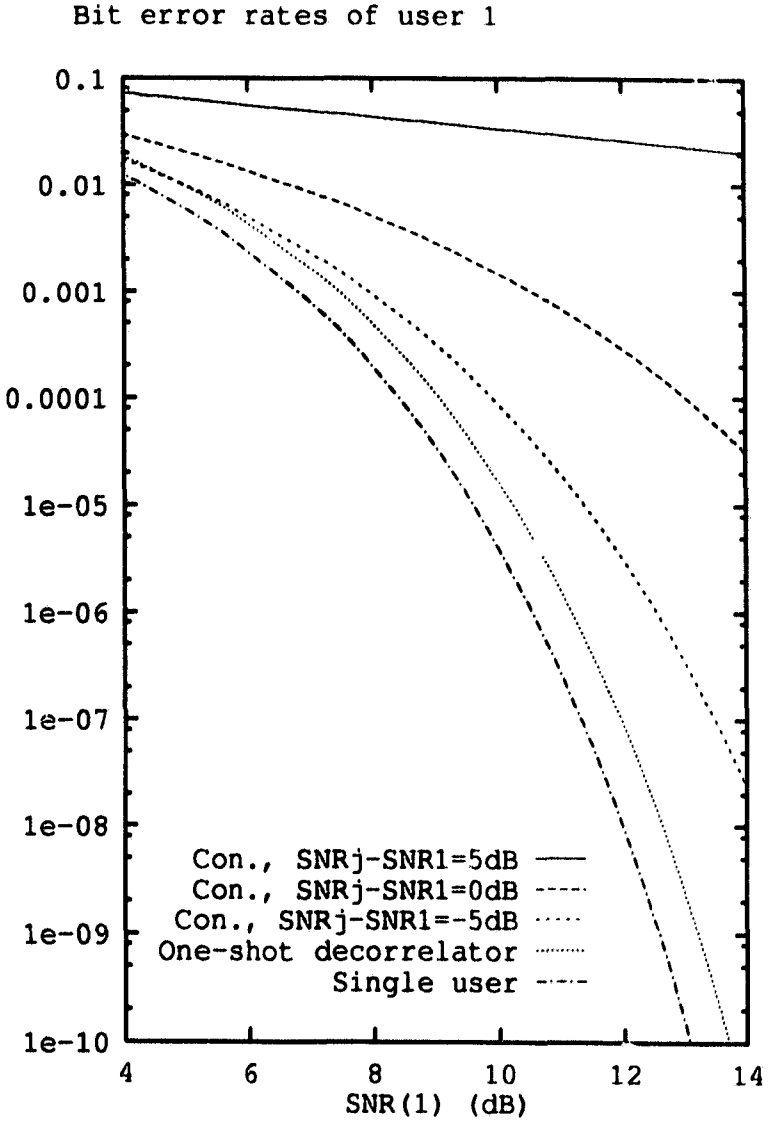

Figure 6.8: Bit error rate of user 1 versus SNR1 for a 6-user system. PN sequences of length 31 are used. This is an example of a good phase-delay distribution of users.

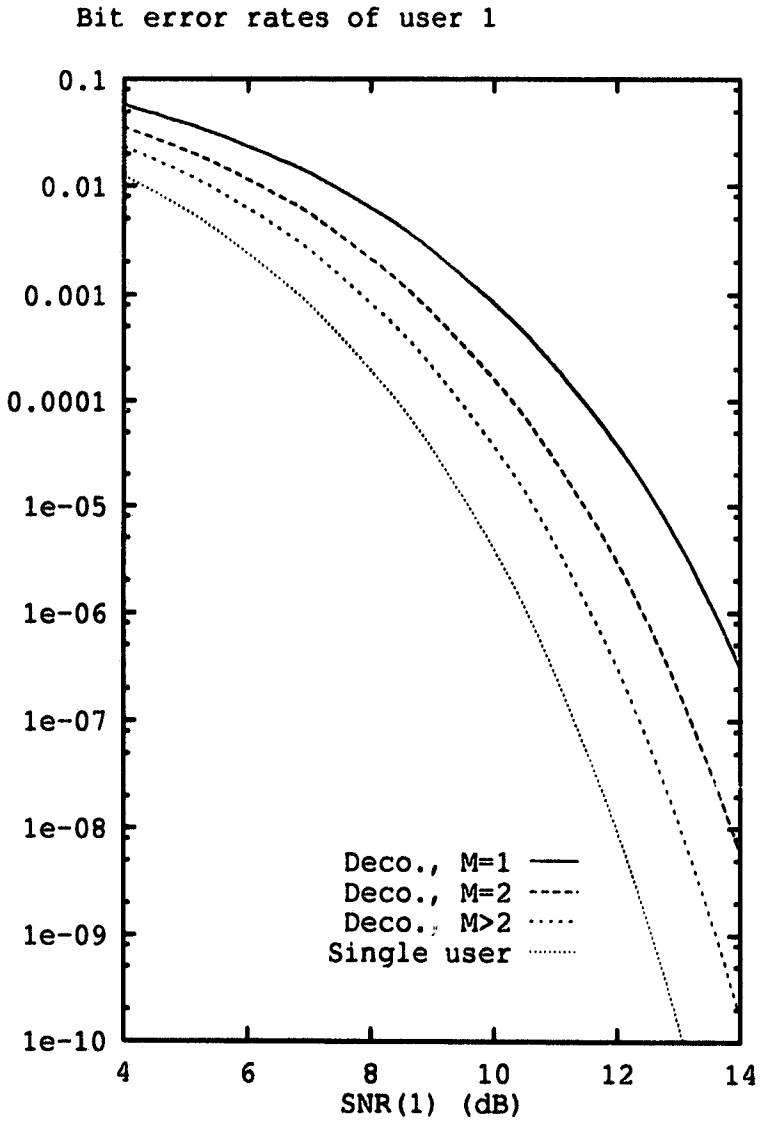

Figure 6.9: Bit-error-rate of a M-shot decorrelating detector for $M = 1, 2, 3, \ldots$. Sequences of length 31 are used for a 6-user system. This is an example of a poor phase-delay distribution of users.

Chapter 7

Acquisitions in Asynchronous CDMA Systems

7.1 Introduction

In chapter 5 and chapter 6, receivers based on multiuser detectors were studied. In practice, there is another type of receivers, which can alleviate the near-far effects, based on cross-correlation cancellation techniques, see [21] [18] [6] [24] [20] and the references therein. The multiuser detectors are able to turn the strong interference signals into useful information for detecting weak signals, and thus completely near-far resistant. The interference-cancellation detector first detects the strongest interference signals, then subtracts them from the compound signals and finally detects the desired signal message from the residual signal. Since the subtraction cannot be made perfect even when the channel noise (assumed to be AWGN) reduces to zero, the interference cancellation receiver is not completely near-far resistant (at least theoretically). However, the cancellation technique can be a useful tool for a receiver to accomplish the PN code acquisition for each component user.

No matter what type of receiver is used, the synchronization process in such a

system becomes more crucial because a receiver has to know exactly the phases of all users' PN codes or at least the phases of those codes which have larger signal powers than the desired code. Unfortunately, the near-far effects cannot be avoided during the acquisitions of those PN codes. While the *equal power* assumption can be accepted when analyzing the bit-error-rate performance since the implementation of automatic power control is possible, the same assumption will not be appropriate for the acquisition process simply because the power control technique cannot work without knowing the phase of each component user's code. In this chapter, we develop a novel acquisition scheme which can alleviate the near-far effects during acquisitions using interference cancellation techniques iteratively until all the PN codes or the desired PN code are captured.

The acquisition model is described in section 7.2 with emphasis on the two proposed acquisition schemes. In section 7.3, we present the performance measure of interest, the probabilities of acquisition for the proposed acquisition schemes. This is followed by the detailed analysis on the statistics of variables which affect the acquisition probability in section 7.4. In section 7.5, some numerical results are presented followed by a short summary in section 7.6.

7.2 Acquisition model

In this section, we describe two acquisition schemes based on cancellation techniques. We continue to use the assumption that the received signal is in baseband form although it may be too ideal to assume that acquisition can be done in baseband. However, the scheme developed in this chapter can be applied to the non-coherent case with different carrier phases by active users. This is listed in the future work in the last chapter.

7.2.1 Preliminaries

In this section, we present the basic estimation scheme for the reconstruction of the detected signals. To acquire PN codes from the received compound signal, the receiver will collect the received baseband signal in data blocks. The collected data blocks are stored in memory for further signal processing. The length of data blocks depends on the computation speed and the size of the memory. In general, the longer the data blocks, the longer the computation time for the acquisition and the larger the memory size but the better the acquisition performance. The reasonable length of the data blocks may vary from 1 to 10 symbols. The receiver will use the current collected data block to conduct signal estimation, cancellation and acquisition. The acquisition process is repeated if there are any more potential users whose PN codes have not yet been captured.

We conduct the acquisition process in a block of length MT, where T is the duration of a single data symbol, and M is a positive integer number. For an asynchronous CDMA system, there will be $M+1$ data bits for each user in general. Thus the received signal can be written as

$$r(t) = S(t,b) + n(t) \tag{7.1}$$

where

$$S(t,b) = \sum_{i=1}^{M+1} \sum_{k=1}^{K} b_k(i) A_k c_k(t - iT - \tau_k) \tag{7.2}$$

where K is the number of users in the system, $b_k(i)$ is the ith data bit of user k in the observation block. A_k is the signal amplitude of user k, and $c_k(t)$ is the unit-amplitude signature waveform of user k and is zero outside the interval $[0,T]$. τ_k is the delay for signal of user k

Using conventional matched filters, it is likely that the strongest signal is detected. Without loss of generality, we assume that signals are numbered such that

their amplitudes satisfy $A_1 \geq A_2 \geq \cdots \geq A_K$ and the delay τ_1 is zero. Then $r(t)$ can be rewritten as

$$\begin{aligned} r(t) &= \sum_{i=1}^{M} b_1(i) A_1 c_1(t - iT) \\ &+ \sum_{i=1}^{M+1} \sum_{k=2}^{K} b_k(i) A_k c_k(t - iT - \tau_k) + n(t) \end{aligned} \tag{7.3}$$

or in the discrete form

$$r = H_1 \theta_1 + J_1 + n \tag{7.4}$$

where

$$\theta_1 = b_1 A_1 = A_1 [b_1(1) \;\; b_1(2) \;\; \ldots \;\; b_1(M)]^T,$$

$$H_1 = [c_1(1) \;\; c_1(2) \;\; \ldots \;\; c_1(M)] \in \{-1, 0, 1\}^{(mM) \times M},$$

$$c_1(i) = [\mathbf{0}^T_{(i-1)m} \;\; c_{1,1} \;\; c_{1,2} \;\; \ldots \;\; c_{1,m} \;\; \mathbf{0}^T_{(M-i)m}]^T,$$

and c_{1p} is the pth sample of the total m samples of PN code $c_1(t)$, and vector $\mathbf{0}_L$ is a column vector with L zero elements. The interference term J_1 with respect to the signal $H_1\theta_1$ at the first cancellation stage is written as

$$J_1 = H_{J_1} \theta_{J_1} \tag{7.5}$$

where the interference parameter θ_{J_1} is

$$\theta_{J_1} = B_{J_1} A_{J_1}$$

the interference amplitude vector is

$$A_{J_1} = [A_2 \;\; A_3 \;\; \ldots \;\; A_K]^T,$$

and the interference data matrix is

$$B_{J_1} = \begin{bmatrix} \text{diag}(b_{J_1}(1)) \\ \text{diag}(b_{J_1}(2)) \\ \vdots \\ \text{diag}(b_{J_1}(M+1)) \end{bmatrix} \tag{7.6}$$

$$b_{J_1}(i) = [b_2(i) \;\; b_3(i) \;\; \ldots \;\; b_K(i)]^T, \quad i = 1, 2, \ldots, M+1.$$

The interference sequence matrix is defined as

$$H_{J_1} = [c_2(1)\, c_3(1) \ldots c_K(1)\, c_2(2)\, c_3(2) \ldots c_K(2) \ldots c_2(M+1)\, c_3(M+1) \ldots c_K(M+1)] \in \{-1, 0, 1\}^{mM \times (K-1)(M+1)},$$

where $c_k(i)$ depends on the delay τ_k. For example, if τ_2 leads to the number of PN code samples to be p_2 for user 2 in the first bit of the observation, we have

$$c_2(1) = [c_{2,m-p_2+1} \;\; \ldots \;\; c_{2,m} \;\; \mathbf{0}^T_{mM-p_2}]^T \in \{-1, 0, 1\}^{mM \times 1},$$

$$c_2(2) = [\mathbf{0}^T_{p_2} \;\; c_{2,1} \;\; \ldots \;\; c_{2,m} \;\; \mathbf{0}^T_{m(M-1)-p_2}]^T \in \{-1, 0, 1\}^{mM \times 1},$$

and

$$c_2(i) = [\mathbf{0}^T_{(i-2)m+p_2} \;\; c_{2,1} \;\; \ldots \;\; c_{2,m} \;\; \mathbf{0}^T_{m(M-i+2)-p_2}]^T \in \{-1, 0, 1\}^{mM \times 1},$$

etc.

Using the conventional matched filter, the first user's signature code is detected by the Automatic Threshold Control (ATC) acquisition scheme described in chapter 4. Thus H_1 is known in (7.4). Then we conduct the estimation on θ_1 including both the sign and the amplitude. We apply the Least-Squares (LS) method to the estimation. The result is given by [27]

$$\begin{aligned} \hat{\theta}_1 &= (H_1^T H_1)^{-1} H_1^T r \\ &= \frac{1}{m} H_1^T r \end{aligned} \tag{7.7}$$

which turns out to be the outputs of the conventional matched filter 1 at the M sampling instants.

To see how the estimation behaves, we calculate its mean and covariance. Substituting r of (7.4) into (7.7), then we get

$$\begin{aligned}\hat{\theta}_1 &= \frac{1}{m}H_1^T(H_1\theta_1 + J_1 + n) \\ &= \theta_1 + \frac{1}{m}H_1^T H_{J_1}\theta_{J_1} + \frac{1}{m}H_1^T n \\ &= \theta_1 + \frac{1}{m}R_{1J_1}\theta_{J_1} + \frac{1}{m}H_1^T n, \end{aligned} \tag{7.8}$$

where the cross-correlation matrix R_{1J_1} between user 1 and other users is given by

$$\begin{aligned} R_{1J_1} &= H_1^T H_{J_1} \\ &= \begin{bmatrix} r_{1J_1}^T(0) & r_{1J_1}^T(1) & 0 & \cdots & 0 \\ 0 & r_{1J_1}^T(0) & r_{1J_1}^T(1) & & \vdots \\ \vdots & & \ddots & \ddots & 0 \\ 0 & \cdots & 0 & r_{1J_1}^T(0) & r_{1J_1}^T(1) \end{bmatrix}, \end{aligned} \tag{7.9}$$

where

$$\begin{aligned} r_{1J_1}^T(0) &= [c_1(1)^T c_2(1) \;\; c_1(1)^T c_3(1) \;\; \ldots \;\; c_1(1)^T c_K(1)] \\ &= [r_{12}(0) \;\; r_{13}(0) \;\; \ldots \;\; r_{1K}(0)], \end{aligned}$$

$$\begin{aligned} r_{1J_1}^T(1) &= [c_1(1)^T c_2(2) \;\; c_1(1)^T c_3(2) \;\; \ldots \;\; c_1(1)^T c_K(2)] \\ &= [r_{12}(1) \;\; r_{13}(1) \;\; \ldots \;\; r_{1K}(1)]. \end{aligned}$$

Once the delays τ_k are fixed, R_{1J_1} is a constant matrix (unknown). The estimation $\hat{\theta}_1$ is a random vector because of the randomness of θ_{J_1} (random data) and the AWGN n. Since each of the data bits in θ_{J_1} is either -1 or 1 with equal probability, the mean of θ_{J_1} is a zero vector. It is obvious that $\bar{\hat{\theta}}_1 = \theta_1$, which means that $\hat{\theta}_1$ is an unbiased estimation.

The variance of $\hat{\theta}_1$ depends on the covariances of $\frac{1}{m}R_{1J_1}\theta_{J_1}$ and $\frac{1}{m}H_1^T n$ (the multi-user interference and the AWGN are independent), which is calculated as

$$\mathrm{Cov}(\hat{\theta}_1) = \frac{1}{m^2}\mathrm{E}\{(R_{1J_1}\theta_{J_1})(R_{1J_1}\theta_{J_1})^T\} + \frac{1}{m^2}\mathrm{E}\{(H_1^T n)(H_1^T n)^T\} \tag{7.10}$$

where the second term is easily found to be

$$\frac{\sigma^2}{m}I_M.$$

I_M is a $M \times M$ identical matrix. To calculate the first term of (7.10), we first calculate a matrix defined as $D_{J_1} = \mathrm{E}\{\theta_{J_1}\theta_{J_1}^T\}$. This is easily obtained by noticing that all the data bits in θ_{J_1} are i.i.d. 1 or -1 random variables with equal probabilities. Thus D_{J_1} is found to be a diagonal matrix

$$D_{J_1} = \begin{bmatrix} (\mathrm{diag}(A_{J_1}))^2 & 0 & \cdots & 0 \\ 0 & (\mathrm{diag}(A_{J_1}))^2 & & \vdots \\ \vdots & & \ddots & 0 \\ 0 & \cdots & 0 & (\mathrm{diag}(A_{J_1}))^2 \end{bmatrix} \tag{7.11}$$

Thus the first term of (7.10) is given by

$$\frac{1}{m^2}R_{1J_1}D_{J_1}R_{1J_1}^T = \begin{bmatrix} \sigma_1^2 & \rho & 0 & \cdots & \cdots & 0 \\ \rho & \sigma_1^2 & \rho & & & \vdots \\ 0 & \ddots & \ddots & \ddots & & \vdots \\ \vdots & & & & \ddots & 0 \\ \vdots & & & \ddots & \ddots & \rho \\ 0 & \cdots & \cdots & 0 & \rho & \sigma_1^2 \end{bmatrix} \tag{7.12}$$

where

$$\begin{aligned} \sigma_1^2 &= \frac{1}{m^2}[r_{1J_1}^T(0)(\mathrm{diag}(A_{J_1}))^2 r_{1J_1}(0) + r_{1J_1}^T(1)(\mathrm{diag}(A_{J_1}))^2 r_{1J_1}(1)] \\ &= \frac{1}{m^2}\sum_{k=2}^{K}(r_{1k}^2(0) + r_{1k}^2(1))A_k^2, \end{aligned} \tag{7.13}$$

$$\begin{aligned}\rho &= \frac{1}{m^2} r_{1J_1}^T(0)(\mathrm{diag}(A_{J_1}))^2 r_{1J_1}(1) \\ &= \frac{1}{m^2}\sum_{k=2}^{K} r_{1k}(0) r_{1k}(1) A_k^2. \end{aligned} \tag{7.14}$$

The ith error variance of the estimation $\hat{\theta}_1$ is given by

$$\mathrm{Var}(\hat{\theta}_1(i)) = \sigma_1^2 + \frac{\sigma^2}{m^2} \tag{7.15}$$

We have seen that the unknown asynchronous multi-user interference introduces correlation ρ among the M estimations. For a synchronous CDMA system, $r_{1k}(1) = 0$, then $\rho = 0$, i.e. the correlation is zero.

In most cases, the estimation $\hat{b}_1 = \mathrm{sign}(\hat{\theta}_1)$ is good enough [1] for the acquisition since $A_1 \geq A_k$, $k \neq 1$. However, the amplitude $\hat{A}_1$ depends on $r_{1k}(0)$, $r_{1k}(1)$ and A_k, $k \neq 1$. To further improve the estimation of A_1, we apply the LS estimation conditioned on that b_1 is estimated correctly, or at least during the M bits data block. Then r in (7.4) can be written as

$$\begin{aligned} r &= H_1 b_1 A_1 + J_1 + n \\ &= \bar{H}_1 A_1 + J_1 + n \end{aligned} \tag{7.16}$$

where $\bar{H}_1 = H_1 b_1$. The unknown variable A_1 is then estimated as

$$\begin{aligned} \hat{A}_1 &= (\bar{H}_1^T \bar{H}_1)^{-1} \bar{H}_1^T r \\ &= \frac{1}{mM} \bar{H}_1^T r \\ &= A_1 + \frac{1}{Mm} \bar{H}_1^T J_1 + \frac{1}{Mm} \bar{H}_1^T n \end{aligned} \tag{7.17}$$

The variance of $\hat{A}_1$ is

$$\begin{aligned} \mathrm{Var}(\hat{A}_1) &= \frac{1}{M^2 m^2} \mathrm{E}\{b_1^T R_{1J_1} \mathrm{E}\{\theta_{J_1} \theta_{J_1}^T\} R_{1J_1}^T b_1\} + \frac{1}{M^2 m^2} \mathrm{E}\{b_1^T H_1^T \mathrm{E}\{nn^T\} H_1 b_1\} \\ &= \frac{\sigma_1^2}{M} + \frac{\sigma^2}{Mm} \end{aligned} \tag{7.18}$$

[1] The performance of $\hat{b}_1$ is often given by the required bit-error rate, a system design specification.

Compared with $\mathrm{Var}(\hat{\theta}_1(i))$ in (7.15), we conclude that the variance has been reduced M times by the second LS estimation. In practice, it is very easy to get $\hat{A}_1$ because it is just the absolute average value of the M samples from the output of matched filter 1.

7.2.2 Acquisition scheme 1

The most straightforward way for acquiring all the PN codes is to apply the above estimation repeatedly until all the stronger signals are removed one by one and the weakest signal is given the chance to be captured. We call this scheme the one-by-one (OBO) cancellation. The acquisition process is shown in figure 7.1. In this chapter, we say that the receiver is in the acquisition stage i when it is detecting the ith signal.

First, the K matched filters try to detect their own PN codes using the ATC acquisition scheme in a certain time period. Some of the matched filters may obtain acquisitions, but the strongest signal is assumed to be the one which corresponds to the largest average correlation output. Then we form an estimated signal for the signal detected

$$\hat{S}(t, b_1) = \sum_{i=1}^{M} \hat{b}_1(i)\hat{A}_1 c_1(t - iT) \tag{7.19}$$

or in the discrete form

$$\hat{S}(b_1) = H_1 \hat{b}_1 \hat{A}_1 \tag{7.20}$$

After the cancellation is done on this M-bit signal, the composite signal is updated by $r - \hat{S}(b_1)$. For this updated signal, the left $K - 1$ matched filters still try to detect their own codes. Once the strongest one is acquired, it will be removed in the same way. This procedure is repeated until all the PN codes are captured. If at the moment when the left L matched filters are not able to detect any signals,

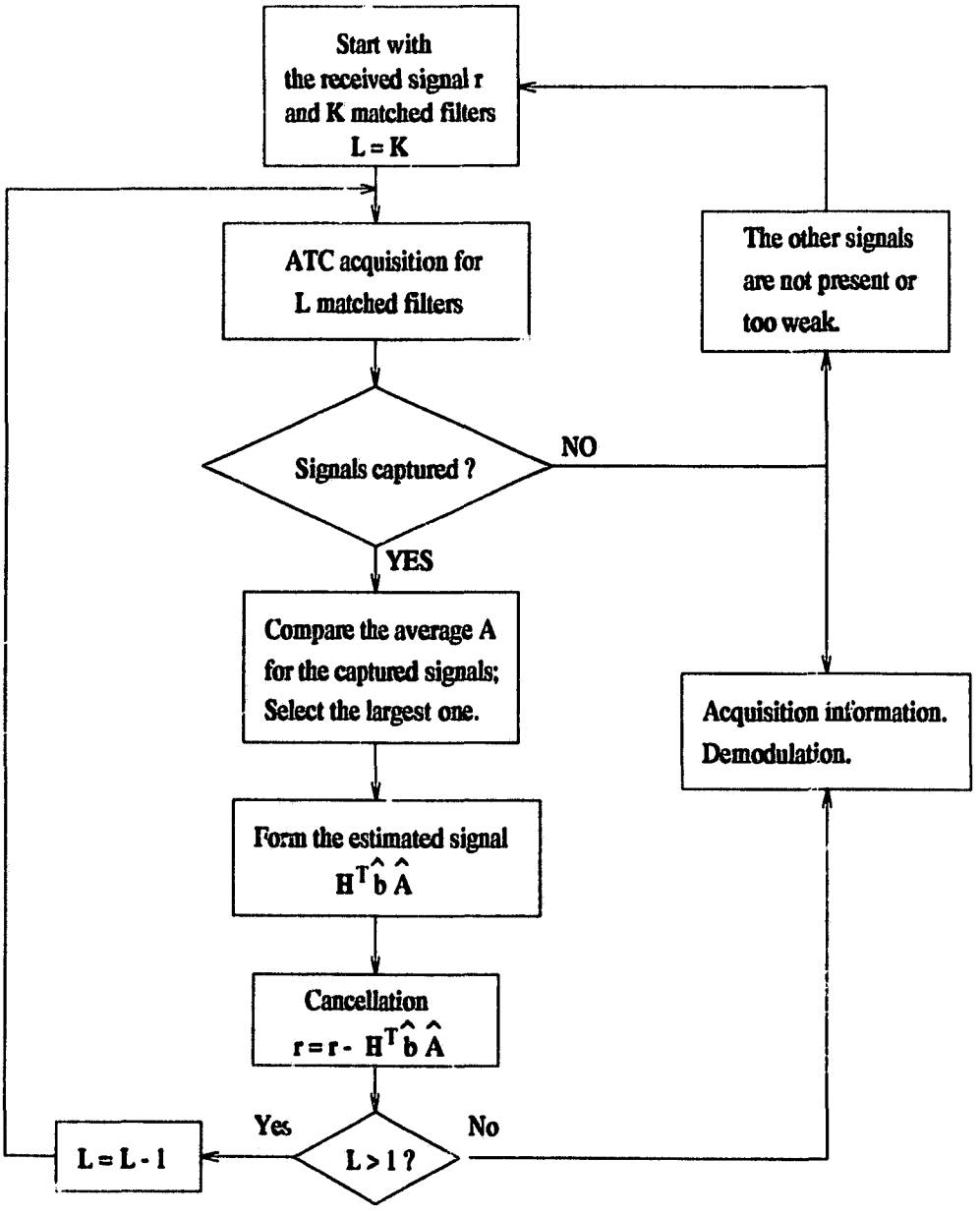

Figure 7.1: Block diagram of one-by-one acquisition process.

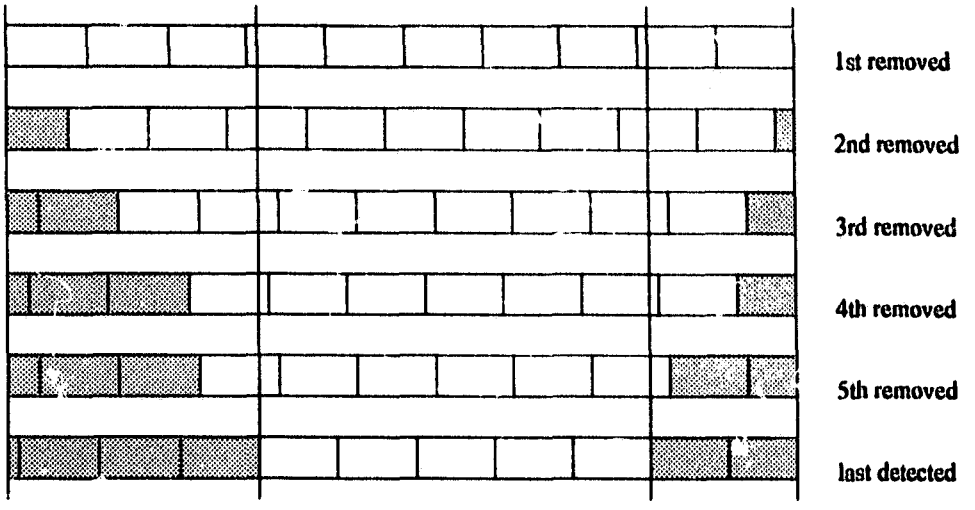

Figure 7.2: Data construction of the received signal. Poorer estimations are represented by the shaded bits.

the signals are assumed to be absent or too weak, and the receiver will pick up another block of data and continue the acquisition, at the same time it will start the demodulation for the captured $K - L$ signals.

Two remarks are addressed here. First, the receiver needs a memory to store signal r or updated signals. Secondly, every time the cancellation is conducted, the detected signal with a number of data bits is removed, and since other users' signals are usually not synchronized with the removed signal, estimations on the two bits at the two ends of the data block are taken from parts of the whole date bits, see figure 7.2. Therefore the estimations on these two bits will be poorer than estimations on other bits. As the cancellation goes on, the effects of the poorer estimations will be passed on to some bits of the next estimation signal due to the cross-correlation. These bits are illustrated by the shaded bits. However, the acquisition detection can be designed not to rely on these bits. In other words, the shaded bits will be omitted for the purpose of acquisitions. As seen from figure 7.2, at the ith stage, i shaded bits (including the partial bits at the two ends) will be omitted, and only

$M - i + 1$ bits are left for the acquisition detection at the stage. Therefore, for a K-user system, if the minimum number of data bits required for acquisitions is M', the number of data bits M required for the first detected signal should be $M = M' + K - 1$. This is clearly shown in figure 7.2 where $M = 10$, $K = 6$ and $M' = 5$.

7.2.3 Acquisition scheme 2

In the OBO acquisition scheme, signals from different users are removed one by one by estimating their waveforms. Since the estimation on any user's signal cannot be perfect, especially when there exists multi-user interference, the updated signal will contain a residue of the cancelled signal. This remainder will be stored with the updated signal until the last detected signal. The residual signals from each stage form a harmful interference to the undetected signals and sometimes make it difficult to capture the relatively weak signals even when the AWGN is negligible.

The shortcoming of the OBO scheme can be alleviated by our second acquisition scheme which is a simultaneous estimation and cancellation (SEC) technique. At each stage, all the signals so far detected are estimated simultaneously and then removed from the original compound signal. It is expected that the cancellation error will be getting smaller as more signals are detected correctly. A special case is that when the AWGN is zero and all the PN codes are captured, the estimations upon all the signals will be perfect (no cancellation error). This is just what the near-far resistant decorrelating detector has achieved. Thus we can say that the SEC scheme is an approximation to the decorrelating detector since it ignores the influence of those weak signals.

Assume that signature sequences of user 1 to user i have been detected. The received signal can be expressed as

$$r = H_i'\theta_i' + J_i' + n \tag{7.21}$$

where the matrix for the detected sequences is given by

$$H_i' = [c_1(1)\, c_2(1) \ldots c_i(1)\, c_1(2)\, c_2(2) \ldots c_i(2) \ldots c_2(M+1)\, c_3(M+1) \ldots c_i(M+1)] \in \{-1, 0, 1\}^{mM \times (i(M+1)-1)},$$

Here we assume that $\tau_k \neq 0$, for $k \neq 1$. The vector of the under-estimated parameter θ_i' is written as

$$\theta_i' = B_{S_i} A_{S_i}$$

where

$$A_{S_i} = [A_1 \quad A_2 \quad \ldots \quad A_i]^T,$$

$$B_{S_i} = \begin{bmatrix} \mathrm{diag}(b_{S_i}(1)) \\ \mathrm{diag}(b_{S_i}(2)) \\ \vdots \\ \mathrm{diag}(b_{S_i}(M+1)) \end{bmatrix}$$

with

$$b_{S_i}(j) = [b_1(j) \;\; b_2(j) \;\; \ldots \;\; b_i(j)]^T, \quad j = 1, 2, \ldots, M,$$

$$b_{S_i}(M+1) = [b_2(M+1) \;\; b_3(M+1) \;\; \ldots \;\; b_i(M+1)]^T,$$

The interference term J_i' in (7.21) is given by

$$J_i' = H_{J_i}' \theta_{J_i}' \tag{7.22}$$

where

$$\theta_{J_i}' = B_{J_i}' A_{J_i}',$$

$$A_{J_i}' = [A_{i+1} \quad A_{i+2} \quad \ldots \quad A_K]^T,$$

$$B'_{J_i} = \begin{bmatrix} \text{diag}(b_J(1)) \\ \text{diag}(b_J(2)) \\ \vdots \\ \text{diag}(b_J(M+1)) \end{bmatrix}$$

$$b_J(j) = [b_{i+1}(j) \;\; b_{i+2}(j) \;\; \ldots \;\; b_K(j)]^T, \quad j = 1, 2, ..., M+1,$$

There could be also two estimation methods in the SEC scheme. For the first one or the simpler one, we estimate θ'_i using

$$\hat{\theta}'_i = [H'^T_i H'_i]^{-1} H'^T_i r \tag{7.23}$$

The estimated waveform is then obtained

$$\hat{S}(\hat{\theta}'_i) = H'_i \hat{\theta}'_i,$$

and the remaining signal after the cancellation based on the estimation is $r - \hat{S}(\hat{\theta}'_i)$.

For the second SEC method, we first calculate B_{S_i} or $b_{S_i}(j), \;\; j = 1, 2, ..., M+1$, using

$$\hat{b}_{S_i} = \text{sign}(\hat{\theta}'_i) \tag{7.24}$$

then the absolute amplitudes of signals from the i users are estimated by

$$\hat{A}_{S_i} = [\bar{H}'^T_i \bar{H}'_i]^{-1} \bar{H}'^T_i r \tag{7.25}$$

where

$$\begin{aligned} \bar{H}'_i &= H'_i \hat{B}_{S_i} \\ &= \left[\sum_{j=1}^{M} c_1(j)\hat{b}_1(j) \quad \sum_{j=1}^{M+1} c_2(j)\hat{b}_2(j) \quad \ldots \quad \sum_{j=1}^{M+1} c_i(j)\hat{b}_i(j) \right] \\ &= \left[\bar{h}_1 \quad \bar{h}_2 \quad \ldots \quad \bar{h}_i \right] \end{aligned} \tag{7.26}$$

The estimated waveform from all the i detected users is

$$\hat{S}(\hat{b}_s) = \bar{H}'_i \hat{A}_{S_i},$$

and the remaining signal after the cancellation is $r - \hat{S}(b_s)$.

The following derivations illustrate how the estimations on amplitudes of the detected signals are updated at each stage when a new signal is detected. Given the estimations $\hat{A}_{S_i}$ on the first i signals, the estimations on the first $i+1$ signals are written as

$$\begin{aligned}
\hat{A}_{S_{i+1}} &= [\bar{H}'^T_{i+1} \bar{H}'_{i+1}]^{-1} \bar{H}'^T_{i+1} r \\
&= \left(\begin{bmatrix} \bar{H}'^T_i \\ \\ \bar{h}^T_{i+1} \end{bmatrix} \begin{bmatrix} \bar{H}'_i & \bar{h}_{i+1} \end{bmatrix} \right)^{-1} \begin{bmatrix} \bar{H}'^T_i \\ \\ \bar{h}^T_{i+1} \end{bmatrix} r \\
&= \begin{bmatrix} \bar{H}'^T_i \bar{H}'_i & \bar{H}'^T_i \bar{h}_{i+1} \\ \\ \bar{h}^T_{i+1} \bar{H}'_i & \bar{h}^T_{i+1} \bar{h}_{i+1} \end{bmatrix}^{-1} \begin{bmatrix} \bar{H}'^T_i \\ \\ \bar{h}^T_{i+1} \end{bmatrix} r
\end{aligned} \tag{7.27}$$

Using the identity [17]

$$\begin{bmatrix} A & D \\ C & B \end{bmatrix}^{-1} = \begin{bmatrix} A^{-1} + E\Delta^{-1}F & -E\Delta^{-1} \\ -\Delta^{-1}F & \Delta^{-1} \end{bmatrix},$$

where $\Delta = B - CA^{-1}D$, $E = A^{-1}D$ and $F = CA^{-1}$, we get

$$\hat{A}_{S_{i+1}} = \begin{bmatrix} \hat{A}_{S_i} - (\bar{H}'^T_i \bar{H}'_i)^{-1} \bar{H}'^T_i \bar{h}_{i+1} \hat{A}_{i+1} \\ \\ \hat{A}_{i+1} \end{bmatrix} \tag{7.28}$$

where

$$\hat{A}_{i+1} = \frac{\bar{h}^T_{i+1}(r - \bar{H}'_i \hat{A}_{S_i})}{\bar{h}^T_{i+1} \bar{Q}'_i \bar{h}_{i+1}} \tag{7.29}$$

with $\bar{Q}_i' = I - \bar{H}_i'(\bar{H}_i'^T\bar{H}_i')^{-1}\bar{H}_i'^T$. It is easy to verify that $\hat{A}_{i+1}$ is an unbiased estimation on A_{i+1} conditioned on the fact that b_{i+1} is correctly detected. From (7.29), it can be seen that the estimation on the amplitude of the new detected user's signal (the $(i+1)$th user) is obtained from taking the output of the $(i+1)$th matched filter with the input equal to the signal cancelled by the previous detected i users' signals and then properly scaled. The scaler in the denominator of (7.29) is different from that for the acquisition scheme 1 where the corresponding scaler is equal to $\bar{h}_{i+1}^T\bar{h}_{i+1} = mM$. Here the scaler is obtained by adding the *weight* Q_i' into the inner product. From (7.28), it is seen that the previous estimations have been modified after detecting the new signal. Recall that the quality of the estimations depend on the undetected multi-user interference J_i' by means of cross-correlations. Thus once any of the interfering user's signal is detected, it can be removed from J_i', and the precision of the estimations on the detected signals is improved. The first acquisition scheme does not have the property because the estimation at each stage will never change throughout the process.

It is interesting to see that the estimation given in (7.24) is in the same form as that of a M-shot decorrelating detector. In fact, while the acquisition process continues, the demodulation on those detected users is also performed by means of any multi-user detections. Therefore, there is no need to keep one specific block of data for acquisition. In practice, the number of active users is usually smaller than K. The receiver has to keep updating its observation data not only for demodulating signal but also for searching any new comers. In addition, the capability of using updated signal data provides a more reliable signal demodulation in the fading environment because the estimation of amplitudes on the previous observation may be quite different from those of the current data due to fading.

7.3 Acquisition probabilities

In this section, we compute the probabilities of acquisitions at all detection stages given the *actual* SNRs of signals and an observation data block. To make this analysis tractable, we make the following assumptions.

1. As many papers did [33][59][32], Gaussian approximation is made for those samples from the outputs of matched filters. For the length of signature sequences and the number of users of the interest, the results of the performance evaluation based on this assumption are very close to the results obtained from simulations.

2. Successive outputs from each of the matched filters are assumed to be statistically independent. In theory, this is not true because of the correlations introduced by the shift registers of the matched filters and the asynchronous interfering users. However, the correlations are very small compared to the estimation variance and thus can be neglected. Combined with the first assumption, this assumption is approximately correct. For the same reason, we have assumption 3.

3. Acquisition decisions on successive bits are approximately independent.

4. Probabilities of acquisitions not in the order of signal power strengths are neglected. Therefore, we only consider the case in which the waveforms are detected in the order of the power strengths from large to small. However, if powers of the signals are similar, every signal gets an approximately equal chance to be captured. The probability analysis will be a little different from the analysis shown in this section. Here we are most interested in the power-dissimilar case, i.e. the near-far environment.

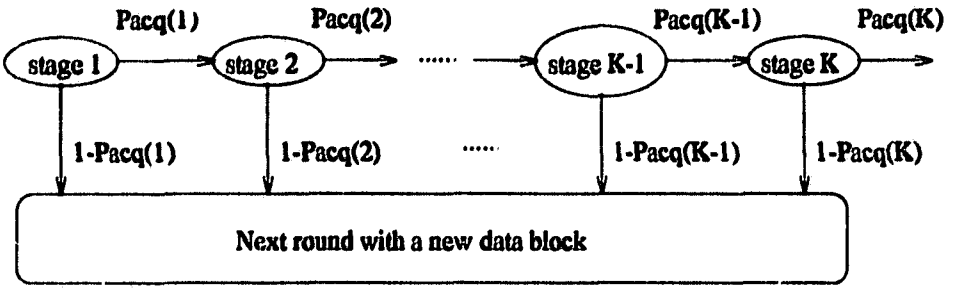

Figure 7.3: Signal flow graph of acquisition process.

From assumption 4, the signal flow graph of the acquisition process at different stages is shown in figure 7.3, where $P_{acq}(i)$ is the probability of the successful acquisition at stage i. It is clearly shown in the figure that the acquisition at a stage depends upon the detections at the previous stages. If the receiver cannot detect any signal at any stage, it will take a new block of data and repeat the acquisition process.

Following the definition in the traditional acquisition process, we use H^0 to denote the hypotheses at non-sync epoches and H^1 to denote the hypotheses at sync epoches. Using the ATC acquisition scheme for the matched filter i and assuming that the detected data bit is $+1$, the sampled outputs of the matched filter yields the decision variables which may be expressed as

$$Z_i(0) = \tilde{A}_i + N_i(0) \qquad \text{at } H^1 \tag{7.30}$$

$$Z_i(n) = N_i(n), \qquad n = 1, 2, ..., m-1 \qquad \text{at } H^0 \tag{7.31}$$

where $\tilde{A}_i$ is the *effective* signal amplitude, $N_i(0)$ and $N_i(n)$ $(n = 1, 2, ..., m-1)$ are mutually independent Gaussian random variables with zero means and variances $\sigma_i^2(0)$ and $\sigma_i^2(n)$, respectively. The values of $\tilde{A}_i$, $\sigma_i^2(0)$ and $\sigma_i^2(n)$ will be evaluated in the next section. The decision is made in favor of the signal corresponding to the largest $|Z_i(n)|$ in a window of length m, while the sign of this term is used to decide whether $+1$ or -1 was transmitted. In the acquisition process, the sign

of the term does not affect the detection result as long as the epoch is picked up. Thus the acquisition epoch is detected if $|Z_i(0)| > |Z_i(n)|$ or $Z_i(0) > |Z_i(n)|$ and $Z_i(0) < -|Z_i(n)|$ for $n = 1, 2, ..., m-1$. However, the probability of $Z_i(0) < -|Z_i(n)|$ for $n = 1, 2, ..., m-1$ is very small and can be neglected when $+1$ was transmitted. Therefore, the probability of an acquisition detection in a window for the ith matched filter can be written as

$$\begin{aligned} P_d(i) &= \Pr\{|Z_i(n)| < |Z_i(0)|, \ n = 1, 2, ..., m-1.\} \\ &\approx \Pr\{|Z_i(n)| < Z_i(0) | Z_i(0) > 0, \ n = 1, 2, ..., m-1.\} \end{aligned} \tag{7.32}$$

Using the assumption 2, we get

$$P_d(i) = \prod_{n=1}^{m-1} \Pr\{|Z_i(n)| < Z_i(0) | Z_i(0) > 0\} \tag{7.33}$$

The acquisition for the ith user's signal is obtained if N out of M such windows have successful detections. By assumption 3, the probability of the successful acquisition for user i's signal will be

$$P_{acq}(i) = \sum_{n=N}^{M} \binom{M}{n} P_d(i)^n (1 - P_d(i))^{M-n} \tag{7.34}$$

The probability that a detector successfully passes stage i is given by

$$P_{pass}(i) = \prod_{k=1}^{i} P_{acq}(k) \tag{7.35}$$

The average number of data blocks a receiver needs to achieve the acquisition at stage i is given by

$$\begin{aligned} N(i) &= \sum_{k=1}^{\infty} k(1 - P_{pass}(i))^{k-1} P_{pass}(i) \\ &= 1/P_{pass}(i) \end{aligned} \tag{7.36}$$

A base-station will be more interested in knowing the average number of data blocks it takes to acquire all the sequences. This is given by

$$N(K) = 1/P_{pass}(K)$$

$$= 1/\prod_{k=1}^{K} P_{acq}(k) \tag{7.37}$$

To calculate $P_{pass}(i)$ and $N(i)$, it remains to calculate $P_d(i)$.

7.3.1 Calculation of $P_d(i)$

We derive $P_d(i)$ using the approximation (7.33). The exact computation is given in the appendix G. However, in most cases, the two approaches produce almost the same result. For notational simplicity, we use Z_n to denote the variable $Z_i(n)$. Thus equation (7.33) is re-expressed as

$$P_d(i) = \prod_{n=1}^{m-1} \Pr\{|Z_n| < Z_0 | Z_0 > 0\} \tag{7.38}$$

Since Z_n are assumed to be Gaussian random variables with zero mean and variance $\sigma_i^2(n)$, we get

$$\begin{aligned} \Pr\{|Z_n| < Z_0 | Z_0 > 0\} &= \frac{1}{\sqrt{2\pi\sigma_i^2(n)}} \int_{-Z_0}^{Z_0} e^{-x^2/(2\sigma_i^2(n))} dx \\ &= \mathrm{erf}(\frac{Z_0}{\sqrt{2\sigma_i^2(n)}}), \end{aligned} \tag{7.39}$$

Since Z_0 is also assumed to be a Gaussian random variable with mean $\tilde{A}_i$ and variance $\sigma_i^2(0)$, $P_d(i)$ is

$$\begin{aligned} P_d(i) &= \int_0^{\infty} p(z_0) \prod_{n=1}^{m-1} \mathrm{erf}(\frac{z_0}{\sqrt{2\sigma_i^2(n)}}) dz_0 \\ &= \frac{1}{\sqrt{\pi}} \int_{-\sqrt{\gamma_i}}^{\infty} e^{-v^2} \prod_{n=1}^{m-1} \mathrm{erf}(\alpha_n v + \alpha_n \sqrt{\gamma_i}) dv \end{aligned} \tag{7.40}$$

where $\alpha_n = \sqrt{\sigma_i^2(0)/\sigma_i^2(n)}$, and $\gamma_i = \tilde{A}_i^2/(2\sigma_i^2(0))$ is the *effective* SNR for the main correlation peak.

7.4 Acquisition detection analysis

In this section, we study the statistical properties of detection variable $\hat{\theta}_i$ conducted by matched filter i at acquisition stage i ($i = 1, 2, ..., K$). Intuitively, the smaller the error variance of estimations from previous stages, the better the acquisition detection at the current stage. In other words, the noise variance produced by a matched filter at a stage will be affected by the error variances of estimations obtained from the previous stages. The relation of those variances at different stages is very complicated due to the nonlinear cross-correlations of the signature sequences. However, we are mostly interested in finding the noise variances generated by matched filters at different stages because acquisition performance can then be determined.

7.4.1 Covariances for acquisition scheme 1

In this subsection, we will look at the estimation variable $\hat{\theta}_i$ for the OBO acquisition scheme. We will soon notice that the estimation conducted by a matched filter is biased after the first stage. Therefore, cancellations based on the estimations in the following stages would not be expected to be better than those based on unbiased estimations.

For the OBO cancellation scheme, after detecting the first signals' PN sequence, the estimation $\hat{\theta}_1$ is

$$\hat{\theta}_1 = H_1^{\dagger} r \tag{7.41}$$

where $H_1^{\dagger} = (H_1^T H_1)^{-1} H_1^T$ is the pseudoinverse of H_1. This has been shown to be an unbiased estimation on θ_1. The residual signal after the first cancellation is given by

$$\begin{aligned} r_c(1) &= r - H_1\hat{\theta}_1 \\ &= r - H_1 H_1^{\dagger} r \\ &= Q_1 r \end{aligned} \tag{7.42}$$

where $Q_1 = I - H_1 H_1^{\dagger}$. Similarly, we obtain the residual signal after the second cancellation

$$\begin{aligned} r_c(2) &= r_c(1) - H_2\hat{\theta}_2 \\ &= r_c(1) - H_2 H_2^{\dagger} r_c(1) \\ &= Q_2 r_c(1) \\ &= Q_2 Q_1 r \end{aligned} \tag{7.43}$$

In general, the residual signal after the jth cancellation is given by

$$\begin{aligned} r_c(j) &= Q_j Q_{j-1} \cdots Q_1 r \\ &= Q_{p_j} r, \end{aligned} \tag{7.44}$$

where $Q_{p_j} = Q_j Q_{j-1} \cdots Q_1$. The estimation on the ith detected signal is given by

$$\begin{aligned} \hat{\theta}_i &= H_i^{\dagger} r_c(i-1) \\ &= H_i^{\dagger} Q_{p_{i-1}} r \\ &= H_i^{\dagger} Q_{p_{i-1}} (H_i\theta_i + J_i + n) \\ &= H_i^{\dagger} Q_{p_{i-1}} H_i\theta_i + H_i^{\dagger} Q_{p_{i-1}} (J_i + n) \end{aligned} \tag{7.45}$$

where $J_i = H_{J_i}\theta_{J_i}$ is the sum of signals of all the K users except the ith user. The definitions of H_{J_i} and θ_{J_i} are similar to the definitions of H_{J_1} and θ_{J_1} by keeping user 1's signal instead of user i's.

The above estimation is biased since $H_i^{\dagger} Q_{p_{i-1}} H_i\theta_i$ is usually not equal to θ_i except for $i = 1$. For the OBO scheme, the acquisition detection before the estimation also

depends on the same variable $\hat{\theta}_i$ because $\hat{\theta}_i = H_i^{\dagger} r_c(i-1)$ is just the output from matched filter i at stage i. Provided that b_i was transmitted, the mean vector of $\hat{\theta}_i$ is given by the first term of (7.45), and the covariance matrix depends on the second term of (7.45). In practical situations, $H_i^{\dagger} Q_{p_{i-1}} H_i$ is a diagonally dominant positive definite matrix which guarantees that the signs of the elements in $H_i^{\dagger} Q_{p_{i-1}} H_i \theta_i$ are not changed from the corresponding elements in θ_i. Since the elements of θ_i are $\{A_i, -A_i\}$ binary random variables with equal probability, the absolute element values of $H_i^{\dagger} Q_{p_{i-1}} H_i \theta_i$ will be different each time a new θ_i is transmitted. For acquisition purpose, we are more interested in the average signal sample energy of each element in $H_i^{\dagger} Q_{p_{i-1}} H_i \theta_i$. These energies are given by the diagonal elements of the following covariance matrix with the expectation respect to θ_i

$$\mathrm{Cov}(H_i^{\dagger} Q_{p_{i-1}} H_i \theta_i) = A_i^2 H_i^{\dagger} Q_{p_{i-1}} H_i H_i^T Q_{p_{i-1}}^T H_i^{\dagger T} \tag{7.46}$$

The *effective* amplitude $\tilde{A}_i$ is then defined as the square-root of the average sample energy.

Now we move to the noise part of $\hat{\theta}_i$ in (7.45). It is a zero mean vector with respect to the mutually independent random data contained in J_i and with respect to the AWGN. Its covariance is given by

$$\begin{aligned}
\mathrm{Cov}(\hat{\theta}_i) &= \mathrm{Cov}(H_i^{\dagger} Q_{p_{i-1}} (J_i + n)) \\
&= \mathrm{E}\{H_i^{\dagger} Q_{p_{i-1}} J_i J_i^T Q_{p_{i-1}}^T H_i^{\dagger T}\} + \mathrm{E}\{H_i^{\dagger} Q_{p_{i-1}} n n^T Q_{p_{i-1}}^T H_i^{\dagger T}\} \\
&= H_i^{\dagger} Q_{p_{i-1}} H_{J_i} \mathrm{E}\{\theta_{J_i} \theta_{J_i}^T\} H_{J_i}^T Q_{p_{i-1}}^T H_i^{\dagger T} + H_i^{\dagger} Q_{p_{i-1}} \mathrm{E}\{n n^T\} Q_{p_{i-1}}^T H_i^{\dagger T} \\
&= H_i^{\dagger} Q_{p_{i-1}} H_{J_i} D_{J_i} H_{J_i}^T Q_{p_{i-1}}^T H_i^{\dagger T} + \sigma^2 H_i^{\dagger} Q_{p_{i-1}} Q_{p_{i-1}}^T H_i^{\dagger T}
\end{aligned} \tag{7.47}$$

where D_{J_i} is

$$D_{J_i} = \begin{bmatrix} (\text{diag}(A_{J_i}))^2 & 0 & \cdots & 0 \\ 0 & (\text{diag}(A_{J_i}))^2 & & \vdots \\ \vdots & & \ddots & 0 \\ 0 & \cdots & 0 & (\text{diag}(A_{J_i}))^2 \end{bmatrix} \tag{7.48}$$

with $A_{J_i} = [A_1 \;\; A_2 \;\; \ldots \;\; A_{i-1} \;\; A_{i+1} \;\; \ldots \;\; A_K]^T$. It is difficult to further simplify (7.47) due to the highly nonlinear dependence of $Q_{p_{i-1}}$. However, the jth detection variance on $\hat{\theta}_i$ is given by the jth diagonal element of $\text{Cov}(\hat{\theta}_i)$ which can be computed from (7.47). It is easy to verify that $\text{Cov}(\hat{\theta}_1)$ derived from (7.47) is the same as that derived from (7.10).

The following example shows how the *effective* amplitudes and the variances of $\hat{\theta}_i$ behave at different acq stages for the OBO scheme.

Example : For a 6-user CDMA system, all users are assumed to be active with *actual* signal-to-noise ratios from user 1 to user 6 being 24, 20, 16, 10, 8 and 6dB, respectively. 6 different m-sequences of length 31 are assigned to the 6 users with sequence phases from user 1 to user 6 being 0, 20, 10, 6, 10 and 3 chips (relative to the first user), respectively. We are interested in finding out the average signal sample energies and the detection variances from matched filter i at stage i by computing (7.46) and (7.47). Knowing them, we can obtain the *effective* bit SNRs for the observation bits.

The *effective* bit SNR for the jth bit of the matched filter i at stage i is defined as

$$\gamma_{ij} = \frac{\tilde{A}_i^2}{2\sigma_{ij}^2(0)} \tag{7.49}$$

where $\sigma_{ij}^2(0)$ is given by the jth diagonal element of the $\text{Cov}(\hat{\theta}_i)$. It is easy to find that $\sigma_{ij}^2(0) = \sigma^2/m$ when there are no interfering signals. In such a case, the defined *effective* SNR will be equal to the *actual* SNR. Usually, it is smaller than the *actual*

Table 7.1: Effective SNR(dB) for the OBO scheme, ($M = 10$).

Stage No.	Bit No.										
	1	2	3	4	5	6	7	8	9	10	11
1	13.0	13.0	13.0	13.0	13.0	13.0	13.0	13.0	13.0	13.0	N/A
2	9.9	11.2	11.2	11.2	11.2	11.2	11.2	11.2	11.2	11.2	7.6
3	4.8	11.4	11.4	11.4	11.4	11.4	11.4	11.4	11.4	11.4	11.8
4	1.1	8.5	8.3	8.3	8.3	8.3	8.3	8.3	8.3	8.3	4.9
5	3.8	4.6	3.6	3.6	3.6	3.6	3.6	3.6	3.6	3.6	3.5
6	-8.8	1.1	0.3	0.3	0.3	0.3	0.3	0.3	0.3	0.3	-0.9

SNR. The *effective* SNRs for $i = 1, 2, \ldots K$ at all observation data bits are listed in table 7.1. Since we are only interested in those bits which have the same value of the *effective* SNR, the subscript j in (7.49) was omitted in section 3 for a notational simplicity. Besides, we use $\sigma_i^2(0)$ to denote the detection variance at a sync epoch and $\sigma_i^2(n)$ $(n = 1, 2, ..., m-1)$ to denote the variances at the non-sync epoches.

From table 7.1, we can see that the *effective* SNRs of those un-shaded bits in figure 7.2 have the same values for a specific matched filter, while the *effective* SNRs of the shaded bits will often have smaller values. The reason has been explained in section 2.2. Therefore, the receiver will skip over those shaded bits and use the left bits for the acquisition detections. We also see that the SNRs of matched filters to detect their own PN sequences are significantly reduced by the multi-user interference compared to their *actual* SNRs. In this example, the amounts of SNR losses from user 1 to user 6 at the corresponding stages are respectively equal to 11, 8.8, 4.6, 1.7, 4.4 and 5.7 dB. Although the stronger signals usually reduce SNRs due to more interfering users, they still have better performances than the weak signals because of their larger *effective* SNRs. Acquisitions often fail for those weak signals.

It should be noted that the analysis we have made is based on the assumption

that a receiver detects signals in the order of signal strengths. In practice, it is also possible that a receiver sometimes detects signals not exactly in the order of strengths. However, in this case, the corresponding *effective* SNRs will be smaller than those obtained in the order of strengths. For the very power-dissimilar signals, the disorder detection rarely occurs. Once they happen, the acquisition detections will often fail because of too large estimation error. For power-similar signals or approximately equal-power signals, the order of detections does not make much difference for the acquisitions.

Finally in this subsection, we need to calculate the noise variance at a non-sync epoch. This is easily done by computing the covariance of (7.45) with $H_i^\dagger$ replaced by its shifted version and taking the first term also as a noise term. We have found that this first term cannot be neglected for the calculation of noise variance. The noise variances are given by their corresponding diagonal elements of the covariance matrix and are denoted by $\sigma_i^2(n)$ where n is the relative time shift with respect to the correct sync epoch 0.

7.4.2 Covariances for acquisition scheme 2

In this subsection, we will discuss the estimation property for the SEC scheme. Unlike the OBO scheme, the estimation on the detected signals is unbiased. The cancellations based on it will be at least better than those by the OBO scheme.

For the SEC scheme, the estimation on the first j detected signals at stage j is written as

$$\begin{aligned} \hat{\theta}'_j &= H_j'^{\dagger} r \\ &= H_j'^{\dagger}(H'_j\theta'_j + J'_j + n) \\ &= \theta'_j + H_j'^{\dagger}(J'_j + n) \end{aligned} \tag{7.50}$$

It is obvious that $\hat{\theta}'_j$ is an unbiased estimation on θ_j. The residual signal after the

cancellation based on $\hat{\theta}'_j$ is

$$\begin{aligned} r_c(j) &= r - H'_j\hat{\theta}'_j \\ &= r - H'_jH'^{\dagger}_j r \\ &= Q'_j r \end{aligned} \tag{7.51}$$

where $Q'_j = I - H'_jH'^{\dagger}_j$.

At the ith stage, the matched filter i will first try to detect its correlation output for the acquisition of the ith signal with the input signal as $r_c(i-1)$. Once the PN sequence H_i is captured, the receiver will reestimate the detected i signals and form the new residual signal $r_c(i)$ for the $(i+1)$th acquisition detection. The performance of the acquisition at stage i depends on the detection variable $\hat{\theta}_i$ conducted by the matched filter i. As for the OBO scheme, we first study $\hat{\theta}_i$ and then find out the *effective* SNRs for the detections.

$$\begin{aligned} \hat{\theta}_i &= H_i^{\dagger} r_c(i-1) \\ &= H_i^{\dagger} Q'_{i-1} r \\ &= H_i^{\dagger} Q'_{i-1}(H_i\theta_i + J_i + n) \\ &= H_i^{\dagger} Q'_{i-1} H_i\theta_i + H_i^{\dagger} Q'_{i-1}(J_i + n) \end{aligned} \tag{7.52}$$

From (7.45) and (7.52), we can see that the MF detection variables for the two schemes are in the same form. However, the difference of the two schemes comes from the difference of the matrices $Q_{p_{i-1}}$ and Q'_{i-1}. Following the same steps in 7.4.1, we obtain the signal covariance as

$$\mathrm{Cov}(H_i^{\dagger} Q'_{i-1} H_i\theta_i) = A_i^2 H_i^{\dagger} Q'_{i-1} H_i H_i^T Q'^T_{i-1} H_i^{\dagger T} \tag{7.53}$$

and the noise covariance of the $\hat{\theta}_i$ as

$$\mathrm{Cov}(\hat{\theta}_i) = H_i^{\dagger} Q'_{i-1} H_{J_i} D_{J_i} H_{J_i}^T Q'^T_{i-1} H_i^{\dagger T} + \sigma^2 H_i^{\dagger} Q'_{i-1} Q'^T_{i-1} H_i^{\dagger T} \tag{7.54}$$

Table 7.2: Effective SNR(dB) for the SEC scheme, ($M = 10$).

Stage No.	Bit No.										
	1	2	3	4	5	6	7	8	9	10	11
1	13.0	13.0	13.0	13.0	13.0	13.0	13.0	13.0	13.0	13.0	N/A
2	9.9	11.2	11.2	11.2	11.2	11.2	11.2	11.2	11.2	11.2	7.6
3	4.2	11.4	11.5	11.5	11.5	11.5	11.5	11.5	11.5	11.5	12.1
4	-4.4	8.8	8.8	8.8	8.8	8.8	8.8	8.8	8.8	8.8	5.9
5	-2.4	6.0	6.1	6.1	6.1	6.1	6.1	6.1	6.1	6.2	4.1
6	-4.7	3.8	4.6	4.6	4.6	4.6	4.6	4.6	4.6	4.6	3.0

The *effective* SNRs for the SEC scheme can be computed using the results from the above two equations.

The sidelobe variances at the non-sync epoches are computed in the same way as that described in 4.1.

We now continue the example in 4.1 by the SEC scheme. While all the parameters are unchanged, we get the *effective* SNRs listed in table 7.2. Compared to table 7.1, we can see that the two schemes have almost the same acquisition performance for the stronger signals. However, the SEC scheme has much better performance than the OBO scheme for the weak signals. For example, the SEC scheme only loses 1.4dB for the last acquisition detection, while the OBO scheme loses 5.7dB, which almost makes the acquisition impossible. Remember that once all the sequences have been acquired, any multi-user detection algorithm will give a better performance than the acquisition algorithms. Thus the acquisition schemes need to be repeated several times or more until all the sequences are captured.

It is noted that the acquisition performance also depends on the degree of similarity of the received signal powers. If the received signals are very similar, the detections for the first few signals may be very difficult. Therefore, it may need

Table 7.3: Effective SNR(dB) for the OBO scheme with equal power of 24dB, ($M = 10$).

Stage	Bit No.										
No.	1	2	3	4	5	6	7	8	9	10	11
1	2.2	2.2	2.2	2.2	2.2	2.2	2.2	2.2	2.2	2.2	N/A
2	-1.3	1.0	1.0	1.0	1.0	1.0	1.0	1.0	1.0	1.0	-2.2
3	-1.1	7.0	7.1	7.1	7.1	7.1	7.1	7.1	7.1	7.1	9.6
4	1.0	14.6	14.1	14.0	14.0	14.0	14.0	14.0	14.0	14.0	6.2
5	10.8	12.1	9.9	9.9	9.9	9.9	9.9	9.9	9.9	9.9	11.9
6	-1.9	7.4	9.5	9.4	9.4	9.4	9.4	9.4	9.4	9.4	7.2

many rounds (data blocks) to acquire the first several signals. Unlike the power-dissimilar case where the detected signals can be demodulated before the last signal is detected, for the power-similar case, not much demodulation can be conducted while the receiver is trying to detect the first several signals. Tables 7.3 and 7.4 show the *effective* SNRs of the OBO and the SEC schemes, respectively, when powers of all the signals are 24dB while other parameters remain as in the previous examples. From these two tables, it is also found that the SEC scheme performs better than the OBO scheme for the later detected signals. However, the first two signals for both schemes are very difficult to be captured in this example because of the very low *effective* SNRs due to the existences of strong interfering signals, no matter how large their *actual* SNRs are (for other phase distributions, the *effective* SNRs could be a little different). It is true that the dissimilar signals will be more suitable for the fast acquisitions in the asynchronous CDMA systems. Fortunately, signals in such systems are more likely to be dissimilar.

Also note that the results given so far in this subsection and 4.1 for the two acquisition schemes are obtained based on cancellations by estimating θ_i or θ'_i. By

Table 7.4: Effective SNR(dB) for the SEC scheme with equal power of 24dB, $(M = 10)$.

Stage No.	Bit No.										
	1	2	3	4	5	6	7	8	9	10	11
1	2.2	2.2	2.2	2.2	2.2	2.2	2.2	2.2	2.2	2.2	N/A
2	-1.3	1.0	1.0	1.0	1.0	1.0	1.0	1.0	1.0	1.0	-2.2
3	-1.7	7.0	7.1	7.1	7.1	7.1	7.1	7.1	7.1	7.1	9.8
4	-4.8	14.7	14.4	14.3	14.3	14.3	14.3	14.3	14.3	14.3	6.9
5	3.2	12.8	11.8	11.8	11.8	11.8	11.8	11.8	11.8	12.2	13.4
6	13.3	21.8	22.6	22.6	22.6	22.6	22.6	22.6	22.6	22.6	21.0

applying the estimation on A_i or A_{S_i} conditioned on $\hat{b}_i$ or $\hat{b}_{S_i}$, the acquisition performance may be further improved.

In the ideal case where $\hat{b}_j = b_j$, $j = 1, 2, \ldots, i-1$, the detection variable at stage i for the OBO scheme is given by

$$\begin{aligned}
\hat{\theta}_i &= H_i^\dagger r_c(i-1) \\
&= H_i^\dagger \bar{Q}_{p_{i-1}} r \\
&= H_i^\dagger \bar{Q}_{p_{i-1}} (H_i\theta_i + J_i + n) \\
&= H_i^\dagger \bar{Q}_{p_{i-1}} H_i\theta_i, + \bar{H}_i^\dagger \bar{Q}_{p_{i-1}} (J_i + n) \qquad (7.55)
\end{aligned}$$

where the first term represents the signal part and the second the noise part, $\bar{Q}_{p_{i-1}} = \bar{Q}_{i-1}\bar{Q}_{i-2}\cdots\bar{Q}_1$ with $\bar{Q}_j = I - \bar{H}_j\bar{H}_j^\dagger$.

Similarly, for the SEC scheme, the detection variable is

$$\begin{aligned}
\hat{\theta}_i &= H_i^\dagger r_c(i-1) \\
&= H_i^\dagger \bar{Q}'_{i-1} r \\
&= H_i^\dagger \bar{Q}'_{i-1} (H_i\theta_i + J_i + n) \\
&= H_i^\dagger \bar{Q}'_{i-1} H_i\theta_i, + H_i^\dagger \bar{Q}'_{i-1} (J_i + n) \qquad (7.56)
\end{aligned}$$

where $\bar{Q}'_{j-1} = I - \bar{H}'_{j-1}\bar{H}'^{\dagger}_{j-1}$. Again the first term is signal part and the second is the noise. Unfortunately, it is virtually impossible to compute the average signal sample energies and the noise covariances from terms in (7.55) and (7.56) due to the highly nonlinear dependence of the expectations on $Q_{p_{i-1}}$ and Q'_{i-1}.

Finally, for comparison, we compute the *effective* SNRs for the conventional single user detectors without conducting any cancellations. The covariance can be calculated by using equation (7.47) or (7.54) on $\hat{\theta}_i$ but with $Q_{p_i} = I$ or $Q'_i = I$. The results are illustrated in tables 7.5 and 7.6 for the cases of unequal and equal powers, respectively. From table 7.5, we see that the acquisitions are affected by the near-far problem, i.e., the last four (weaker) signals have *effective* SNRs which are lower than 0dB, thus making these signals almost undetectable. Even for the second signal, its acquisition also becomes difficult since the sidelobes from the matched filter 2 are also very high. We should bear in mind that acquisitions depend not only on the effective SNRs listed in those tables but also on the variances $\sigma_i^2(n)$ of those sidelobes which can be calculated for a given phase distribution. For the above phase distribution, the *effective* SNR for the main correlation peaks from the second conventional matched filter is pretty high, which means that the estimations on these main peaks is very precise. However, if we look at its correlation output, which is plotted in figure 7.5, we can see how much effect the sidelobes have on the detection of the main peaks. From table 7.6, all signals are still unable to get an equal chance to be captured due to their random phase distribution. However no signals suffer severe near-far effects. The performance is worse than any of the cancellation acquisition schemes although all the received signal powers are extremely high.

Table 7.5: Effective SNR(dB) for the conventional scheme with unequal powers as 24, 20, 16, 10, 8, 6dB and the same phase distribution as previous tables. ($M = 10$).

Stage	Bit No.										
No.	1	2	3	4	5	6	7	8	9	10	11
1	13.0	13.0	13.0	13.0	13.0	13.0	13.0	13.0	13.0	13.0	N/A
2	9.9	11.0	11.0	11.0	11.0	11.0	11.0	11.0	11.0	11.0	6.9
3	-9.4	-2.3	-2.3	-2.3	-2.3	-2.3	-2.3	-2.3	-2.3	-2.3	-2.0
4	-17.8	-4.8	-4.8	-4.8	-4.8	-4.8	-4.8	-4.8	-4.8	-4.8	-0.7
5	-15.7	-9.7	-9.7	-9.7	-9.7	-9.7	-9.7	-9.7	-9.7	-9.7	-10.1
6	-18.5	-13.5	-13.5	-13.5	-13.5	-13.5	-13.5	-13.5	-13.5	-13.5	-14.7

Table 7.6: Effective SNR(dB) for the conventional scheme with equal powers of 24dB and the same phase distribution as previous tables. ($M = 10$).

Stag	Bit No.										
No.	1	2	3	4	5	6	7	8	9	10	11
1	2.2	2.2	2.2	2.2	2.2	2.2	2.2	2.2	2.2	2.2	N/A
2	-1.3	1.1	1.1	1.1	1.1	1.1	1.1	1.1	1.1	1.1	-1.9
3	-5.4	2.6	2.6	2.6	2.6	2.6	2.6	2.6	2.6	2.6	4.3
4	-8.2	5.7	5.7	5.7	5.7	5.7	5.7	5.7	5.7	5.7	5.8
5	-3.3	2.2	2.2	2.2	2.2	2.2	2.2	2.2	2.2	2.2	-0.8
6	-4.7	1.0	1.0	1.0	1.0	1.0	1.0	1.0	1.0	1.0	-0.3

7.5 Numerical results and discussions

In this section, we compare the two acquisition schemes by computing their acquisition probabilities and the average number of blocks required to complete the ith stage acquisition. The comparisons will be conducted under two cases. The first one corresponds to the case where the estimation for acquisition detection is based on the parameter θ_i only. The second one is the case where the estimations are based on b_i and A_i. For the latter case, we only give the simulation results due to the difficulties of computing equations (7.55) and (7.56).

The system parameters are the same as those in the example of the section 3. Here we list them again for convenience.

System parameters:

$K = 6$;

$m = 31$;

$SNR = [24\ \ 20\ \ 16\ \ 10\ \ 8\ \ 6]$ dB;

$Phase = [0\ \ 20\ \ 10\ \ 6\ \ 10\ \ 3]$ chips;

$M = 10$ bits;

$M' = M - K + 1 = 5$ bits;

$N = 3$.

From table 7.7, we see that results obtained from the simulations and the theoretical computations are very close for both acquisition schemes. To capture all the 6 users in this numerical example, the OBO scheme needs about 21 data blocks while the SEC scheme only needs about 6 blocks which is faster than the OBO scheme.

Table 7.8 lists the simulation results for case 2. For convenience of comparison, the simulation results are again listed in this table. It is found that the acquisition performance of the OBO scheme based on the estimation on θ_i has been significantly improved by further conducting estimation on the amplitude A_i which is capable

Table 7.7: Acquisition probabilities and average number of acquisition blocks for case 1. (N=3).

Stage No.(i)	OBO scheme				SEC scheme			
	$P_{acq}(i)$		$N(i)$		$P_{acq}(i)$		$N(i)$	
	Comp.	Simu.	Comp.	Simu.	Comp.	Simu.	Comp.	Simu.
1	1.0000	1.000	1	1	1.0000	1.000	1	1
2	1.0000	0.998	1	1	1.0000	1.000	1	1
3	0.9999	0.998	1	1	0.9999	0.998	1	1
4	0.8309	0.765	1.2	1.3	0.9317	0.876	1.1	1.1
5	0.3480	0.280	2.9	3.6	0.5867	0.502	1.7	2.0
6	0.0573	0.049	17.5	20.4	0.2133	0.173	4.7	5.8

of shrinking the estimation variances. The performance of the SEC scheme is not improved as much as that of the OBO scheme. The reason is still unclear. The two schemes almost have the same performance after the second estimation.

Finally, we plot some typical correlation outputs from matched filters for conventional, OBO and SEC acquisition schemes. Figure 7.4 to figure 7.7 plot the normalized detection variables from matched filters 1 to 4 using the conventional detection technique. From these figures, we see that signals from all the users except the first (largest) one are difficult to be detected due to the near-far effects. Figure 7.8 to figure 7.18 illustrate the detection variables from the outputs of matched filters at each corresponding stage for the OBO and SEC the schemes. We can see that the weak signals get a higher chance to be detected by conducting cancellations.

7.6 Summary

In this chapter, a new PN code acquisition technique based on interference cancellation is developed for asynchronous CDMA communication systems. The acquisition

Table 7.8: Simulations for acquisition probabilities and average number of acquisition blocks for case 2. (N=3).

Stage No.(i)	OBO scheme				SEC scheme			
	$P_{acq}(i)$		$N(i)$		$P_{acq}(i)$		$N(i)$	
	Case1	Case2	Case1	Case2	Case1	Case2	Case1	Case2
1	1.000	1.000	1	1	1.000	1.000	1	1
2	0.998	1.000	1	1	1.000	1.000	1	1
3	0.998	1.000	1	1	0.998	1.000	1	1
4	0.765	0.786	1.3	1.3	0.876	0.779	1.1	1.3
5	0.280	0.561	3.6	1.8	0.502	0.570	2.0	1.8
6	0.049	0.365	20.4	2.7	0.173	0.396	5.8	2.5

scheme is robust because the near-far problem is alleviated by the cancellation process. Two schemes are proposed. One is based on a one-by-one cancellation, in which the estimated strongest signal is removed from the current composite signal at one stage and never re-estimated in the following stages. The signals are removed one by one until the weakest signal is detected. The other scheme is based on a simultaneous estimation and cancellation technique, in which all the signals so far detected are estimated together and removed from the original composite signal at each stage. The latter scheme has a better acquisition performance if the second estimation on signal amplitudes is not conducted. Furthermore, the SEC scheme is able to merge into the multiuser detection process naturally because it provides the signature sequence matrix of users detected as well as their current amplitudes at each stage. In fact, the SEC scheme at any detection stage can be viewed as an M-shot decorrelating detector for the detected users.

The effect of a false acquisition at a stage is not considered in this chapter. In practice, this will cause a wrong cancellation, which further increases the interference for the undetected signals. This will of course result in longer acquisition time for

the system. However, by using the automatic threshold control scheme, the false alarm rate can be greatly reduced. From the simulation, we can see that this effect can be neglected.

Since the near-far problem is alleviated by the cancellation process, fast acquisition is possible for most of the signals in a cell. Therefore, it is indeed suitable for packet radio communications provided that the processing time of the cancellation procedure is fast enough. This raises another challenging project, which is how to design the algorithm in the most efficient way to update the matrix H_i' upon each new detected signal and compute its pseudoinverse matrix.

For the carrier modulated signals, coherent detection of multiuser signals is possible. In this case, the acquisition schemes should include the estimation of the carrier phases which are uniformly distributed random variables. This is going to be our future work.

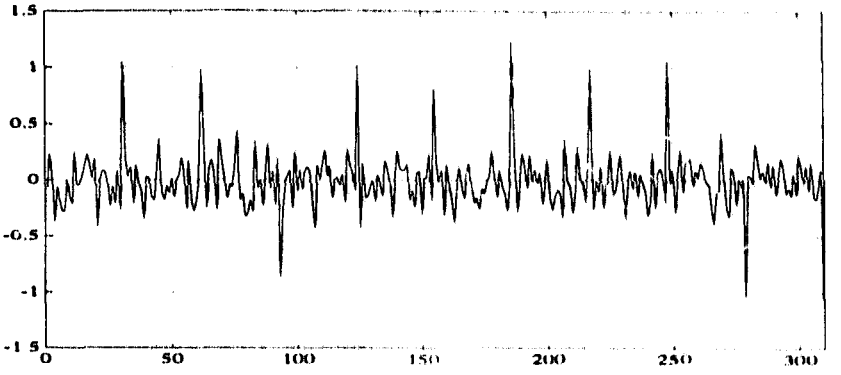

Figure 7.4: Outputs of MF 1 by conventional scheme

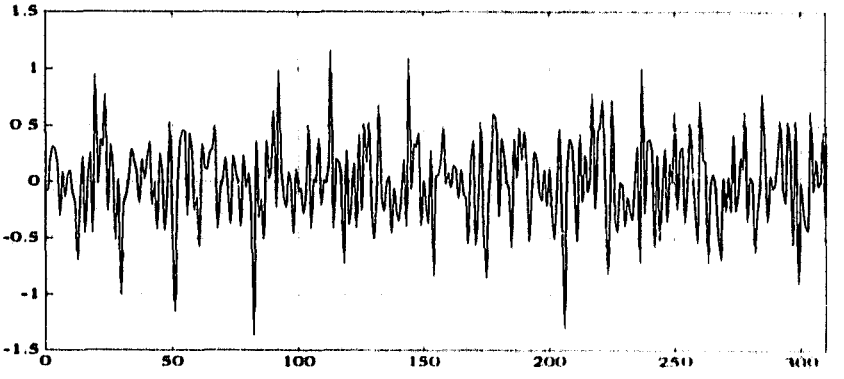

Figure 7.5: Outputs of MF 2 by conventional scheme

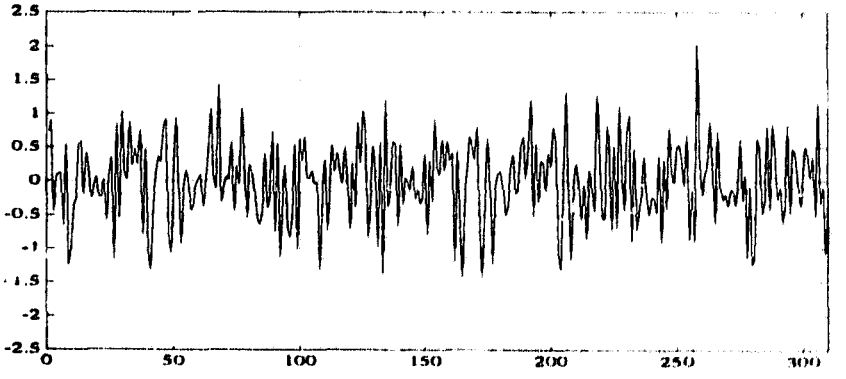

Figure 7.6: Outputs of MF 3 by conventional scheme

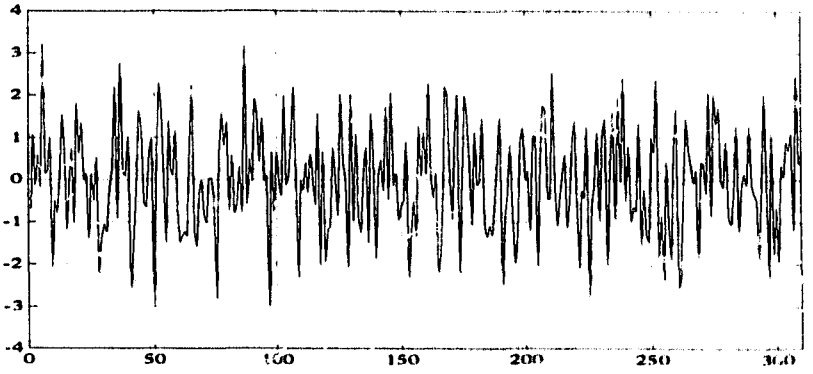

Figure 7.7: Outputs of MF 4 by conventional scheme

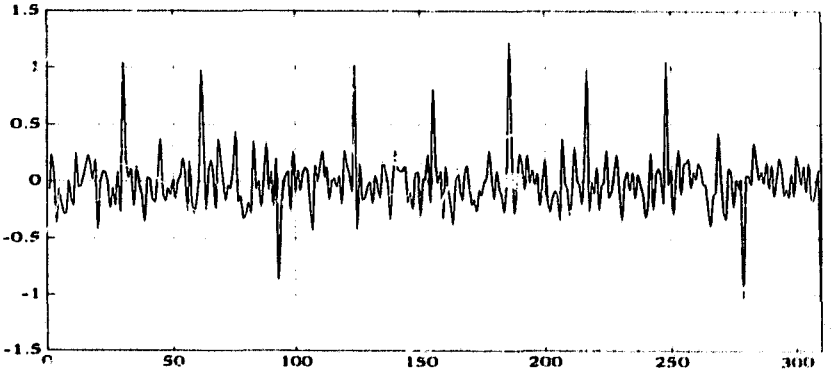

Figure 7.8: Outputs of MF 1 by OBO scheme

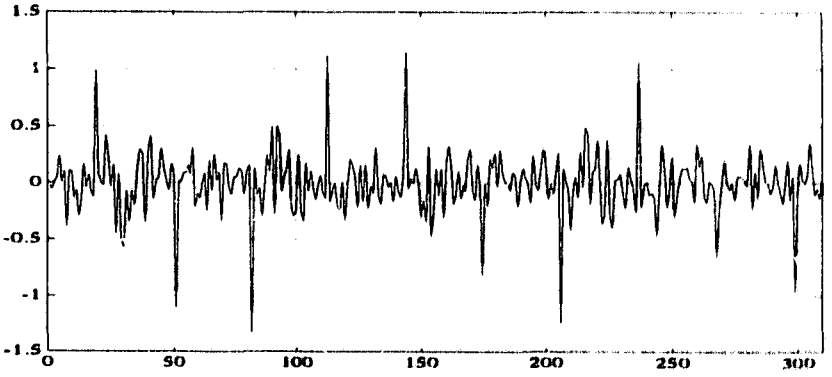

Figure 7.9: Outputs of MF 2 by OBO scheme

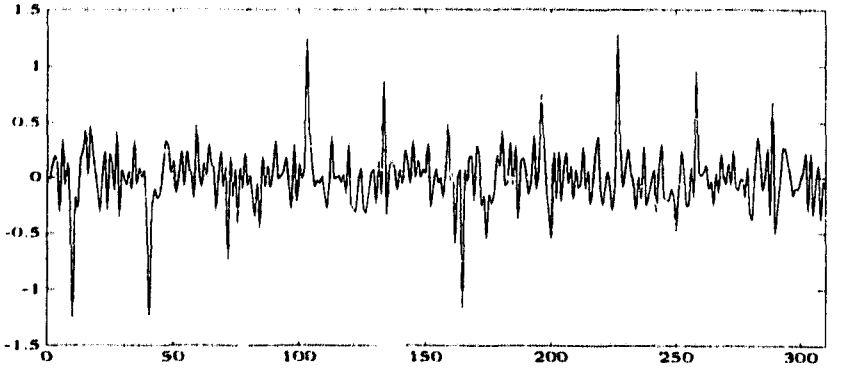

Figure 7.10: Outputs of MF 3 by OBO scheme

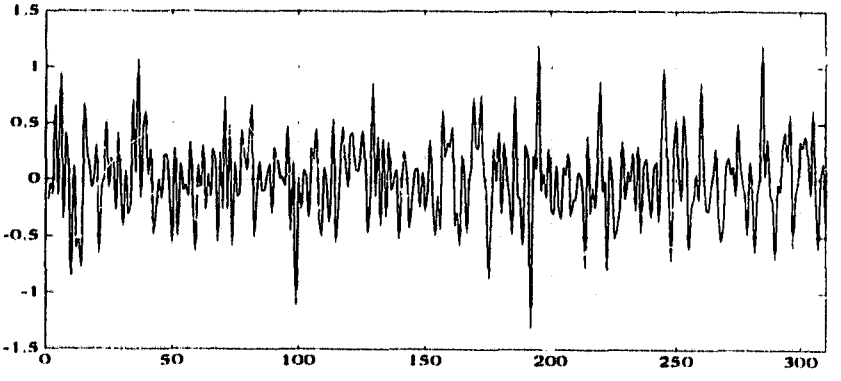

Figure 7.11: Outputs of MF 4 by OBO scheme

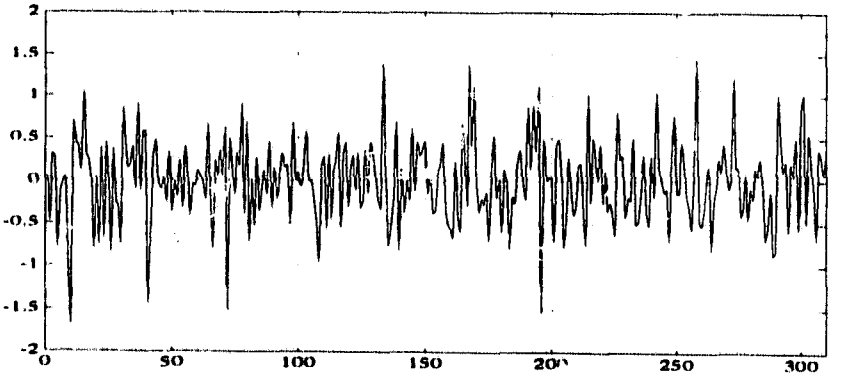

Figure 7.12: Outputs of MF 5 by OBO scheme

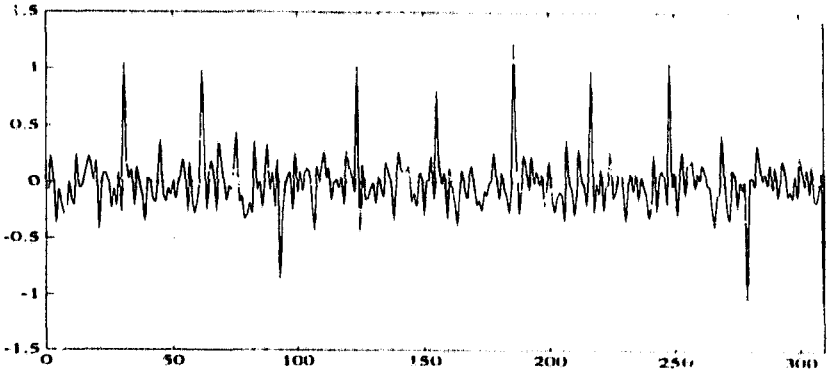

Figure 7.13: Outputs of MF 1 by SEC scheme

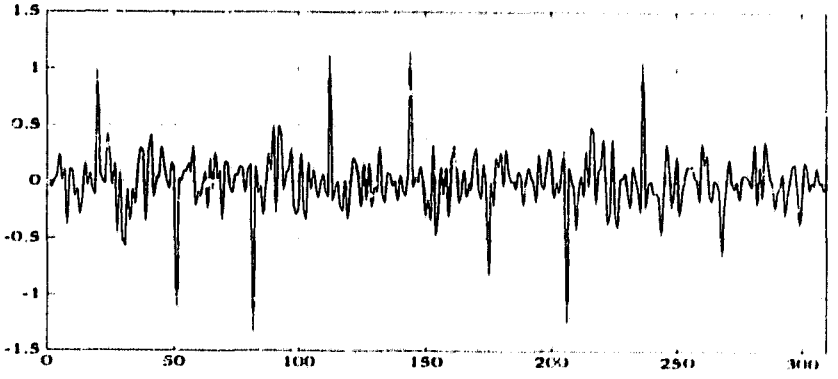

Figure 7.14: Outputs of MF 2 by SEC scheme

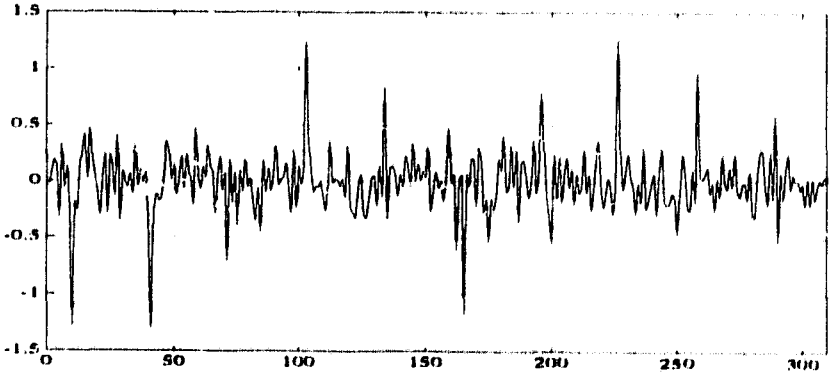

Figure 7.15: Outputs of MF 3 by SEC scheme

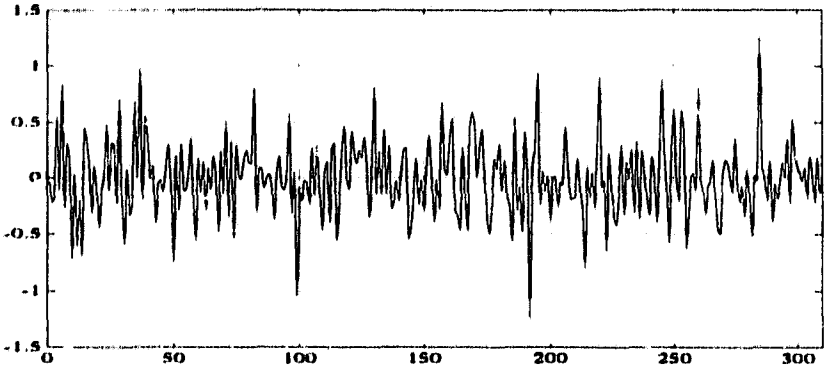

Figure 7.16: Outputs of MF 4 by SEC scheme

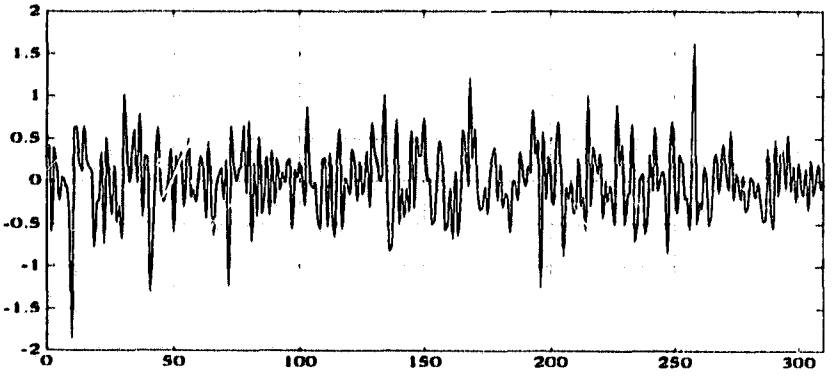

Figure 7.17: Outputs of MF 5 by SEC scheme

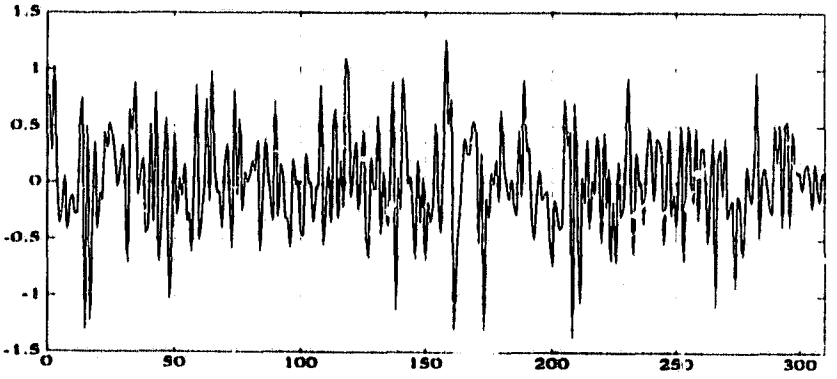

Figure 7.18: Outputs of MF 6 by SEC scheme

Chapter 8

Conclusions

A brief summary is addressed in section 8.1 followed by suggestions for further research in section 8.2.

8.1 Summary of thesis

The thesis studies several aspects of acquisition techniques for spread spectrum direct sequence packet radio communications. For burst mode DS spread spectrum communications, where a fixed length preamble is used at the beginning of each data packet for synchronization, packet acquisition using the preamble appears to be very important. It has been found that the conventional scheme, which only utilizes one period of PN sequence for acquisition followed by acquisition coincidence detection, does not yield reliable enough performance due to the channel noise. Since error control coding techniques can be used to compensate the performance loss due to the noise for data demodulation, most of the packet losses are caused by acquisition failures. Reliable synchronizations can be achieved by employing a bank of matched filters followed by a bank of long active correlators [35, 58]. However, the receiver complexity may hinder the practical use of this approach. In chapter

2 of this thesis, we introduced a multiple prefix acquisition scheme to increase the acquisition reliability at low SNR while maintaining simple receiver construction. The *masking effect* existing in preamble acquisition can be completely eliminated by using a hardlimiting matched filter instead of a linear one which was analyzed in chapter 3. Compared to the other existing acquisition schemes, the proposed scheme achieves a highly reliable acquisition performance with a minimum receiver complexity.

Spread spectrum packet radio often operates in CDMA environment. Thus the received signal is the superposition of many spread spectrum waveforms. Linear demodulation schemes will be required to make full use of the information from interfering users. Demodulation schemes with a hardlimiter, while simpler to implement, may lose too much information from the interfering users. For this reason, we proposed the automatic threshold control acquisition scheme for linear matched filters in chapter 4. Using the ATC, the masking effect no longer exists while the linearity of the transmitted signals remains at the output of the matched filter. In CDMA systems, the masking effect is caused not only by the variation of the SNR of the desired signal but also by the signals from the undesired users. Synchronization will be extremely difficult without using the ATC scheme since the number of active users and their received powers are random variables, resulting in more serious masking effects.

To probe more insight of the acquisition property in CDMA, in chapter 5 and chapter 6, we studied multi-user detectors which are near-far resistant.

For the conventional spread spectrum detector, a receiver only uses one unique signature sequence to correlate the incoming compound signal and pick up the message modulated by the same signature sequence. Thus the information about the mutual interference among users is ignored, even though the receiver possesses the knowledge (structure and phase) of the signature sequence of each component user.

The conventional single-user detector is vulnerable to the *near-far effects* and its performance is only acceptable for the case of low-bandwidth efficiency where the signature sequences can be designed such that the inter-user interference is negligible. Furthermore, elaborate power control technique has to be implemented in the system to make all the signals' powers approximately equal at the receiver. Unfortunately, power control dictates significant reduction in the transmitted powers of the strong users in order for the weaker users to achieve reliable communication. Thus, power control can become self-defeating since it actually decreases the overall multiple-access and antijamming capabilities of the system [54].

Multiuser detectors are near-far resistant. Once it is implemented, the capacity of the system can be expected to be higher than that of the conventional system. One of the important multi-user detectors is the nonlinear multi-user detector, which utilizes both the sequence and energy information of users. The nonlinear detector will usually outperform the linear type detectors which only use sequence information. The multistage detector (nonlinear) proposed in [50] can greatly improve the detection performance over linear detectors. However, performance difference between this detector and the optimal one is not trivial. In chapter 5, we developed a new multistage detector. The algorithms are based on the continuous approach to the optimal 0-1 solution. By modifying a single diagonal element of the Hessian matrix of the quadratic function, all the elements of the estimated vector are modified in one stage. The algorithms are shown to achieve more reliable signal detection than the multistage algorithm of [50], especially in the case of higher cross-correlations between any pair of the users' id codes.

To apply the proposed multistage detector to asynchronous CDMA systems, one-shot and M-shot detectors were developed in chapter 6. Both are near-far resistant. It is found that the performance of the one-shot detector varies with the sequence phase delays. However, the amount of the variation is not very large for a carefully

designed system. The M-shot detector can reduce the performance variation at the expense of slight increase in computation complexity. We have found that a 3-shot detector may be the most cost-effective. The one-shot and M-shot multi-user detectors are very useful for the future CDMA systems, especially the narrow-band CDMA system such as CDMA cellular system. They can be used for the reverse link data demodulation of a CDMA cellular system without using the complicated power control technique.

In chapter 7, emphasis was placed to the acquisition for CDMA signals. We have noticed that to date little attention has been paid to the sequence acquisition issue in CDMA although lots of acquisition schemes are available for the conventional the single-user receiver. It should not be difficult to see that acquisition in a CDMA system, especially in the system equipped with multiuser detectors, becomes more crucial than acquisition in single user case, because the receiver has to acquire the phases of all the active users' PN sequences. Furthermore, the near-far problem cannot be avoided during acquisition since any near-far multiuser detectors cannot work perfectly without knowing the phase information of the active users' signature sequences. The conventional matched filter acquisition technique designed for a single user will encounter a great amount of interference when working in a CDMA system. In chapter 7, two acquisition schemes based on interference cancellation were studied for CDMA signals. In general, the acquisition scheme consists of two basic steps. In the first step, the receiver searches the PN code phase of the strongest signal. In the second step, the estimation of the detected signal amplitudes (powers and signs) is obtained, thus the waveform of the detected signal(s) can be reconstructed and removed (cancelled) from the original signal. In practice, the acquisitions for the currently active users' signals may not be obtained in the same observation data block due to the non-coordination of asynchronous users, i.e., some users' signals are captured earlier because they arrive earlier. In fact, while a receiver

is maintaining the demodulation for the detected users' signals, it also removes the waveform constructed by these signals from the original received signal and check the residual to see if there are any new comers. The most important achievement by the new schemes is their approximately near-far resistances. Without the acquisition schemes developed in this chapter, near-far detection of CDMA signals using multi-user detectors will be impossible.

8.2 Further research

In this thesis, we are mainly concerned with the signal detection and acquisition problems for CDMA systems. However, for simplicity and the purpose of tackling the main problem in CDMA, i.e., the near-far problem, coherent detection for each user's signal is assumed. Therefore, the signal processing algorithms can exclusively deal with the baseband signals which can be expressed in discrete forms. Furthermore, the channel is assumed to be AWGN for the same reason.

In practice, coherent receptions for multi-user detections are still possible if the carrier phase of each component signal can be tracked. In some cases, where the received signals are subject to severe fading, oscillator phase instability at the transmitter makes the coherent reception extremely difficult. In such situations, some kind of non-coherent multi-user detectors need to be developed. In [50], a DPSK linear multi-user detector was studied. For the detector, no knowledge of the energies and carrier phases of any of the component signals is assumed at the receiver. However, estimation of signal energies may be possible by the proposed acquisition scheme in chapter 7. Nonlinear multi-user detectors for non-coherent detection may be used to improve performance. Study of such detectors is one of the further research topics.

In any cases, the acquisition of each of the component signals based on baseband

signals is too ideal to be accepted. The main purpose of chapter 7 is to show the robustness of the cancellation schemes combined in the acquisition scheme. Our further research will focus on the non-coherent signal acquisition using the cancellation schemes. Of course, for coherent demodulation, carrier phase for each component signal is another important parameter which needs to be estimated during synchronization. This will not be too difficult if all the PN sequences can be captured non-coherently.

The future work should also include the extension of the analysis of the proposed detection and acquisition schemes in fading channel. It will be very interesting to look at the ways to obtain the near-far resistant multi-user detectors and synchronizers in fading channel for CDMA systems. Neural network combined with blind equalization may be one of the efficient theoretical tools to solve this kind of problems.

Bibliography

[1] B. Aazhang and H.V. Poor. "Performance of DS/SSMA Communications in Impulsive Channels - Part 2 : Hard-Limiting Correlation Receivers". *IEEE Transactions on Communications*, 36(1), January 1988.

[2] A. Baier. "A Low-Cost Digital Filter For Arbitrary Constant-Envelope Spread Spectrum Waveforms". *IEEE Transactions on Communications*, 32(4):354 361, April 1984.

[3] M. W. Carter. "The Indefinite Zero-One Quadratic Problem". *Discrete Applied Mathematics*, (7):23–44, 1984.

[4] G.M. Comparetto. "A Generalized Analysis for a Dual Threshold Sequential Detection PN Acquisition Receiver". *IEEE Transactions on Communications*, 35(9), September 1987.

[5] S. Davidovici, L.B. Milstein, and D. Schilling. "A New Rapid Acquisition Technique for Direct Sequence Spread-spectrum Communications". *IEEE Transactions on Communications*, 32(11), November 1984.

[6] P. Dent, B. Gudmundson, and M. Ewerbring. "CDMA-IC: A Novel Code Division Multiple Access Scheme Based on Interference Cancellation". In *Proceedings of the Third IEEE International Symposium on Personal, Indoor and Mobile Radio communications*, pages 98–102, Oct. 1992.

[7] P.F. Driessen "Binary Frame Synchronization Sequences for Packet Radio". *IEE Electronic Letter*, 23, 1987.

[8] P.F. Driessen. "Performance of Frame Synchronization in Packet Transmission Using Bit Erasure Information". *IEEE Transactions on Communications*, 39(4), April 1991.

[9] P.F. Driessen and Z.L. Shi. "A New Rapid Acquisition Scheme For Burst Mode DS Spread Spectrum Packet Radio". In *IEEE Military Communications Conference*, pages 809–913, Nov. 1991.

[10] J.H. Fischer, J.H. Cafarella, C.A. Bouman, G.T. Flynn, V.S. Dolat, and R. Boisvert. "Wide-Band Packet Radio for Multipath Environments". *IEEE Transactions on Communications*, 36(5):564–576, May 1988.

[11] S.G. Glisic. "Modified Twolevel-Doublesearch Synchronization of Direct Sequence Spread Spectrum Systems". 1984.

[12] S.G. Glisic. "Automatic Decision Threshold Level Control in Direct-Sequence Spread Spectrum Systems Based on Matched filtering". *IEEE Transactions on Communications*, 36(4):519–527, April 1988.

[13] V. P. Gulati, S. K. Gupta, and A. K. Mittal. "Unconstrained Quadratic Bivalent Programming Problem". *European Journal of Operational Research*, 15:121–125, 1981.

[14] J.F. Hayes. *Modeling and Analysis of Computer Communications Networks.* Plenum Press, 1984.

[15] A.S. Householder. *The Theory of Matrices in Numerical Analysis.* Blaisdell, New York, 1963.

[16] R.E. Kahn, S.A. Gronemeyer, J. Burchfiel, and R.C. Kunzelman. "Advances in Packet Radio Technology". *Proceedings of The IEEE*, 66(11):1468 1496. November 1978.

[17] T. Kailath. *Linear Systems*. Prentice-Hall Information and System Sciences Series, 1980.

[18] A. Kajiwara and M. Nakagawa. "Crosscorrelation Cancellation in SS/DS Block Demodulator". *Trans. IEICE*, E-74(9), September 1991.

[19] Richard Kerr. "The CDMA Digital Cellular System An ASIC Overview In *Proc. of the third IEEE international symposium on Personal, Indoor and Mobile Radio Communications*, pages 36–41, October 1992.

[20] A. Klein and P.W. Baier. "Simultaneous Cancellation of Cross Interference and ISI in CDMA Mobile Radio Communications". In *Proceedings of the Third IEEE International Symposium on Personal, Indoor and Mobile Radio communications*, pages 118–122, Oct. 1992.

[21] R. Kohno, H. Imai, and M. Hatori. "Cancellation Techniques of Co-Channel Interference in Asynchronous Spread Spectrum Multiple Access Systems". *Trans. IEICE*, J66-A(5), May 1977.

[22] M. Kowatsch. "Application of Surface Acoustic Wave Technology to Burst Format Spread Spectrum Communications". *IEE Proceedings*, 131(7), December 1984.

[23] M. Kowatsch, J.T. Lafferl, and A. Ersoy. "An Application of SAW Convolvers to Spread-Spectrum Transmission of Packet Voice". *IEEE Transactions on Sonics and Ultrasonics*, 32(5), September 1985.

[24] S. Kubota, S. Kato, and K. Feher. "Inter-Channel Interference Cancellation Technique for CDMA Mobile/Personal Communication systems". In *Proceedings of the Third IEEE International Symposium on Personal, Indoor and Mobile Radio communications*, pages 112–117, Oct. 1992.

[25] R. Lupas and S. Verdu. "Linear Multiuser Detectors for Synchronous Code-Division Multiple-Access Channels". *IEEE Transactions on Information Theory*, 35(1):123–136, January 1989.

[26] R. Lupas and S. Verdu. "Near-Far Resistance of Multiuser Detectors in Asynchronous Channels". *IEEE Transactions on Communications*, 38(4):496–508, April 1990.

[27] Jerry M. Mendel. *Lessons in Digital Estimation Theory.* Prentice-Hall Signal Processing Series, 1987.

[28] L.B. Milstein, J. Gevargiz, and P.K. Das. "Rapid Acquisition for Direct Sequence Spread- Spectrum Communications Using Parallel SAW Convolvers". *IEEE Transactions on Communications*, 33(7):593–600, July 1985.

[29] M. Mowatsch. "Application of Surface Acoustic Wave Technology to Burst Format Spread Spectrum Communications". *IEE Proceedings*, 131(7):734–741, December 1984.

[30] Jim K. Omura. "Spread Spectrum Radios for Personal Communication Services". In *Proceedings, Spread Spectrum - Potential Commercial Applications, Myth or Reality?*, pages 5.1.1–5.1.3, May 1991.

[31] Andreas Polydoros. "A Unified Approach to Serial Search Spread-Spectrum Code Acquisition-Part I: General Theory". *IEEE Transactions on Communications*, 32(5):542–549, May 1984.

[32] Andreas Polydoros. "A Unified Approach to Serial Search Spread-Spectrum Code Acquisition-Part II: A Matched-Filter Receiver". *IEEE Transactions on Communications*, 32(5):550–560, May 1984.

[33] Michael B. Pursley. "Performance Evaluation for Phase-Coded Spread-Spectrum Multiple-Access Communication-Part I: System Analysis". *IEEE Transactions on Communications*, 25(8):795–799, August 1977.

[34] S.S. Rappaport and D.M. Grieco. "Spread-Spectrum Signal Acquisition: Methods and Technology". *IEEE Communications Magazine*, 22(6):6–21, 1984.

[35] S.S. Rappaport and D.L. Schilling. "A Two-Level Coarse code Acquisition Scheme for Spread Spectrum Radio". *IEEE Transactions on Communications*, 28(9):1734–1742, September 1934.

[36] Sheldon M. Ross. *Stochastic Processes*. John Wiley & Sons, 1983.

[37] D.L. Schilling, L.B. Milstein, R.L. Pickholtz F. Bruno, E. Kanterakis, M. Kullback, V. Erceg, W. Biederman, D. Fishman, and D. Salerno. "Broadband CDMA for Personal Communications Systems". *IEEE Communications Magazine"*, 29(11):86–93, November 1991.

[38] D.L. Schilling, L.B. Milstein, R.L. Pickholtz M. Kullback, and F. Miller. "Spread Spectrum for Commercial Communications". *IEEE Communications Magazine"*, 29(4):66–79, April 1991.

[39] D.L. Schilling, R.L. Pickholtz, and L.B. Milstein. "Spread Spectrum Goes Commercial". *IEEE Spectrum*, pages 40–45, August 1990.

[40] K.S. Schneider. "Optimum Detection of Code Division Multiplexed Signals". *IEEE Transactions on Aerosp. Electron. Syst.*, AES-15:181–186, January 1979.

[41] R.A. Scholtz. "Frame Synchronization Techniques". *IEEE Transactions on Communications*, 28(8):1204–1212, August 1980.

[42] M. Schwartz, W.R. Bennett, and S. Stein. *Communications Systems and Techniques.* New York: McGraw-Hill, 1966.

[43] Z. L. Shi and C. S. Li. "A New Acquisition Technique for Spread Spectrum System Using Burst Format Message Signalling". In *International Conference on Communications Technology, Nanjing, China*, October 1987.

[44] M. Simon, J. Omara, R.Scholtz, and B. Levitt. *Spread Spectrum Communications.* Rockville, MD: Computer Science Press, 1985.

[45] L.B. Sklar. "Efficiency Factors in Data Communications". *IEEE Communications Magazine*, 22(6), June 1984.

[46] G.W. Stewart. *Introduction to Matrix Computations.* Academic Press, 1973.

[47] B. Tuch. "An Engineer's Summary of an ISM Band Wireless LAN". *A report from NCR Systems Engineering Utrecht*, Nov. 1991.

[48] G.L. Turin. "An Introduction to Digital Matched Filters". *Proceedings of IEEE*, 64(7), July 1976.

[49] M. K. Varanasi and B. Aazhang. "Multistage Detection in Asynchronous Code-Division Multiple-Access Communications". *IEEE Transactions on Communications*, 38(4):509–519, April 1990.

[50] M. K. Varanasi and B. Aazhang. "Near-Optimum Detection in Synchronous Code-Division Multiple-Access Systems". *IEEE Transactions on Communications*, 39(5):725–736, May 1991.

[51] M. K. Varanasi and B. Aazhang. "Optimally Near-Far Resistant Multiuser Detection in Differentialiy Coherent Synchronous Channels". *IEEE Transactions on Information Theory*, 37(4):1006–1018, July 1991.

[52] S. Verdu. "Minimum Probability of Error for Asynchronous Gaussian Multiple-Access Channels". *IEEE Transactions on Information Theory*, IT-32(1):85–96, January 1986.

[53] S. Verdu. "Optimum Multi-User Asymptotic Efficiency". *IEEE Transactions on Communications*, 34(9):890–897, Sept. 1986.

[54] S. Verdu. "Recent Progress in Multiuser Detection". *Advances in Communications and Signal Processing, Lecture Notes in Control and Information Sciences*, 129, Springer Verlag 1988.

[55] A.J. Viterbi and R. Padovani. "Implications of Mobile Cellular CDMA". *IEEE Communications Magazine*, 30(12), December 1992.

[56] R.B. Ward and K.P. Yiu. "Acquisition of Pseudonoise Signals by Sequential Estimation". *IEEE Transactions on Communications*, 25(8):784–794, August 1977.

[57] A.D. Whalen. *Detection of Signal in Noise.* Academic Press New York and London, 1971.

[58] N.D. Wilson, S.S. Rapaport, and M.M. Vasudevan. "Rapid Acquisition Scheme for Spread Spectrum Radio in a Fading Environment". *IEE Proceedings*, 135(1):95–104, February 1988.

[59] K. Yao. "Error Probability of Asynchronous Spread-Spectrum Multiple-Access Communication Systems". *IEEE Transactions on Communications*, 25(8):803–809, August 1977.

[60] R.E. Ziemer and R.L. Peterson. *Digital Communications and Spread Spectrum Systems.* Macmillan Publishing Company, 1985.

Appendix A
Accurate Computation of P_L

As an alternative to the simplified method in Section 2.3.2, an accurate approach is presented in this appendix to obtain the probability of packet loss caused by synchronization failure. For this purpose, we define the waiting time w as the time elapsed from the starting point of the arrival of a packet to the point that the receiver just switches back to the idle state. From the construction of the preamble and figure 2.4, we know that, $w = 0$ if the packet drops in an idle interval I on arrival, and $w > 0$ if the packet falls in a block interval on arrival. When $0 < w < N_h T$, the packet is recoverable. When $N_h T \leq w \leq T_2$, the packet will be lost. w is actually a random variable with its probability density denoted as $w(t)$.

To find P_L, we need to find the probability density of the waiting time $w(t)$ after a packet arrival at $t = 0$. Note that there is a finite probability that the waiting time is exactly zero. Then

$$P_L = 1 - w_0 P_{syn}(0) - \sum_{k=1}^{N_h m - 1} w_k P_{syn}(k) \tag{A.1}$$

where

$$w_0 = Pr\{w = 0\} \tag{A.2}$$

$$w_k = Pr\{(k-1)T_c \leq w \leq kT_c\} = \int_{(k-1)T_c}^{kT_c} w(t)dt \tag{A.3}$$

and $P_{syn}(k)$ is computed by 2.17.

To find w_0 and w_k, we must find $w(t)$. To find $w(t)$, we require the probability density $f(t)$ of the blocking periods B. By construction of the sync technique,

$$f(t) = p_1\sigma(t - T_1) + p_2\sigma(t - T_2) \tag{A.4}$$

where $p_1 = 1 - P_{fcn}$ and $p_2 = P_{fcn}$. P_{fcn} is the probability that at least one false marker detection occurs in noise during N_k marker tests, and is determined by 2.24 and 2.25.

We assume that the arrival of a packet during a busy period B does not affect p_1 and p_2. This assumption is reasonable if the PN code is a near-ideal autocorrelation function.

We follow [14] to determine w_0, w_k and $w(t)$ in terms of $f(t)$ and two additional parameters λ_f and λ_p. We have defined $\lambda_f = P_{f0n}/T_c$ as the number of arrivals of false acquisitions in T_c seconds when the receiver is idle. λ_p is defined as the number of arrivals of packets in T_c seconds. Both arrivals are assumed to be Poisson.

By definition, $w(t)$ concerns the waiting time caused by false acquisitions, and does not include waiting time because the receiver is busy processing a previous packet. Thus in using the method of [14], we assume that the arrival rate of packets is vanishingly small (i.e. there is only one packet arrival for all time, and we wish to determine P_L for this packet). Thus we consider the case $\lambda_p T_2 \ll 1$.

To find w_0, we note that in figure 2.4, the random variable w is equal to zero if the packet arrives during one of the intervals I_0, I_1,..., I_n,.... Summing over disjoint events we find [14]

$$\begin{aligned} w_0 &= \sum_{n=0}^{\infty} Pr[\sum_{i=0}^{n}(I_i + B_i) < \tau < \sum_{i=0}^{n}(I_i + B_i) + I_{n+1}] \\ &= \frac{\lambda_p}{\lambda_f + \lambda_p - \lambda_f F(\lambda_p)} \end{aligned} \tag{A.5}$$

where $F(\lambda_p) = p_1 e^{-\lambda_p T_1} + p_2 e^{-\lambda_p T_2}$ is the Laplace transform of the density function $f(t)$ of the random variable B_i.

Similarly, $w(t)$ can be found by

$$w(t)dt = Pr[t < w < t + dt] = \sum_{n=0}^{\infty} Pr[t < \sum_{i=0}^{n+1}(I_i + B_i) - \tau \leq t + dt] \qquad (A.6)$$

Following [14] for $f(t)$ given by (A.4)

$$w(t) = \frac{\lambda_f}{\lambda_f + \lambda_p - \lambda_f F(\lambda_p)} \int_t^{\infty} \lambda_p e^{-\lambda_p(\tau - t)} f(\tau) d\tau \qquad (A.7)$$

$$= \frac{\lambda_f \lambda_p}{\lambda_f + \lambda_p - \lambda_f F(\lambda_p)} [p_1 e^{-\lambda_p(T_1 - t)} g_1(t) + p_2 e^{-\lambda_p(T_2 - t)} g_2(t)] \qquad (A.8)$$

where

$$g_i(t) = u(t) - u(t - T_i) \qquad i = 1, 2 \qquad (A.9)$$

We can now evaluate the w_k terms in (A.1) using (A.3) and (A.8) when $k < N_h m$.

$$w_k = \int_{(k-1)T_c}^{kT_c} \frac{\lambda_f}{\lambda_f + \lambda_p - \lambda_f F(\lambda_p)} \lambda_p F(\lambda_p) e^{\lambda_p t} dt$$

$$= \frac{\lambda_f}{\lambda_f + \lambda_p - \lambda_f F(\lambda_p)} F(\lambda_p) e^{\lambda_p k T_c} (1 - e^{-\lambda_p T_c}) \qquad (A.10)$$

When $N_h T \leq w \leq T_2$, the packet will be blocked and then lost. The corresponding probability is given by

$$P_b = P[N_h T < w \leq T_2]$$

$$= \int_{N_h T}^{T_1} \frac{\lambda_f}{\lambda_f + \lambda_p - \lambda_f F(\lambda_p)} \lambda_p F(\lambda_p) e^{\lambda_p t} dt$$

$$+ \int_{T_1}^{T_2} \frac{\lambda_f}{\lambda_f + \lambda_p - \lambda_f F(\lambda_p)} \lambda_p p_2 e^{-\lambda_p T_2} e^{\lambda_p t} dt$$

$$= \frac{\lambda_f}{\lambda_f + \lambda_p - \lambda_f F(\lambda_p)} [1 - p_1 e^{-\lambda_p(T_1 - N_h T)} - p_2 e^{-\lambda_p(T_2 - N_h T)}], \qquad (A.11)$$

In the limit $\lambda_p T_2 \ll 1$, we have

$$w_0 = \frac{1}{1 + \frac{\lambda_f}{\lambda_p}(1 - p_1 e^{-\lambda_p T_1} - p_2 e^{-\lambda_p T_2})}$$

$$\begin{aligned} &\approx \frac{1}{1+\frac{\lambda_f}{\lambda_p}(1-p_1+p_1\lambda_p T_1-p_2+p_2\lambda_p T_2)} \\ &= \frac{1}{1+\lambda_f(p_1T_1+p_2T_2)} \\ &= \frac{1}{1+\alpha} \end{aligned} \tag{A.12}$$

Using the same argument, w_k from (A.10 can be reduced to

$$w_k = \frac{P_{f0n}}{1+\alpha} \tag{A.13}$$

and

$$P_b = P_{f0n}[N_s - 1 + P_{fcn}L_D]m/(1+\alpha). \tag{A.14}$$

Therefore with the condition of $\lambda_p T_2 \ll 1$, P_L from A.1 can be expressed as

$$P_L = \frac{1}{1+\alpha}P_{syn}(0) + \frac{P_{fan}}{1+\alpha}\sum_{k=1}^{N_h m-1} P_{syn}(k) \tag{A.15}$$

which is the same as the result obtained from (2.16) and (2.18).

Appendix B
Computations of q, p, s, q_n, p_n, s_n for Linear Receiver

In this appendix, we determine the probabilities q, p, s, q_n, p_n, s_n for the non-coherent receiver of Figure 2.3. Two matched filters are used for the marker test. We assume that the two input signals are orthogonal, where u_1 and u_0 corresponding to "1" and "0" respectively are the outputs of the envelopes normalized to σ.

The distribution at each MF output is written [5]

$$p(u_1) = u_1 \exp(-\frac{u_1^2 + 2\gamma_0}{2}) I_0(\sqrt{2\gamma_0} u_1) \tag{B.1}$$

$$p(u_0) = u_0 \exp(-\frac{u_0^2}{2}) \tag{B.2}$$

provided that "1" was sent. For reliable coincidence detection ($P(h_e, h_x, N_s) \simeq 1$) without excessive false alarms ($P_{fn} \simeq 0$), it is necessary to use a normalized threshold $b_1 \neq 0$ with the comparison device, thus erasure may occur if both MF outputs are less than b_1. If we define

$$Q(\alpha, \beta) = \int_{\beta}^{\infty} x exp(-\frac{x^2 + \alpha^2}{2}) I_0(\alpha x) dx \tag{B.3}$$

then q, p, s, q_n, p_n, s_n are calculated as follows:

$$\begin{aligned} s &= \int_0^{b_1}\int_0^{b_1} p(u_1,u_0)du_1du_0 \\ &= [1-Q(\sqrt{2\gamma_0},b_1)][1-\exp(-\frac{{b_1}^2}{2})] \end{aligned} \tag{B.4}$$

$$\begin{aligned} q &= \int_{b_1}^{\infty} P_r[U_0<u_1|U_1=u_1]p(u_1)du_1 \\ &= \int_{u_1=b_1}^{\infty}\int_{u_0=0}^{u_1} p(u_0)du_0p(u_1)du_1 \\ &= \int_{b_1}^{\infty}[1-exp(-u_1^2/2)]p(u_1)du_1 \\ &= Q(\sqrt{2\gamma_0},b_1)-\frac{1}{2}\exp(-\frac{\gamma_0}{2})Q(\sqrt{\gamma_0},\sqrt{2}b_1) \end{aligned} \tag{B.5}$$

$$p = 1-q-s \tag{B.6}$$

$$\begin{aligned} q_n &= p_n = \int_{u_1=b_1}^{\infty}\int_{u_0=0}^{u_1} u_0exp(-\frac{u_0^2}{2})du_0u_1exp(-\frac{u_1^2}{2})du_1 \\ &= \exp\{-\frac{b_1^2}{2}\}-\frac{1}{2}\exp\{-b_1^2\} \end{aligned} \tag{B.7}$$

$$s_n = 1-2q_n \tag{B.8}$$

Appendix C
Computation of $P_{acq}(i,k)$ for Two-Level Threshold

In this appendix, $P_{acq}(i,k)$ of 2.19 of the new scheme introduced in section 2.3.2 with the two-level threshold is calculated from the flow graph of figure C.1 with the indicated states and gains. The contents of the $H(i,j)$ gain blocks are illustrated in figure C.2. For each $H(i,j)$ block, there are two gains: one is from the input to an acquisition state, which is denoted as $H_a(i,j)$, and the other is from the input to a false alarm state, which is denoted as $H_f(i,j)$. With the initial searching point $k+1 = (i_o-1)m + j_o$, the probability $P_{acq}(i,k)$ of reaching an acquisition state Acq(i,k) at the ith PN period may be written in terms of the probabilities $S_{i,j}$ of reaching the intermediate states (i,j) and the gains $H_a(i,j)$ as

$$P_{acq}(i,k) = \begin{cases} \sum_{j=j_o}^{m} S_{i_o,j} H_a(i_o,j), & i = i_o, j_0 = 1,2,\ldots,m \\ \\ \sum_{j=1}^{m} S_{i,j} H_a(i,j), & i > i_o. \end{cases} \tag{C.1}$$

The $S_{i,j}$ are found from the recursive equations

$$S_{i_o,j_o} = 1, \tag{C.2}$$

$$S_{i,j} = S_{i,j-1}(1 - P_{fd}(j-1)), \quad 1 \le i \le N_h, \; j \le m, \tag{C.3}$$

and

$$S_{i,1} = S_{i-1,m}(1 - P_d). \tag{C.4}$$

The gains $H_a(i,j)$ are obtained from figure C.2, where the additional h subscript attached to the gains P_d and $P_{fd}(j)$ means that the higher threshold b_{0h} is used in the corresponding definitions (2.5), (2.6). From figure C.2,

$$H_a(i,j) = (P_{fd}(j) - P_{fdh}(j)) \prod_{k=j+1}^{m-1} (1 - P_{fdh}(j))P_{dh}, \quad 1 \le i \le N_h, \quad j \le m-1 \tag{C.5}$$

and

$$H_a(i,m) = P_{dh} + (P_d - P_{dh}) \prod_{k=1}^{m-1} (1 - P_{fdh}(k)), \tag{C.6}$$

$$H_a(N_h,m) = P_{dh}. \tag{C.7}$$

This completes the calculation of $P_{acq}(i,k)$.

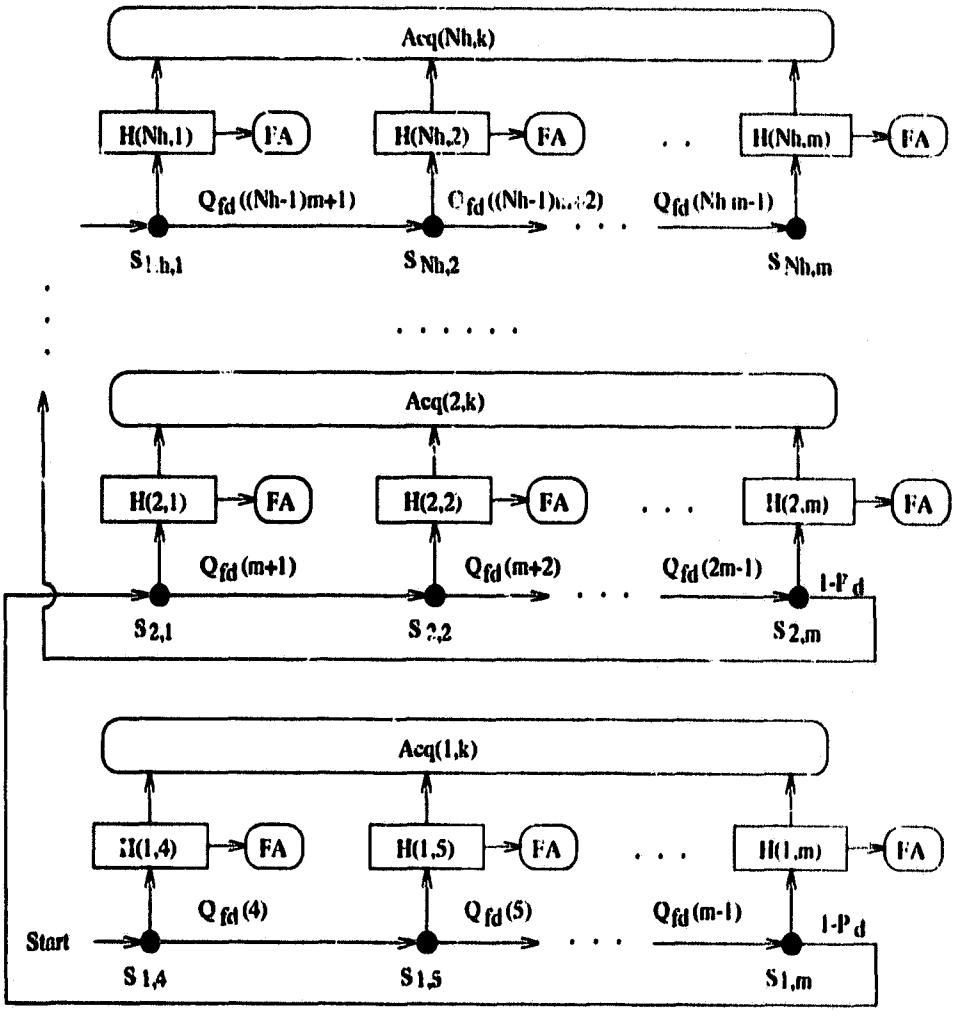

Figure C.1: Signal flow graph for acquisition with two-level threshold

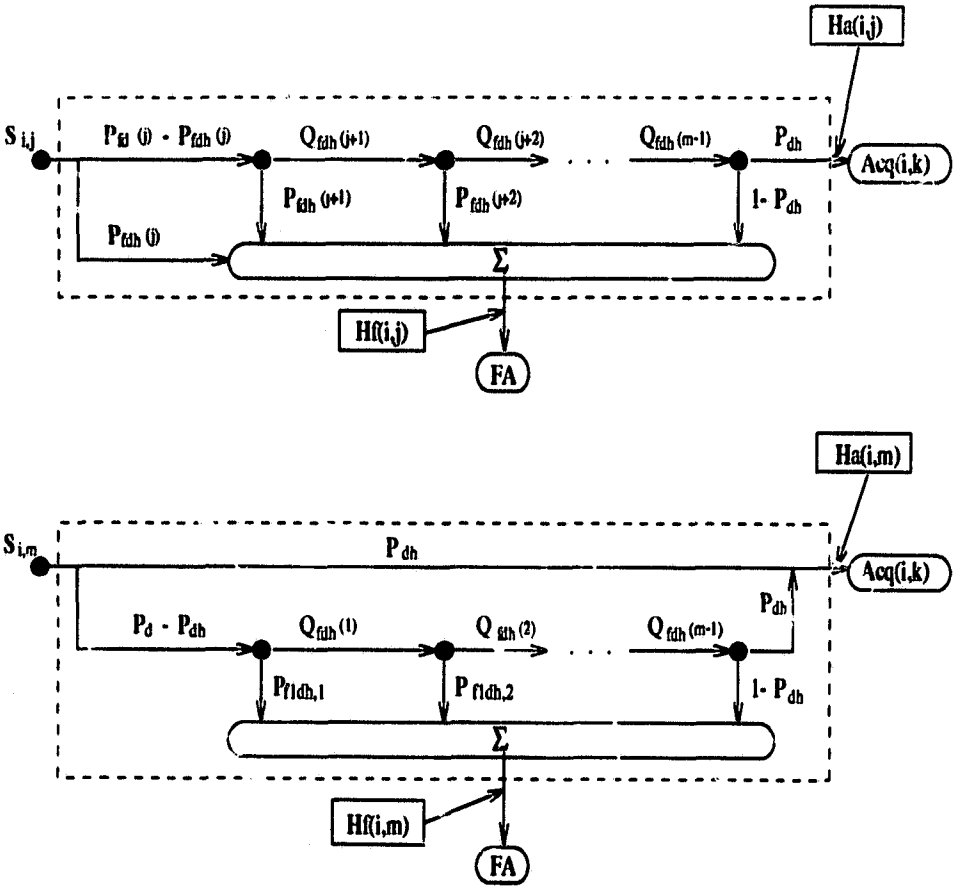

$i = 1, 2, \ldots, Nh-1$; $Ha(Nh,m) = P_{dh}$

Figure C.2: Details of $H(i,j)$ gain block

Appendix D
A Modified Analysis of the TL Scheme

In this appendix, some modifications on performance of the TL method in [35, 58] are presented for convenience of comparison between the new scheme proposed in chapter 2 and the TL scheme. For example, the original analysis did not take the blocking probability/rate as the criterion. Since the blocking rate is more appropriate in packet radio communications, it is necessary to modify the analysis.

For the TL scheme the packet will be lost if it is blocked or if the synchronization fails when no blocking occurs. The expression for this probability is simply

$$P'_L = 1 - (1 - P_{B_{TL}})P'_{syn} \tag{D.1}$$

where $P_{B_{TL}}$ is the blocking probability and P'_{syn} the sync probability for the TL method.

Since the receiver may be falsely locked into the in-sync condition, it is possible for a coming packet to be blocked by the unavailable receiver engaged by a previous false lock signal. The probability that a code start signal of a packet finds the receiver to be in a false lock state is

$$P'_B = \frac{B'}{B' + I'} \tag{D.2}$$

where $B' = L_D T' = L_D m T_c$ is the total time that the receiver stays in the false lock state. $I' = 1/\lambda' = T_c/P_{FL}$ is the average time interval in which the receiver is not in the false lock condition. Here Possion arrival are assumed for the false lock signals. P_{FL} is the probability of the false lock.

A code start signal will be also blocked when it finds all the active correlators engaged, even though the receiver is not in the false lock condition. This probability is given by the Erlang B formula $B(c, a)$ [35, 58] where $a = [1-(1-P_{f0})^{N_{pc}}]M$ is the offered load and c is the number of active correlators. N_{pc} is the number of prefixes in the preamble. P_{f0} is the probability of false start by the passive correlators. Given b'_0 as the threshold of the passive correlator, P_{f0} will be

$$P_{f0} = \exp(-\frac{b_0'^2}{2}) \tag{D.3}$$

Thus the blocking probability $P_{B_{TL}}$ for the TL scheme can be written

$$\begin{aligned} P_{B_{TL}} &= P'_B + (1 - P'_B)B(c, a) \\ &= \frac{\alpha' + B(c, a)}{1 + \alpha'} \end{aligned} \tag{D.4}$$

where

$$\begin{aligned} \alpha' = B'/I' &= L_D m P_{FL} \\ &= L_D m[1 - (1 - P_{f0})^{N_{pc}}](1 - B(c, a))P_{f1}. \end{aligned} \tag{D.5}$$

In the above equation, the expanded expression for P_{FL} is taken from (4) in [58]. P_{f1} is the probability of false coincidence by the active correlators given b'_1 as the threshold.

$$P_{f1} = \exp(-\frac{b_1'^2}{2}) \tag{D.6}$$

The probability P'_{syn} of successful synchronization in (D.1) is

$$\begin{aligned} P'_{syn} &= [1-(1-P'_{d0})^{N_{pc}}]P'_{d1} \\ &= [1-(1-Q(\sqrt{2m\gamma_{in}}, b'_0))^{N_{pc}}]Q(\sqrt{2M\gamma_{in}}, b'_1) \end{aligned} \tag{D.7}$$

where P'_{d0} and P'_{d1} are the detection probabilities of the passive correlators and the active correlators respectively, and given by

$$P'_{d0} = Q(\sqrt{2\gamma_0}, b'_0) \tag{D.8}$$

$$P'_{d1} = Q(\sqrt{2\gamma'_0}, b'_1) \tag{D.9}$$

where $\gamma'_0 = M\gamma_{in} = M\frac{E_c}{N_0}$.

The thresholds b'_0 and b'_1 are determined so that the overall performance or the dynamic range is optimized.

Appendix E
Computations of q, p, s, q_n, p_n, s_n for HL Receiver

In this appendix, symbol detection probability q, symbol error probability p and symbol erasure probability s to compute $P(h_e, h_x, \tilde{n})$ in section 2.3.2, are derived for coincidence detection. In addition, when signal is absent, the probabilities q_n, p_n and s_n that the outcome of a symbol test of coincidence is "1", "-1" and "erasure" in 2.3.2 are also derived.

To calculate q, p and s, we assume that symbol "1" is transmitted. Noting that the digital threshold for coincidence is h_2, the probability q that the output Y_m is not less than h_2 is given

$$q = Pr\{Y_m \geq h_2\} \tag{E.1}$$

By Gaussian approximation, q will be

$$q = \int_{h_2}^{\infty} f_{Y_m}(y)dy \tag{E.2}$$

Similarly, p and s can be obtained from

$$\begin{aligned} p &= Pr\{Y_m \leq -h_2\} \\ &= \int_{-\infty}^{-h_2} f_{Y_m}(y)dy \end{aligned} \tag{E.3}$$

$$\begin{aligned} s &= Pr\{|Y_m| < h_2\} \\ &= 1 - q - p \end{aligned} \tag{E.4}$$

Bearing in mind that the probability density function $f_{Y_m}(y) = f_{Y_{\bar{m}}}(y)$ is according to Gaussian distribution with mean and variance given in section 3.3.2, q, p and s are easily obtained as

$$q = 0.5 \operatorname{erfc}\left(\frac{h_2 - (1-2p_e)m}{\sqrt{8mp_e(1-p_e)}}\right) \tag{E.5}$$

$$p = 0.5 \operatorname{erfc}\left(\frac{h_2 + (1-2p_e)m}{\sqrt{8mp_e(1-p_e)}}\right) \tag{E.6}$$

$$s = 1 - q - p \tag{E.7}$$

When signal is absent, we can easily calculate q_n, p_n and s_n by letting $p_e = 0.5$ in (E.5), (E.6) and (E.7). Thus we get

$$q_n = 0.5 \operatorname{erfc}\left(\frac{h_2}{\sqrt{2m}}\right) \tag{E.8}$$

$$p_n = q_n = 0.5 \operatorname{erfc}\left(\frac{h_2}{\sqrt{2m}}\right) \tag{E.9}$$

$$s_n = 1 - 2q_n \tag{E.10}$$

Appendix F
Numerical Computation of Minimum P_L

In this appendix, we show the method to calculate $\min P_L$ with respect to SNR in chapter 4. As described in section 4.4.4, the optimal thresholds (b_0, b_c) as the function of SNR can be obtained by doing the minimization

$$\min\ P_L(b_0, b_c), \quad b_0 \text{ and } b_c \geq 0. \tag{F.1}$$

Since $P_L(b_0, b_c)$ is related to b_0 and b_c in a nonlinear manner, the problem cannot be easily solved by setting $\frac{\partial P_L}{\partial b_0} = 0$ and $\frac{\partial P_L}{\partial b_c} = 0$. Fortunately, P_L as a function of b_0 with b_c as a constant appears to be unimodal, i.e., P_L has a single minimum within a certain interval $b_m \leq b_0 \leq b_M$. This feature is shown in figure F.1 and figure F.2. Thus any of the linear search techniques such as the three-point search, the Fibonacci search and the Golden-ratio section search can be used. The optimization procedure is illustrated by the following steps. Step 1. Transfer the 2-dimensional problem into an unidimensional search by fixing b_c. Step 2. Applying one of the above search techniques, find the optimal function value and b_0. Step 3. Change b_c, and repeat step 2. Step 4. Select optimal (b_0, b_c) at the minimum P_L point. In fact, b_c has little effect on the minimum P_L as long as it is not too small.

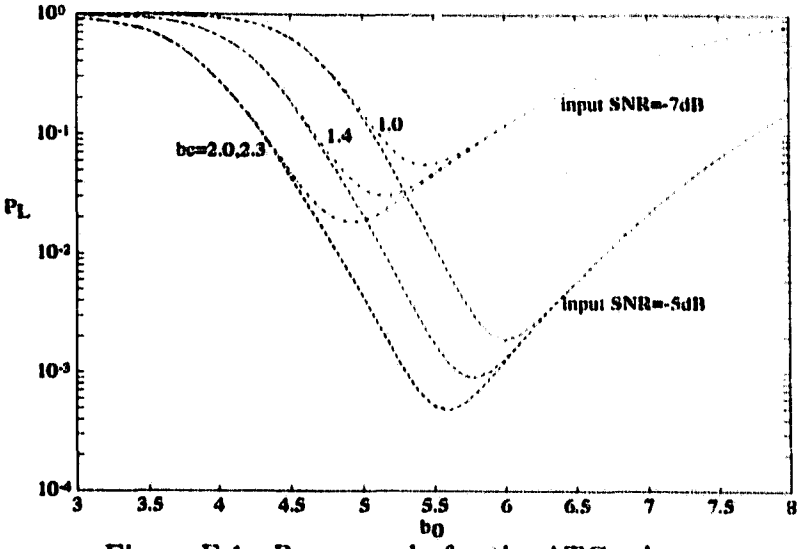

Figure F.1: P_L versus b_0 for the ATC scheme.
b_c is a parameter, $L_d = 1000, L = 8, l = 6$.

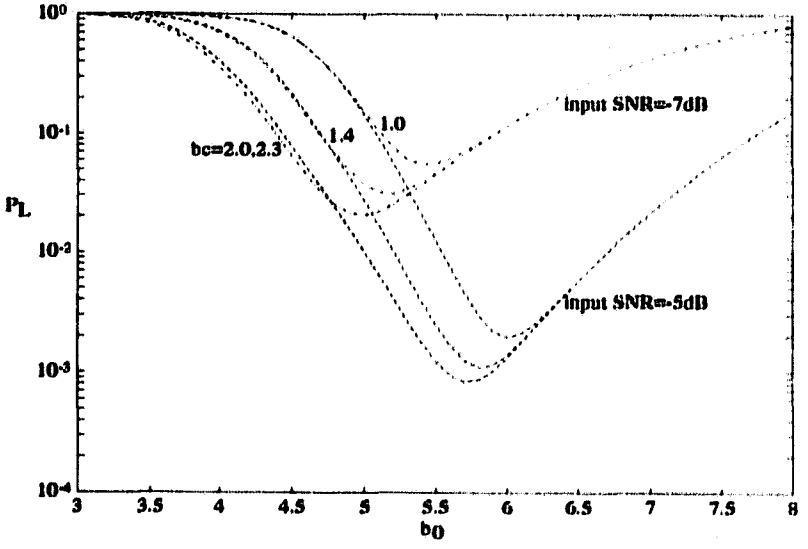

Figure F.2: P_L versus b_0 for the CT scheme.
b_c is a parameter. $L_d = 1000, L = 8, l = 6$.

Appendix G
Exact Computation of $P_d(i)$

In this appendix, we show the method to precisely compute $P_d(i)$ from $P_d(i) = \prod_{n=1}^{m-1} \Pr\{|Z_n| < |Z_0|, n = 1, 2, ..., m-1.\}$ in section 7.3. To do this, we first derive the probability density functions of $U_n = |Z_n|$ and $U_0 = |Z_0|$. The probability distribution function of U_n is

$$\begin{aligned} P_{U_n}(u_n) &= \Pr(U_n \le u_n) \\ &= \Pr(|Z_n| \le u_n) \\ &= \Pr(-u_n \le Z_n \le u_n) \\ &= \Pr(Z_n \le u_n) - \Pr(Z_n \le -u_n) \end{aligned} \tag{G.1}$$

By differentiating (G.1) with respect to u_n, we get the probability density function of U_n in term of the density function of Z_n. It is

$$p_{u_n}(u_n) = p_{z_n}(u_n) + p_{z_n}(-u_n), \quad u_n \ge 0. \tag{G.2}$$

Since Z_n is zero mean Gaussian random variable, we have $p_{z_n}(-u_n) = p_{z_n}(u_n)$. Thus

$$p_{u_n}(u_n) = 2p_{z_n}(u_n), \quad u_n \ge 0. \tag{G.3}$$

Similarly, we have

$$p_{u_0}(u_0) = p_{z_0}(u_0) + p_{z_0}(-u_0)$$

$$= \frac{1}{\sqrt{2\pi\sigma_i^2(0)}}(e^{-\frac{(u_0-\bar{A}_i)^2}{2\sigma_i^2(0)}} + e^{-\frac{(u_0+\bar{A}_i)^2}{2\sigma_i^2(0)}}) \tag{G.4}$$

Now $P_d(i)$ can be written as

$$P_d(i) = \int_0^\infty \prod_{n=1}^{m-1} \Pr(U_n < u_0 | U_0 = u_0) p_{u_0}(u_0) du_0 \tag{G.5}$$

where

$$\begin{aligned} \Pr(U_n < u_0 | U_0 = u_0) &= \int_0^{u_0} p_{u_n}(u_0) du_n \\ &= \int_0^{u_0} 2p_{z_n}(u_0) du_n \\ &= \text{erf}(\frac{u_0}{\sqrt{2\sigma_i^2(n)}}) \end{aligned} \tag{G.6}$$

Substitute (G.6) into (G.5), we have

$$\begin{aligned} P_d(i) &= \int_0^\infty \prod_{n=1}^{m-1} \text{erf}(\frac{u_0}{\sqrt{2\sigma_i^2(n)}}) p_{u_0}(u_0) du_0 \\ &= \frac{1}{\sqrt{2\pi\sigma_i^2(0)}} \int_0^\infty \prod_{n=1}^{m-1} \text{erf}(\frac{u_0}{\sqrt{2\sigma_i^2(n)}})(e^{-\frac{(u_0-\bar{A}_i)^2}{2\sigma_i^2(0)}} + e^{-\frac{(u_0+\bar{A}_i)^2}{2\sigma_i^2(0)}}) du_0 \\ &= \frac{1}{\sqrt{\pi}} \int_{-\sqrt{\gamma_i}}^\infty e^{-v^2} \prod_{n=1}^{m-1} \text{erf}(\alpha_n v + \alpha_n \sqrt{\gamma_i}) dv \\ &\quad + \frac{1}{\sqrt{\pi}} \int_{\sqrt{\gamma_i}}^\infty e^{-v^2} \prod_{n=1}^{m-1} \text{erf}(\alpha_n v - \alpha_n \sqrt{\gamma_i}) dv \end{aligned} \tag{G.7}$$

However the second term in (G.7) is very small in most cases compared to the first term, thus can be neglected. The first term is just the approximation we obtained in (7.40).